



**HAL**  
open science

# Deep learning approaches for neurological disorders detection based on brain activity analysis

Asma Baghdadi

► **To cite this version:**

Asma Baghdadi. Deep learning approaches for neurological disorders detection based on brain activity analysis. Bioinformatics [q-bio.QM]. Université Paris-Est; Université de Sfax (Tunisie), 2021. English. NNT : 2021PESC0067 . tel-04163090

**HAL Id: tel-04163090**

**<https://theses.hal.science/tel-04163090v1>**

Submitted on 17 Jul 2023

**HAL** is a multi-disciplinary open access archive for the deposit and dissemination of scientific research documents, whether they are published or not. The documents may come from teaching and research institutions in France or abroad, or from public or private research centers.

L'archive ouverte pluridisciplinaire **HAL**, est destinée au dépôt et à la diffusion de documents scientifiques de niveau recherche, publiés ou non, émanant des établissements d'enseignement et de recherche français ou étrangers, des laboratoires publics ou privés.



# THESIS

*Presented at*

**National Engineering School of Sfax**

*In order to obtain the degree of*

**DOCTORATE**

in

***Computer Systems Engineering***

By

**Asma BAGHDADI**

[Eng. in Computer Science]

## **Deep learning approaches for neurological disorders detection based-on brain activity analysis**

*Defended on December 9, 2021 before the jury composed of:*

M. Ahmed BEN HAMIDA (Professor, ENIS)	President
M. Mohamed Hédi BEDOUI (Professor, FMM)	Reviewer
M. Laetitia JOURDAN (Professor, University of Lille)	Reviewer
M. Su RUAN (Professor, University of Rouen)	Examiner
M. Adel M. ALIMY (Professor, ENIS)	Supervisor
M. Patrick SIARRY (Professor, UPEC)	Supervisor
M. Yassine ARIBI (Assistant professor, ENIS)	Co-Supervisor



# Deep learning approaches for Neurological disorders detection based-on brain activity analysis

Asma BAGHDADI

**الخلاصة:** كان مجال الذكاء الاصطناعي والتعرف على الأنماط مساهماً رئيسياً في العلوم والطب. صحة البشر هي الهدف النبيل لهذه الأطروحة التي عملنا عليها لاقتراح حلول وقائية لنوعين من الأمراض العصبية الشائعة: الجرع والصرع. ان الدراسات المشمولة في هذه الأطروحة مخصصة للكشف عن مستويات الجرع لدى الأفراد المعاقين والتي أدت بالأساس إلى تطبيق شامل وقاعدة بيانات متاحة للباحثين. أظهر نظام الكشف الذي يعتمد بشكل أساسي على استخراج وتصنيف مجموعة من الخصائص أداءً متفوقاً على الموجود في البحوث. الطريقة المشتركة بين جزأي هذه الأطروحة هي استخدام إشارات EEG على الرغم من ندرة التحقيق في مثل هذه التطبيقات نظراً لتعقيدها. لتعزيز العمل على الصرع قمنا بتنفيذ المهام المختلفة التي تخدم أطباء الأعصاب والمرضى: الكشف عن أنواع النوبات وتصنيفها باستخدام مناطق الدماغ الأكثر مساهمة في المرحلة الحاسمة والتنبؤ بنوبات الصرع من أجل للوقاية منها وتقليل خطر الموت المفاجئ. النماذج العميقة المقدمة قوية و قابلة للتفسير لامتداد الاطباء بالأسس التي قام عليها التنبؤ.

## **Résumé :**

Le domaine de l'intelligence artificielle et de la reconnaissance des formes a été un contributeur majeur à la science et à la médecine. Le bien-être de l'homme est le noble objectif de cette thèse, sur laquelle nous avons travaillé pour proposer des solutions préventives pour deux types de maladies neurologiques courantes : l'anxiété et l'épilepsie. Les études incluses dans cette thèse étaient dédiées à la détection des niveaux d'anxiété chez les individus sains, résultant en une application de bout en bout et une base de données accessible aux chercheurs. Le système de détection basé principalement sur l'extraction et la classification d'un ensemble de caractéristiques a montré des performances supérieures à l'existant. La modalité commune entre les deux parties de cette thèse est l'utilisation des signaux EEG malgré leur investigation minimale dans de telles applications compte tenu de leur complexité. Pour approfondir les travaux sur l'épilepsie, nous avons réalisé les différentes missions au service des neurologues et des patients : la détection et la classification des types de crises à l'aide des régions du cerveau contribuant le plus à la phase décisive et la prédiction des crises d'épilepsie afin de les prévenir et de diminuer le risque de mort subite. Les modèles profonds proposés sont robustes et surtout interprétables.

## **Abstract:**

The field of artificial intelligence and pattern recognition has been a major contributor to science and medicine. The well-being of humans is the noble goal of this thesis, which we have worked on to propose preventive solutions for two types of common neurological diseases: anxiety and epilepsy. The studies included in this thesis were dedicated to detecting anxiety levels in healthy individuals, resulting in an end-to-end application and a database accessible to researchers. The detection system based mainly on the extraction and classification of a set of characteristics showed performance levels superior to the existing one. The common modality between both parts of this thesis is the use of EEG signals despite their minimum investigation in such applications given their complexity. To further develop the work on epilepsy, we carried out the different tasks serving neurologists and patients: detection and classification of seizure types using regions of the brain contributing the most in the decisive phase and the prediction of epileptic seizures in order to prevent them and decrease the risk of sudden death. The deep models offered are robust and above all interpretable.

**المفاتيح:** إشارات EEG ، كشف القلق ، كشف النوبات وتصنيفها ، التنبؤ بالنوبات ، التعلم العميق ، الشبكة العصبية المتكررة ، النماذج القابلة للتفسير

**Mots clés :** Signaux EEG, détection d'anxiété, détection et classification des crises, prédiction des crises, apprentissage en profondeur, réseau de neurones récurrents, modèles interprétables

**Key-words:** EEG signals, anxiety detection, seizure detection and type classification, seizure prediction, deep learning, Recurrent Neural Network, Explainability



**Thèse de doctorat de l'Université Paris-Est**

Pour l'obtention du  
**Doctorat en Signal, Image et Automatique**

Rédigée par  
**ASMA BAGHDADI**

---

**DEEP LEARNING APPROACHES FOR NEUROLOGICAL  
DISORDERS DETECTION BASED ON  
BRAIN ACTIVITY ANALYSIS**

APPROCHES D'APPRENTISSAGE PROFOND POUR LA DÉTECTION DES  
TROUBLES NEUROLOGIQUES BASÉE SUR  
UNE ANALYSE DE L'ACTIVITÉ CÉRÉBRALE

---

*Soutenue le 09 décembre 2021 devant le jury composé de :*

<b>M. Ahmed BEN HAMIDA</b> (Professeur, ENIS)	Président
<b>M. Mohamed Hédi BEDOUI</b> (Professeur, FMM)	Rapporteur
<b>Mme. Laetitia JOURDAN</b> (Professeur, Université de Lille)	Rapporteuse
<b>Mme. Su RUAN</b> (Professeur, Université de Rouen)	Examinatrice
<b>M. Adel M. ALIM</b> (Professeur, ENIS)	Directeur de thèse
<b>M. Patrick SIARRY</b> (Professeur, UPEC)	Directeur de thèse
<b>M. Yassine ARIBI</b> (Maître-assistant, Université de Taif)	Co-Superviseur

## Résumé

L'électroencéphalographie est une technique d'enregistrement des signaux électriques du cerveau. Cet outil est intensivement utilisé dans le service de neurologie et de psychiatrie. L'analyse de l'activité cérébrale est une étape critique, qui apporte des informations sur les états émotionnel, mental et neurologique d'un patient.

Un état d'anxiété légère ou sévère altère l'activité cérébrale d'un individu. Les changements qui peuvent se manifester lors d'un état d'anxiété sont détectables par l'analyse de l'activité cérébrale. C'est aussi le cas pour le diagnostic de l'épilepsie, qui repose essentiellement sur l'électroencéphalogramme, qui aide les neurologues à diagnostiquer l'épilepsie et appliquer le traitement adéquat. Plusieurs recherches ont montré l'efficacité des signaux EEG à refléter les changements émotionnels, mentaux et les problèmes neurologiques.

La lecture des enregistrements EEG par l'expert du domaine est considérée comme un processus chronophage et fastidieux. L'automatisation de ce processus dans le but de détecter un état mental ou une maladie est de haute importance pour les neurologues. Les systèmes de reconnaissance intelligente, basée sur l'analyse de l'activité cérébrale, peuvent servir ainsi, pour les patients à domicile, à surveiller leur état, afin de se contrôler et d'avoir des préventions utiles.

Nous avons suivi l'approche typique utilisée en neuroscience pour le diagnostic des troubles cérébraux reposant sur les signaux EEG. La première étape est la collecte des données physiologiques à l'aide d'un casque EEG, suivie par le prétraitement. Cette étape comprend la préparation des données à analyser, soit en sélectionnant la partie optimale de l'enregistrement contenant les informations pertinentes, soit en appliquant certaines méthodes pour améliorer la qualité des données enregistrées. L'étape d'extraction des caractéristiques est appliquée après le prétraitement. Cependant, les données sont modélisées afin d'en extraire les informations pertinentes. Les caractéristiques les plus puissantes sont sélectionnées pour passer à l'étape de classification.

Etant donnée la nature des signaux EEG, qui sont réellement des séries temporelles, l'utilisation d'un réseau de neurones récurrents semble la manière la plus adéquate pour gérer ces signaux. Dans ce travail, trois contributions sont proposées, afin d'extraire une meilleure représentation des séries temporelles (prétraitées et brutes) et de les classer. Tout au long de ce travail, nous avons

accentué la richesse des signaux EEG bruts, l'importance des méthodes d'apprentissage profond et l'importance de l'analyse des résultats, pour fournir aux médecins des modèles interprétables et affermir leur confiance en cette technologie.

Le manuscrit de thèse commence par un **chapitre introductif** dans lequel le contexte et la problématique abordée sont expliqués. En outre, l'architecture générale, résumant les trois contributions, est présentée dans une figure explicative. À la fin de ce chapitre, l'organisation de la thèse est décrite, en mentionnant les différentes publications scientifiques en relation avec la thèse.

L'état de l'art de cette thèse est présenté dans le **chapitre 2**. Tout concept lié à la détection du niveau d'anxiété, à la classification des types de crises ou bien à la prédiction des crises a été évoqué, pour permettre au lecteur d'assimiler le contexte. Un aperçu des bases de données existantes, exploitées dans chaque partie de la thèse, est aussi donné. Le chapitre présente clairement les défis à relever dans cette thèse. En fait, la diversité des techniques de décomposition, d'apprentissage de caractéristiques et le domaine d'application rendent assez difficile notre contribution utilisant une nouvelle approche. De plus, la comparaison avec les travaux existants n'est pas aisée, vu que, dans chaque travail, un contexte bien défini a été considéré comme type d'expérimentation : modèle pour chaque participant ou modèle pour tous les participants, nombre de participants fixé, durée de l'expérimentation, nombre d'électrodes, et sélection des caractéristiques.

L'apprentissage profond basé sur les signaux EEG a commencé à émerger au début de 2015. Puisque l'extraction manuelle des caractéristiques est chronophage et nécessite un expert du domaine pour trouver la technique la plus convenable, l'apprentissage en profondeur a été proposé essentiellement pour faire l'apprentissage automatique des caractéristiques par le réseau de neurones. Dans les trois contributions, nous proposons une architecture basée sur l'apprentissage profond, suivi d'une étape d'interprétabilité du modèle créé. L'interprétabilité des résultats valorise le travail et donne des explications radicales aux médecins concernant le comportement caché du modèle. Pour comparer les techniques, nous avons aussi implémenté des méthodes basées sur l'extraction manuelle des caractéristiques.

Inspiré par ce principe, le présent travail a relevé le défi, en confiant l'étape d'extraction de caractéristiques et de classification à un réseau de neurones récurrents, convolutionnels.

Les contributions sont réparties en deux parties comme suit.

### **1<sup>ère</sup> partie : Détection de niveau d'anxiété**

- **Chapitre 3 :** Ce chapitre détaille tous les travaux élaborés afin de fournir un produit fini pour la détection du niveau d'anxiété. Vu le manque de travaux dédiés à l'étude de l'anxiété, comme l'état transitoire qu'un individu peut subir, nous avons eu du mal à trouver une base de données EEG exploitable à cette fin. Nous avons constaté une absence de bases de données publiques, puisque la plupart des travaux sur l'anxiété testent leurs méthodes sur des données purement cliniques et donc privées, ou bien collectent des signaux limités à un usage unique dans ces méthodes et sont privés. Il fallait donc penser à proposer une base de données pour la reconnaissance des niveaux d'anxiété. Dans ce cadre, une coopération a été établie avec une thérapeute de l'hôpital universitaire Hédi Chaker, afin de concevoir un protocole expérimental de stimulation d'anxiété. La collecte de données a été réalisée à l'aide d'un casque EMOTIV EPOC+ sur 23 participants. Une étude approfondie a été élaborée, produisant un protocole expérimental pour la stimulation de l'anxiété chez des individus sains. Le protocole a été validé par une psychothérapeute, pour qu'il contienne une phase de récitation d'une situation stimulante et une phase d'auto-rappel individuel. Le choix des six situations en premier lieu a été fait à travers la distribution d'un questionnaire proposé par la thérapeute à des personnes autres que celles engagées pendant l'enregistrement. Ce questionnaire a pour objectif de déterminer les six situations sources d'anxiété, à partir des réponses données. La durée de l'expérience est de 15 minutes. Tout au long de l'expérience, le volontaire est confronté à six situations différentes de la vie réelle et doit évaluer ses émotions durant chaque situation, en remplissant l'échelle SAM (*Self-Assessment Manikin*). La psychothérapeute a évalué le niveau d'anxiété chez les participants avant et après l'expérience, à travers l'échelle d'anxiété HAMILTON. Les données EEG collectées au moyen du neuro-casque EMOTIV EPOC+, qui contient 14 canaux et 2 références, ont été labélisées selon deux méthodes : en se basant sur l'échelle SAM (les valeurs *Valence et Arousal*) et en se basant sur les scores du test HAMILTON. Une étape de prétraitement des signaux EEG vis-à-vis

du bruit et des artefacts internes et externes est très importante pour avoir un modèle pertinent. Les données brutes sous format .edf et les données prétraitées ont été mises à la disposition de la communauté scientifique sur IEEE DataPort. L'approche proposée pour la détection du niveau d'anxiété est basée sur l'extraction d'un ensemble de caractéristiques, qui ont été étudiées dans la littérature et ont prouvé leur pertinence comme marqueurs d'anxiété dans les signaux EEG. Cet ensemble contient des caractéristiques temporelles, spectrales et spatio-temporelles. Nous avons utilisé deux classificateurs pour la classification en multi-classes (4 niveaux d'anxiété) : SVM et KNN. Nous avons comparé les résultats en utilisant chaque type de caractéristique indépendamment, et en combinant plusieurs types ensemble. Les meilleurs résultats ont été obtenus pour l'ensemble des caractéristiques (*ALLfeatures*), en utilisant SSAE comme classificateur : 86.70%.

À la fin de ce chapitre, une première utilisation d'un réseau de neurone récurrent *LSTM* a été faite dans le cadre d'une démonstration de l'application '*Anxiety checker*', avec une amélioration remarquable du taux de détection (de 86.70% à 93.32%).

**Le travail présenté dans ce chapitre a donné lieu à un article publié dans la revue « Journal of Ambient Intelligence and Humanized Computing ».**

## **2<sup>ème</sup> partie : Détection/Prédiction des crises et classification des types de crise**

- **Chapitre 4** : La classification des crises d'épilepsie présente un défi pour les neurologues durant le processus de diagnostic. Il est très important que le médecin détecte le type d'épilepsie, pour la prescription du traitement adéquat. En 2017, la ligue internationale contre l'épilepsie (*ILAE*) a proposé une nouvelle classification des types de crises. Le système automatisé de classification des crises proposé dans ce chapitre peut aider les professionnels de la santé à diagnostiquer la maladie, en réduisant le temps nécessaire et en améliorant potentiellement la précision et la fiabilité. Ce chapitre propose un nouveau modèle *LSTM* basé sur l'attention par régions et démontre l'intérêt de la couche d'attention et des poids calculés, liés à la contribution des canaux améliorant les performances de la classification. De cette

manière, le modèle et les résultats sont plus explicables, en montrant des corrélations entre l'interprétation neurologique par un expert et la lecture des *Heatmaps* des sorties déduites de notre modèle. Le modèle LSTM-attention procure une amélioration significative de la précision de la classification, atteignant 94,40% sur l'ensemble de données TUSZ lors de la classification de 8 types de crises d'épilepsie et 96,78% pour une classification binaire (crise Vs normale).

Le nombre de paramètres dans nos modèles est d'un peu plus d'un million, avec un temps d'inférence d'environ 1,2 ms sur un GPU NVIDIA GTX960m. Le modèle se généralise également bien à travers différents types de crises minoritaires.

Selon la description par session jointe aux données, il existe une corrélation significative entre les conclusions scientifiques et nos résultats. Le plus grand score d'attention signifie que la probabilité d'apparition de crises sur cette zone est plus élevée. En résumé, l'étude de cas indique que nous pouvons apprendre des scores d'attention avec des représentations interprétables par nos modèles basés sur l'attention par canal, qui, non seulement améliore les performances de détection/classification, mais aussi identifie les causes cliniques de l'apparition des crises. Dans nos expériences, il a été observé que des poids relativement importants étaient attribués à des canaux qui contribuent à caractériser un type de crise. Pour un exemple de crise focale non spécifique, le neurologue a signalé un état pathologique épileptique non convulsif chez un patient atteint d'épilepsie pharmaco-résistante. L'EEG tracé montre une crise temporo-occipitale, qui coïncidait avec les poids de la couche attention de 21 canaux, pour les segments de crise correspondants. Les canaux (O1, O2) et (T5, T6) ont un poids important par rapport aux autres canaux au début de la crise. Les travaux futurs peuvent se concentrer sur l'amélioration des performances de cette étude pour les classes mineures, en utilisant des données multimodales, principalement des vidéos EEG.

**Le travail présenté dans ce chapitre a donné lieu à un article soumis à la revue « IEEE Journal of Biomedical and Health informatics ».**

- **Chapitre 5 :** Dans ce chapitre, nous avons présenté la troisième contribution de cette thèse, qui concerne le problème de prédiction des crises épileptiques. Afin de

conceptualiser un système robuste de prédiction des crises épileptiques à partir des signaux EEG, il est important d'étudier les approches d'apprentissage pour la reconnaissance des états épileptiques. Ce processus comprend en général, une étape d'acquisition, dans laquelle les signaux EEG sont collectés sur des patients épileptiques, une phase de prétraitement visant à supprimer la ligne de base et les artefacts, une phase d'extraction de caractéristiques et des étapes de classification. Récemment, le processus a été renouvelé en incluant une étape d'apprentissage des caractéristiques via les réseaux profonds, à la place de l'extraction manuelle, qui nécessite une expertise et une familiarité avec les caractéristiques des crises d'épilepsie.

Les modèles profonds proposés dans cette thèse sont conceptualisés pour gérer la nature complexe du signal EEG, par l'ajout de plusieurs couches au modèle LSTM et par l'augmentation du nombre d'unités de mémoire cachées. Nous avons aussi proposé des modèles plus sophistiqués, en exploitant le mécanisme de l'attention, pour avoir des résultats déchiffrables '*EXPLAINABILITY*'. Ce processus vise à permettre un meilleur apprentissage des caractéristiques. Nos modèles sont plus adaptés aux applications en temps réel que d'autres basés sur des techniques d'extraction de caractéristiques, qui sont mises en œuvre dans un but de comparaison.

La représentation typique des caractéristiques est apprise par nos modèles, ce qui conduit à des résultats très satisfaisants pour la prédiction des crises. De plus, nous pouvons appliquer la même architecture pour la détection des crises, en incluant des segments critiques au processus global. Au début de ce chapitre, nous avons étudié différentes approches pour extraire les caractéristiques liées aux crises EEG. La prédiction des crises dans la première approche a été traitée comme un problème d'apprentissage automatique. Les principales étapes de ce problème de classification sont : l'extraction des caractéristiques pertinentes et la conception d'un classifieur adéquat. Une fois les caractéristiques extraites, il reste essentiel de définir la méthode de prise de décision. Le classifieur doit être capable de bien généraliser et de montrer de bonnes performances. Les annotations faites par un neurologue sont souvent considérées comme le point de référence dans le cadre de

ce problème. Cette approche repose sur la détermination préalable des moments statistiques à calculer, comme la moyenne, la variance, l'asymétrie et l'aplatissement dans le signal EEG. La contribution majeure est la proposition d'un nouveau modèle pour l'apprentissage des caractéristiques spatio-temporelles du signal EEG, avec une couche d'attention pour les fragments d'entrée. Nous avons également implémenté un modèle LSTM pour l'apprentissage des dépendances temporelles, afin de montrer l'amélioration obtenue par le nouveau modèle spatio-temporel ConvLSTM proposé par [Xingjian et al., 2015].

L'objectif derrière l'intégration d'un mécanisme d'attention dans le modèle spatio-temporel ConvLSTM2D proposé est d'analyser en profondeur la contribution des fragments temporels construits dans la décision finale du système. Ainsi, nous identifions un horizon de prédiction justifiable, indépendant du patient, contenant les fragments les plus efficaces. Cette analyse peut aider le neurologue à rechercher les raisons de l'apparition de la crise, en identifiant les déclencheurs, suivant les fragments les plus contributifs. La définition de la période préictale optimale (OPP) peut également reposer sur les poids d'attention des fragments inclus dans la période préictale sélectionnée (SPP). Plus précisément, si le choix du SPP est fait à moins d'1h pour tous les patients, les scores d'attention calculés sur tous les segments de 1h peuvent fournir des informations importantes sur la contribution de chaque fragment ; ainsi le SPP peut être réduit de 1h à 15min. Nous supposons qu'il existe une phase préictale pour toutes les crises et qu'il existe un point d'inflexion entre les états interictal et préictal et nous travaillerons pour montrer cela.

Pour une période préictale égale à 15 minutes, suivant les travaux de [Tsiouris et al.], nous avons obtenu des résultats de prédiction très compétitifs par rapport à l'état de l'art, avec une précision de 94.45% et 90.62% pour les modèles ConvLSTMatt et ConvLSTM respectivement.

L'objectif principal de cette étude est de concevoir des modèles d'apprentissage en profondeur pour la prédiction des crises d'épilepsie, indépendamment du patient. De tels modèles peuvent être utilisés dans des situations où les sujets de l'ensemble de données ont moins d'exemples étiquetés (enregistrements EEG). Nous reconnaissons qu'il s'agit d'un cas typique dans les scénarios de surveillance des

unités de soins intensifs, où un nombre adéquat d'échantillons ne peut pas être obtenu pour former un modèle de prédiction.

**Une partie du travail présenté dans ce chapitre a donné lieu à un article pour la conférence « International Joint Conference on Neural Networks ».**

**La méthode proposée dans la deuxième partie de ce chapitre fera l'objet d'un article soumis à la revue « IEEE Transactions on Neural Networks and Learning Systems ».**

Le présent manuscrit se termine, dans le **chapitre 6**, par un rappel sur les différentes contributions présentées et par la proposition de deux perspectives intéressantes pour la poursuite de ce travail.

La première perspective est une étude de la relation entre l'anxiété et les crises épileptiques. La question que l'on pose est la suivante : un état d'anxiété élevé peut-il provoquer une crise chez les patients épileptiques ? Les biomarqueurs de l'électroencéphalographie (EEG) sont un ensemble de manifestations neurologiques détectées dans le signal EEG, qui sont exploitées pour donner une empreinte à une réaction cérébrale, face à une émotion traumatique, à l'anxiété ou au stress. Beaucoup de personnes ont du mal à gérer leurs émotions, c'est pourquoi, elles ont une forte probabilité que leur système de défense se bloque. Les patients épileptiques peuvent être confrontés à une Pseudo-épilepsie (PNES). Celle-ci n'est pas du même type que les crises neurologiques causées par une activité incontrôlée dans le cerveau. Les PNES sont plutôt une réponse extrême au stress et à l'anxiété et sont donc considérées de nature psychiatrique. Si une réponse extrême du cerveau d'un patient non-épileptique au stress et à l'anxiété peut provoquer une PNES, combien de biomarqueurs d'anxiété peuvent être présents dans l'état préictal d'une crise ? Comme nous savons que certains biomarqueurs EEG ont une grande corrélation avec un état anxieux, comme discuté dans le chapitre 3, nous proposons de rechercher la présence de ces empreintes dans les segments préictaux. L'étude doit fournir une comparaison entre les valeurs des états préictal, ictal et interictal du biomarqueur choisi. Si une corrélation est trouvée, un modèle peut être proposé pour discriminer entre les trois états, en fonction de la caractéristique extraite. Ce travail peut être appliqué pour la prédiction ou la détection des crises.

La deuxième perspective est relative au problème de l'insuffisance de données EEG pour la classification des types des crises, via un réseau de neurones profond. Le modèle « *Generative*

*Adversarial Network* » (GAN) peut servir d'approche comme générateur de nouvelles données EEG, très similaires aux données réelles. Une telle génération enrichit la base d'apprentissage et non pas celle de test. De cette manière, l'apprentissage d'un réseau de neurones profond sera plus pertinent.

# Dedications

The sake of Allah, my Creator and my Master, my sincere thanks to you, who endowed me to complete this PhD research.

I dedicate this thesis:

**To my father *Chaouki*,**

who had the dream of witness this dissertation and who never stopped supporting me during the challenges of post-graduate studies.

**To my mother *Roya*,**

who has been a constant source of support and help, taking care of my family during the challenging times of my thesis.

Thank you for having always loved me unconditionally. Thank you for your prayers that facilitate the hardest missions

**To my husband *Walid*,**

I can't forget your support and encouragement during all the life challenges. I am truly thankful for having you in my life. Thank you for lending a helping hand every time I need you. For your patience, faith and love.

**To my beloved kid *Mohamed Jude*,**

as a sign of the strong woman I became after your birth.

**To My beloved brother *Ahmed Yassine*,**

who stands by my side when things look bleak.

**To**

my friends who encourage and support me,

All the people in my life who touch my heart, all those who helped me from near or far.

Those who felt one day to me a sense of respect and love.

---

# Acknowledgments

The writing of this dissertation has been one of the most significant challenges in my academic life. Without the support and guidance of a number of people, this study would not have been completed. It is to them that I am greatly indebted.

I would like to express my deepest gratitude and appreciation to Professor *Adel M. Alimi*, my supervisor and director of *REGIM-Lab* (REsearch Groups in Intelligent Machines), whose constant guidance and patient revision have all been crucial in the realisation of this dissertation.

I am also grateful to my supervisor Professor *Patrick Siarry* from the *LiSSi* (Laboratoire Images, Signaux et Systèmes intelligents) for providing an invaluable effort of unwavering support, for his imminent presence, his continuous supervision and his human qualities.

I would like to acknowledge Doctor *Yassine Aribi*, my co-supervisor, Assistant University College of Ranyah Taif for his help with my first steps in this project, his cooperation and his support.

I am also indebted to Doctors, *Najla Halouani*, Assistant University Hospital in Psychiatry at Hedi Chaker university hospital center of Sfax, *Sawsen Daoud* Assistant University Hospital in Neurology at Habib Bourguiba, university hospital of Sfax for helping during the anxiety experiment design and EEG data collection and assistance and guidance for the scientific interpretations.

I would also like to thank Professor *Mohamed Hédi Bedoui* and Professor *Laetitia Jourdan* for accepting to review my thesis and for their relevant comments on my research work.

My gratitude goes to Professor *Ahmed Ben Hamida* for the honor he had accorded me for agreeing to be the committee chair of this thesis. My distinguished thanks go also to Professor *Su Ruan* for the valuable service to examine this work and to be a member of my committee.

I would like to sincerely thank my friend, Doctor *Rahma Fourati* in the *REGIM-Lab* for her imminent presence, helpful hand, support in many occasions, for providing scientific advice on the research's experiment, discussions and constant perusal of my work, her scientific rigor and breadth of her knowledge.

Of course, I could not have achieved this purpose without making deep gratitude to teachers

---

and researchers who have guided me in my quest for knowledge during my years of studies.

Last but not least, I could not have made a success of my work without my family; words can never express my gratitude to them for their patience, care, encouragements, and faith in what I am doing.

In short, and not to forget anyone, I take this opportunity to dedicate my thanks to all those who helped and encouraged me during my university studies.

# Contents

<b>List of Figures</b>	<b>vii</b>
<b>List of Tables</b>	<b>x</b>
<b>1 Introduction</b>	<b>1</b>
1.1 Context and motivation . . . . .	1
1.2 Thesis contributions . . . . .	4
1.3 Thesis outline . . . . .	6
1.4 Thesis publications . . . . .	7
<b>2 Literature Review on Health-Related Artificial Intelligence Applications</b>	<b>9</b>
2.1 Introduction . . . . .	10
2.2 Health-Related Artificial Intelligence Applications . . . . .	11
2.2.1 Electroencephalography . . . . .	11
2.2.2 Anxiety state . . . . .	15
2.2.3 Epilepsy disorder . . . . .	16
2.3 Review of EEG-based approaches for anxiety detection . . . . .	20
2.3.1 Available benchmarks . . . . .	20
2.3.2 Existing works on anxiety levels recognition . . . . .	21
2.4 Review on EEG-based approaches for epileptic seizures prediction . . . . .	23
2.4.1 Available benchmarks . . . . .	23
2.4.2 Existing works on epileptic seizures detection and prediction . . . . .	25
2.5 Review of EEG-based approaches for seizures types recognition . . . . .	33
2.5.1 Available benchmarks . . . . .	33
2.5.2 Existing works on seizures types recognition . . . . .	37
2.6 Conclusion . . . . .	38
<b>3 EEG-based anxiety levels recognition using a psychological stimulation</b>	<b>39</b>
3.1 Introduction . . . . .	40
3.2 DASPS: a new database for anxiety levels detection based on a psychological stimulation . . . . .	41
3.2.1 Anxiety stimulation . . . . .	41
3.2.2 Psychological evaluation . . . . .	42
3.2.3 Subjects . . . . .	44

## Contents

---

3.2.4	EEG recording . . . . .	45
3.2.5	Experiment protocol . . . . .	46
3.2.6	Data analysis . . . . .	48
3.2.7	Artifacts removal . . . . .	51
3.3	Feature-based Machine Learning Approach for anxiety levels recognition . . .	52
3.3.1	Time Domain Features . . . . .	53
3.3.2	Frequency domain features . . . . .	55
3.3.3	Time-frequency domain features . . . . .	55
3.3.4	Other features . . . . .	57
3.4	Anxiety detection results and discussion . . . . .	58
3.4.1	SAM-based results . . . . .	58
3.4.2	HAM-based improved results . . . . .	63
3.5	A mobile application for anxiety level recognition based on deep LSTM model	66
3.5.1	Broader impact and overview . . . . .	67
3.5.2	Evaluation of LSTM architectures . . . . .	68
3.5.3	Overview of the application . . . . .	69
3.6	Conclusion . . . . .	71
<b>4</b>	<b>A novel region-aware attention with deep LSTM for EEG epileptic seizure classification</b>	<b>72</b>
4.1	Introduction . . . . .	73
4.2	A region-aware attention mechanism for seizure types classification from raw EEG signals . . . . .	75
4.2.1	Attention mechanism for multi-channel epileptic signals . . . . .	75
4.2.2	LSTM model with an attention mechanism . . . . .	78
4.3	Experiment results for seizure detection and seizure type classification . . . . .	80
4.3.1	Experiment design . . . . .	80
4.3.2	Experimental results . . . . .	82
4.4	Cases study . . . . .	91
4.4.1	Myoclonic seizure . . . . .	91
4.4.2	Tonic-clonic seizure . . . . .	93
4.4.3	Complex partial seizure . . . . .	95
4.5	Conclusion . . . . .	97
<b>5</b>	<b>A spatio-temporel attention network for epileptic seizures prediction from EEG signals</b>	<b>98</b>
5.1	Introduction . . . . .	99

## Contents

---

5.2	Epileptic states . . . . .	100
5.2.1	Interictal state . . . . .	100
5.2.2	Preictal state . . . . .	100
5.2.3	Ictal state . . . . .	101
5.2.4	Postictal state . . . . .	101
5.3	Preictal biomarkers . . . . .	102
5.4	Method . . . . .	103
5.4.1	Feature extraction . . . . .	104
5.4.2	Spatio-temporal representation based on Convolutional Long Short-Term Memory model . . . . .	107
5.4.3	Attention-based ConvLSTM model . . . . .	111
5.5	Experimental results and discussion . . . . .	114
5.5.1	EEG dataset and data preparation . . . . .	115
5.5.2	Results on patient-dependent epileptic seizure prediction . . . . .	116
5.5.3	Results on subject-independent epileptic seizure prediction . . . . .	123
5.6	Conclusion . . . . .	130
<b>6</b>	<b>Conclusion and Future Works</b>	<b>132</b>
6.1	Summary of contributions . . . . .	133
6.2	Future works . . . . .	134
6.2.1	Investigation of the relation between anxiety and epileptic seizures . . . . .	135
6.2.2	Data augmentation using adversarial neural network for the TUHSZ dataset addressing the issue of imbalanced classification task . . . . .	136
6.2.3	Automated hyper-parameters optimization . . . . .	136
	<b>Bibliography</b>	<b>138</b>

# List of Figures

1.1	The three major methodologies considered in this thesis. . . . .	5
2.1	EEG rhythms (Gamma, Beta, Alpha, Theta, Delta) . . . . .	13
2.2	The international 10-20 system of electrodes placement . . . . .	14
2.3	An example of artifact-contamination, Left: ECG is identified by its fixed period and morphology and is limited to T3-A1 channel, Right: The focal slowing in the T4-T6 and T6-O2 channels has no fields beyond T6 electrode and has the oscillation typical of rhythmic electrode movement . . . . .	15
3.1	Self-Assessment Manikin (SAM) proposed by Bradley and Lang (1994). Self-evaluation scales for the dimensions of valence (top row), arousal (middle row), and dominance (bottom row) in a 9-point scale. . . . .	44
3.2	Hamilton anxiety rating scale (HAM-A) proposed by [Hamilton, 1959] [Maier et al., 1988]. 14 questions about feelings and thoughts during the last month in a 4-point scale. . . . .	45
3.3	The Emotiv EPOC EEG headset with 14 channels . . . . .	46
3.4	The experimental protocol of anxiety stimulation . . . . .	47
3.5	Presentation of participant rating in two-dimensional space . . . . .	49
3.6	Head plots of the distribution of mean power per frequency band. The warmer colors indicate higher relative power (scaled from minimum to maximum values of the total group) . . . . .	51
3.7	Architecture of the proposed system for anxiety levels detection . . . . .	53
3.8	Overall class distribution across all participants for two and four anxiety levels. . . . .	59
3.9	PCA score plot of PC1 and PC2 for (a) 5s trial duration and (b) 1s trial duration . . . . .	60
3.10	Improved results across all features extracted from the SAM-based and HAM-based databases . . . . .	62
3.11	Confusion matrix for (a) SVM, (b)k-NN and (c) SSAE summarizing the targeted (y-axis) and predicted (x-axis) anxiety level, where 0: Normal, 1: Severe, 2: Moderate and 3: Light . . . . .	65
3.12	ROC curve of 2-levels anxiety using SSAE with 4 types of features. . . . .	66
3.13	Business model canvas of an EEG-based mobile application for anxiety levels recognition . . . . .	67
3.14	The process of an anxiety levels recognition application with all implicated parts . . . . .	68
3.15	Confusion matrix of anxiety levels recognition for the LSTM model evaluated with a test set from DASPS . . . . .	69
3.16	ScreenShots of the anxiety checker application, Top: Topographic map option, Bottom: Anxiety level recognition . . . . .	70

## List of Figures

---

4.1	The overall workflow of our proposed method including the three main phases .	75
4.2	The structure diagram of our attention-based LSTM model . . . . .	76
4.5	LSTM-att model performance in term of accuracy and loss for seizure detection with TUSZ dataset . . . . .	84
4.6	Confusion matrix of our LSTM-att model validated on TUSZ . . . . .	85
4.8	Mean attention weights on channels for a set of seizure samples from CHB-MIT	89
4.9	EEG bands topographical distribution of an ictal segments from the CHBMIT dataset . . . . .	89
4.10	Left:Visualization of a multi-channel signal containing a Focal Non-specific seizure from TUSZ, Right: Correspondent Heatmap of calculated weights . . .	90
4.11	Position of high-weighted channels: Fz, Cz, Pz, (O1,O2) and (P5,P6) according to the 10-20 electrode system placement. . . . .	91
4.12	Visualization of a multi-channel signal containing a seizure from TUSZ: Myoclonic seizure . . . . .	92
4.13	Heatmap of calculated weights of a Myoclonic seizure . . . . .	92
4.14	Position of high-weighted channels according to the 10-20 electrode system placement. Fz, Cz, Pz, O1 and P4 are central and posterior channels . . . . .	93
4.15	Tonic-Clonic seizure . . . . .	94
4.16	Heatmap of calculated weights of a tonic-clonic seizure . . . . .	94
4.17	Position of high-weighted channels according to the 10-20 electrode system placement. P4, O1, O2, Pz and Cz are central and posterior channels . . . . .	95
4.18	Complex partial seizure . . . . .	96
4.19	Heatmap of calculated weights of a complex partial seizure . . . . .	96
5.1	Spectrum of two random signals from CHB-MIT and TUH EEG Corpus, Segment of 5 seconds and channels are averaged . . . . .	103
5.2	Overall diagram of the proposed method comportsing the two approaches for seizure prediction . . . . .	104
5.3	6 levels decomposition of the original EEG signal, the decomposition level was chosen based on the frequency sampling. fs=256 Hz . . . . .	106
5.4	Power bands feature extraction . . . . .	107
5.6	The inner architecture of a ConvLSTM model . . . . .	109
5.5	An instance of LSTM module . . . . .	109
5.7	The proposed spatio-temporal ConvLSTM model is depicted by the three blocks of ConvLSTM. The attention block captures the relevance of each segment to the final decision. . . . .	111
5.8	Frame-based vs Conv-based ConvLSTM attention model . . . . .	112
5.9	Different states representation of an epileptic patient's EEG segment . . . . .	116
5.10	T-sne projection of data from chb01 . . . . .	121

## List of Figures

---

5.11 T-sne projection of data from chb12 . . . . .	121
5.12 T-sne projection of raw data from the test set (left) and of learnt features (right)	122
5.13 Results of all cases grouped by the number of seizures, for patients who have the same number of seizure we plotted the mean values . . . . .	122
5.14 Results of all cases grouped by SENS, SPEC and ACC . . . . .	122
5.15 Improved results by the proposed LSTM-att method . . . . .	123
5.16 Confusion matrix of the ConvLSTM model . . . . .	126
5.17 Confusion matrix of the frame-based attention ConvLSTM model . . . . .	126
5.18 Illustration of the prediction process . . . . .	128
5.19 EEG Signal plot vs Spectrogram vs attention Heatmap of 15 minutes from a preictal state . . . . .	129

# List of Tables

2.1	EEG frequency bands signification for diseases causing mental disorders . . . . .	17
2.2	Previous works on EEG-based anxiety detection . . . . .	24
2.3	Details of all 24 cases included in the CHB-MIT database . . . . .	26
2.4	Previous works on EEG-based seizure prediction . . . . .	34
2.5	Summary of TUH dataset . . . . .	35
2.6	Previous works on EEG-based seizure types classification . . . . .	36
3.1	Anxiety triggers categories and stimuli . . . . .	42
3.2	Mean rating and Standard Deviation across all participants for each situation . .	49
3.3	Participants Number in each quadrant according to SAM ratings . . . . .	50
3.4	Participants number by anxiety levels according to Hamilton scores . . . . .	50
3.5	EEG signal frequency bands and decomposition levels at fs=128 Hz . . . . .	56
3.6	EEG quantitative features . . . . .	57
3.7	Anxiety detection results of 4 and 2 levels . . . . .	59
3.8	Anxiety detection results using SSAE . . . . .	62
3.9	Performance comparison of the proposed work with the state-of-the-art methods	63
3.10	Anxiety detection improved results for 4 levels . . . . .	64
4.1	Proposed LSTM architecture parameters . . . . .	81
4.2	Results on TUSZ dataset for seizure detection . . . . .	83
4.3	Results on TUSZ dataset for seizure classification . . . . .	83
4.4	Comparison with state-of-the-art methods validated on TUSZ dataset . . . . .	86
4.5	Results on CHB-MIT dataset . . . . .	87
4.6	Comparison with state-of-the-art methods on seizure detection with CHB-MIT dataset . . . . .	87
5.1	EEG signal frequency bands and decomposition levels at fs=256 Hz . . . . .	107
5.2	Parameters and hyperparameters of the a ConvLSTM model . . . . .	110
5.3	EEG-based seizure prediction results . . . . .	120
5.4	Performance comparison of the proposed work with a raw EEG-based approach	123
5.5	The parameter settings of the proposed Convolution based ConvLSTM atten- tion . . . . .	124
5.6	Results of the proposed ConvLSTM and ConvLSTM attention . . . . .	125
5.7	Results of patient-independent seizure prediction approaches . . . . .	127
5.8	Evaluation of the system's behavior for three different seizures . . . . .	128

# List of Abbreviations

<b>AAR</b>	Automatic Artifact Removal
<b>AE</b>	Autoencoder
<b>AI</b>	Artificial Intelligence
<b>ANN</b>	Artificial Neural Network
<b>AUC</b>	Area Under Curve
<b>BSS</b>	Blind Source Separation
<b>CBT</b>	Cognitive Behavioral Therapy
<b>DEAP</b>	Database for Emotion Analysis using Physiological Signals
<b>DASPS</b>	Database for Anxious States based on a Psychological Stimulation
<b>DNN</b>	Deep Neural Network
<b>DSAE</b>	Denoising Sparse AutoEncoder
<b>DWT</b>	Discrete Wavelet Transform
<b>EEG</b>	ElectroEncephaloGraphy
<b>ECG</b>	ElectroCardioGram
<b>ED</b>	Epileptiform Discharges
<b>EOG</b>	ElectrOculoGram
<b>EMG</b>	muscle artifacts
<b>EMD</b>	Empirical Wavelet Transform
<b>ESN</b>	Echo State Network
<b>FIR</b>	Finite Impulse Response
<b>fMRI</b>	functional Magnetic Resonance Imaging
<b>FD</b>	Fractal Dimension
<b>GAN</b>	Generative Adversarial Networks
<b>GSCCA</b>	Group Sparse Canonical Correlation Analysis
<b>HAM-A</b>	Hamilton Anxiety Rating Scale
<b>HBN</b>	Healthy Brain Network
<b>HFD</b>	Higuchi's Fractal Dimension
<b>HOP</b>	Hyper-parameters Optimization
<b>HHS</b>	Hilbert-Huang Spectrum

## Chapter 0. List of Abbreviations

---

<b>IADS</b>	International Affective Digitized Sounds
<b>IAPS</b>	International Affective Picture System
<b>iEE</b>	Intracranial ElectroEncephaloGram
<b>ICA</b>	Independent Component Analysis
<b>ILAE</b>	International League Against Epilepsy
<b>LSTM</b>	Long Short Term Memory
<b>LVHA</b>	Low Valence and High Arousal
<b>MI</b>	Mutual Information
<b>ML</b>	Machine Learning
<b>MLP</b>	Multi-Layer Perceptrons
<b>MSCE</b>	Magnitude Square Coherence Estimation
<b>MVAR</b>	MultiVariate AutoRegressive
<b>OPP</b>	Optimal Preictal Period
<b>PNES</b>	Psychogenic NonEpileptic Seizures
<b>PSD</b>	Power Spectral Density
<b>PSS</b>	Perceived Stress Scale
<b>RBF</b>	Radial Basis Function
<b>RER</b>	Relative Energy Ratio
<b>RMS</b>	Root Mean Square
<b>RNN</b>	Recurrent Neural Network
<b>ROC</b>	Receiver Operating Characteristic
<b>SAE</b>	Stacked AutoEncoder
<b>SAM</b>	Self Assessment Manikin
<b>SCARED</b>	Screen for Child Anxiety Related Disorders
<b>SPP</b>	Selected Preictal Period
<b>SUDEP</b>	Sudden Unexpected Death in Epilepsy
<b>t-SNE</b>	t-Distributed Stochastic Neighbor Embedding
<b>TQWT</b>	Tunable Q Wavelet Transform

# Introduction

---

## Contents

<b>1.1</b>	<b>Context and motivation . . . . .</b>	<b>1</b>
<b>1.2</b>	<b>Thesis contributions . . . . .</b>	<b>4</b>
<b>1.3</b>	<b>Thesis outline . . . . .</b>	<b>6</b>
<b>1.4</b>	<b>Thesis publications . . . . .</b>	<b>7</b>

---

## 1.1 Context and motivation

Since the introduction of Artificial Intelligence (AI) in the world of clinical applications, advances of the neural architecture behind this technology has resolved many problems. The main key of AI is the ability to mimic the cognitive behavior of humans, which includes problem solving and learning. AI is exploited to address various kinds of resolving tasks, especially when it takes bio-signals as input. It can provide a very helpful hand for clinicians in the quotidian routine of checkup and diagnosis. Starting from simple tasks of making decisions based on a set of inputs to the more complex task of nonlinear signals analysis and the detection of emotional states, epileptic seizures and even tumor location detection.

Health-related Artificial Intelligence has attracted many researchers in the last decade. One of the advantages is that the developed applications serve more than one party. Benefits of remote monitoring, real-time diagnosis and detection and prediction systems were made available to the patients. Clinicians were offered numerous decision making and early diagnosis tools rendering their job easier and reducing the tedious time of reading and analysing information. AI have been also used for the rehabilitation of anxious patient in complement with

## Chapter 1. Introduction

---

the biofeedback. The patient is able to control his emotional state or his anxiety level to avoid an anxiety attack. New trends of therapeutic environments for patients rehabilitation with serious mental disorders, implement effective detection algorithms. Biofeedback systems can help children, adolescents and adults control and manage their levels of anxiety, and facilitate real life challenges. Anxiety is a mental health issue that has physical consequences on our bodies. However, it can affect the immune system, and unfortunately, there is evidence that too much anxiety can actually weaken the immune system dramatically [Felman, 2018]. Anxiety management is not one-size-fits-all, thus, the need to detect when anxiety is manifesting and how the body and neurological system react to such special emotional state is very essential. Anxiety detection is an underlying part of affective computing. It can also be an effective module in many frameworks, and can be adapted to early diagnosis of anxiety disorders, to digital marketing and even to serious games. This field is still immature, and related researches should involve biosignals in the affective computing more frequently.

Nowadays, and according to latest statistics [Scheffer et al., 2017], epilepsy affects 1% of the world population and come third place as the most common neurological disease after migraine and dementia.

The International League Against Epilepsy (ILAE) defined Epilepsy as a disorder of the brain characterized by an enduring predisposition to generate epileptic seizures, and also by the neurobiologic, cognitive, psychological, and social consequences of this condition [Scheffer et al., 2017]

Epileptic seizures are considered neurological dysfunctions manifested by an abnormal electrical activity of the brain. Sometimes seizures are accompanied with convulsions, but there are also silent seizures that do not manifest with external abnormal activity. These types of seizures require an EEG monitoring to be detected.

The occurrence of some seizures within dangerous conditions can be fatal and causes the famous SUDEP (Sudden Unexpected Death in Epilepsy). As healthy people die suddenly and unexpectedly, SUDEP concerns sudden death for epileptic patients. However, the risk is greater with epilepsy. It is very important that affected persons as well as their relatives be conscience and familiar with this fact to help reduce the risk of SUDEP.

Only a few epileptic seizures are fatal. There is danger when a seizure occurs in waters,

## Chapter 1. Introduction

---

when no one is nearby, whether during swimming or in the tub. Some seizures do not stop on their own and can become what is called status epilepticus or status epileptic, which sometimes results in death. SUDEP, drowning and status epilepticus contribute significantly to the slight statistical decline in the life expectancy of people with epilepsy compared to the general population.

The application of artificial intelligence in the field of medical monitoring can help avoid the cases of SUDEP by preventing an incoming seizure within a sufficient period of time and with high sensitivity and low false prediction rate.

Seizure prediction domain has attracted researchers in the last decade. Neuroscientists have investigated EEG, ECG biomarkers to define the triggers of seizure within a defined preictal period. Features engineering has also played a crucial role in analysing the characteristics of the different epileptic states. Thus, defining relevant biomarkers that contribute the most in distinguishing two or more states. Despite the advances made in the field of Health-related AI, many critical challenges and open questions pushing researchers to investigate more and more still exist. Brain activity analysis is the main and crucial step for neurological disorders diagnosis. It is also used to understand the behind-the-scenes of anxiety attacks [Quesney and Gloor, 1985]. Electroencephalogram EEG is the only way to record the electrical brain activity, through electrodes placed non-invasively on the scalp or during a brain surgery to measure intracranial discharges. EEG is the most used tool for epilepsy diagnosis and seizure monitoring. Extensive efforts in neuroscience and psychology were made. However, despite the high capability of intelligent approaches, especially deep learning based ones, the neuroscience community is still not entirely confident with this technology and avoids it due to the lack of explainability of these so-called 'black boxes'. So many questions are presented: What are the best approaches to simulate a person's anxiety in order to record EEG for an effective anxiety detection study? How can we develop adaptive anxiety detection systems that can address the variability between individuals and environment settings? How deep model can be explainable and give more relevant information to the neurologist? When Deep learning can effectively replace handcrafted features and how learned feature can be interpretable? Does computational models have the ability to detect the highest important temporal fragments for onsets prediction ? How the according results can be used effectively in the seizure prediction systems ? In this study,

we will explore some parts of these questions.

### 1.2 Thesis contributions

Electroencephalography (EEG) is considered as the first step in the diagnosis of epilepsy. It is also employed for anxiety disorders. In order to respect the clinical process of neurological disorders diagnosis, EEG recorders are considered as the single modality in this thesis. The three major contribution of this dissertation are based on the intelligent analysis of the brain activity aiming to concept a computational model for recognition, detection and prediction. Multi-channel EEG signals are gathered using neuro-headset or neuro-caps including a set of sensors. The recorded brain activity is used by real-time application in many fields.

In this thesis, we explore the theoretical basis, models, algorithms, and experimental validation of some models conceptualized for Health-related AI applications. The main contributions are as follows.

During our first contribution, a modernistic approach to anxiety stimulation following a face-to-face psychological incitement was presented. We constructed a dataset comprising EEG data that we gathered during the trial. We then presented insights in order to analyze acquired data demonstrating the efficiency of the pursued approach. The strategy showed success in inciting anxiety levels, which were then validated by HAM-A Test Scores, calculated before and after the test. A varied series of emotion recognition features based on EEG signals, in particular anxiety and stress, are reviewed and applied.

In the second contribution, an automated seizure classification system is proposed aiming to assist clinical professionals in diagnosing the disease, reducing time and potentially improves accuracy and reliability. We propose a novel Region-wise attention-based LSTM model and demonstrates the capability of the attention layer and the calculated weights related to the channels contribution enhancing the classification performances. As such, the model and results are more explainable showing correlations between neurological interpretation by an expert and the reading of the Heatmaps of deduced outputs of our model.

In the third contribution, we further enhance the feature learning by introducing the ConvLSTM neural Network to demonstrate its capabilities in learning spatio-temporal information.

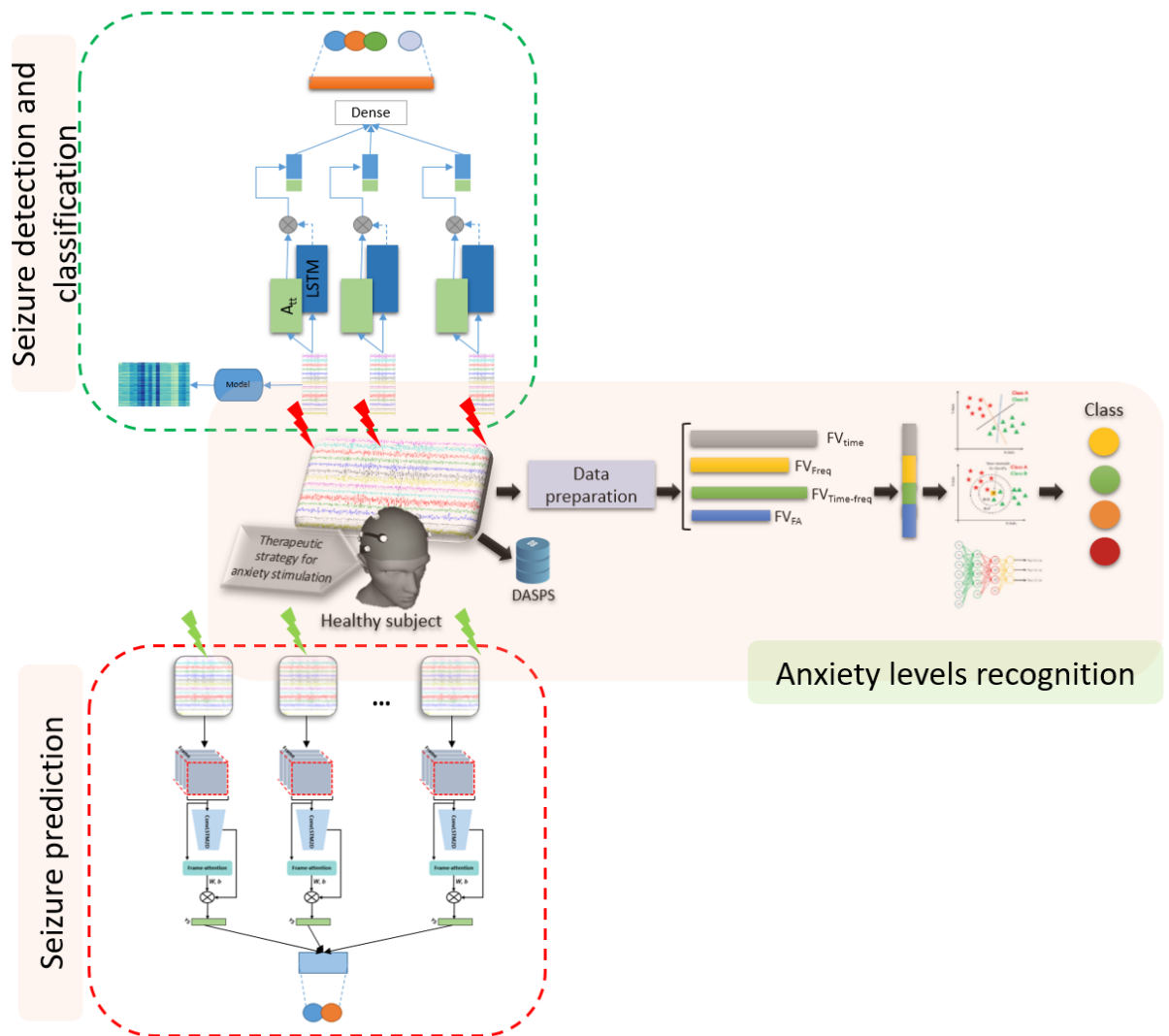


Figure 1.1: The three major methodologies considered in this thesis.

Also we have implemented a LSTM model for the learning of temporal dependencies in order to show the improvement achieved by the novel Spatio-temporal ConvLSTM model. The leading purpose of this contribution is designing deep learning models for patient-independent epileptic seizure prediction. Said models can be utilized in situations where subjects in the dataset have fewer classified examples (EEG recordings). We noticed that this is a common case in Intensive Care Unit monitoring scenarios where an acceptable number of samples cannot be obtained to train a prediction model.

### 1.3 Thesis outline

The three major contributions of this theses are presented in Figure 1.1. We followed the steps used in neuroscience for the automatic detection of brain disorders with the help of EEG in our investigations. The first step is collecting physiological data with the help of an EEG headset. The following step is preprocessing, which includes the data preparation for analysis, either by selecting the recording optimal portion to be analyzed or by applying a number of methods to improve the recorded data quality. The feature extraction step is then applied after preprocessing. At this stage, the data is modeled to extract relevant information. The said relevant information is labeled using features describing the EEG signals, which features are subsequently used for classification. Namely, in the feature selection process, which is also called dimensionality reduction, in the case a considerable number of features were extracted, the most dominant features for the classification step are usually selected. The final step is classification, which is carried out using supervised classifiers. In a number of instances, the feature selection step can be bypassed. In this instance, the extracted features performance is evaluated during the classification process. The arrangement of this document follows the same arrangement as the afore-mentioned typical steps. The arrangement of the present thesis can be summed up as follows:

- **Chapter Two:** In this chapter, EEG and Epilepsy are theoretically introduced in order to highlight the basics required to comprehend the study. Then a review of state of the art literature, and particularly recent studies related to the three main contributions are described. A review of the principals concepts is presented in this chapter. First we describe EEG, the investigated recording method. Then the essential points of anxiety and epilepsy are described. At the final part of this chapter, the main scientific reports that perform anxiety levels recognition and seizures prediction/detection using EEG are detailed.
- **Chapter Three:** A novel approach to anxiety stimulation following a face-to-face psychological incitement was presented in this chapter. We then presented insights in order to analyze acquired data demonstrating the efficiency of the pursued approach. We detailed the used set of emotion recognition features based on EEG signals, in particular

## Chapter 1. Introduction

---

anxiety and stress. Additionally, we examined which trial duration were most auspicious and which features were most efficient. This contribution yields the first public dataset of EEG data recorded using a portable device for anxiety detection.

- **Chapter Four:** This chapter presents the proposed novel Region-wise attention-based LSTM model and demonstrates the capability of the attention layer and the calculated weights related to the channels contribution enhancing the classification performances. This way, the model and results are more explainable showing correlations between neurological interpretation by an expert and the reading of the Heatmaps of deduced outputs of our model
- **Chapter Five:** The chapter begins with an explanation of the convolutional LSTM neural network. After which, a technical overview of the applied convolutions and the model setting is provided. Different architectures of the proposed novel spatio-temporal ConvLSTM model for epileptic seizure detection are detailed. Finally, the results of the model validation on a public dataset was discussed and a case of study was elaborated.

The thesis ends with a conclusion that provides a summary of our contributions, outlines the conclusions and the limitations of this research and also suggests several directions for future research.

## 1.4 Thesis publications

The proposed contributions through this thesis work led to four communications in international conferences, to one accepted journal paper, as follows:

- Paper in international journals
  1. [Baghdadi et al., 2020a] Baghdadi, A., Aribi, Y., Fourati, R., Halouani, N., Siarry, P. and Alimi, A. M. (2020). Psychological stimulation for anxious states detection based on EEG-related features. *Journal of Ambient Intelligence and Humanized Computing*. 2021 Aug;12(8):8519-33.
- Papers in proceedings of peer-reviewed international conferences

## Chapter 1. Introduction

---

1. [Baghdadi et al., 2020b] Baghdadi, A., Fourati, R., Aribi, Y., Siarry, P. and Alimi, A. M. (2020). Robust feature learning method for epileptic seizures prediction based on long-term EEG signals. In the International Joint Conference on Neural Networks (IJCNN) 2020 Jul 19 (pp. 1-7). IEEE.
2. [Baghdadi and Aribi, 2019] Baghdadi, A., Aribi, Y. (2019). Effectiveness of dominance for Anxiety Vs Anger detection. In the Fifth International Conference on Advances in Biomedical Engineering (ICABME), 2019 Oct 17 (pp. 1-4). IEEE.
3. [Baghdadi et al., 2017] Baghdadi, A., Aribi, Y. and Alimi, A. M. (2017). Efficient human stress detection system based on frontal alpha asymmetry. In International Conference on Neural Information Processing (ICONIP), Nov 14 (pp. 858-867). Springer
4. [Baghdadi et al., 2016] Baghdadi, A., Aribi, Y. and Alimi, A. M. (2016). A survey of methods and performances for eeg-based emotion recognition . Improved recurrent neural network architecture for SVM learning. In the International conference on hybrid intelligent systems (HIS), Nov 21 (pp. 164-174).

# Literature Review on Health-Related Artificial Intelligence Applications

---

## Contents

---

<b>2.1</b>	<b>Introduction</b>	<b>10</b>
<b>2.2</b>	<b>Health-Related Artificial Intelligence Applications</b>	<b>11</b>
2.2.1	Electroencephalography	11
2.2.1.1	EEG rhythms	12
2.2.1.2	10-20 system	14
2.2.1.3	EEG artifacts	14
2.2.2	Anxiety state	15
2.2.2.1	Anxiety state definition	15
2.2.2.2	Changes on EEG waves	15
2.2.3	Epilepsy disorder	16
2.2.3.1	Epilepsy definitions	17
2.2.3.2	Prediction vs detection of epileptic seizures	17
2.2.3.3	Seizures types	18
2.2.3.4	Seizures vs Artifacts	19
<b>2.3</b>	<b>Review of EEG-based approaches for anxiety detection</b>	<b>20</b>
2.3.1	Available benchmarks	20
2.3.2	Existing works on anxiety levels recognition	21
<b>2.4</b>	<b>Review on EEG-based approaches for epileptic seizures prediction</b>	<b>23</b>
2.4.1	Available benchmarks	23
2.4.1.1	Bonn dataset	23
2.4.1.2	CHB-MIT dataset	25
2.4.2	Existing works on epileptic seizures detection and prediction	25
<b>2.5</b>	<b>Review of EEG-based approaches for seizures types recognition</b>	<b>33</b>
2.5.1	Available benchmarks	33
2.5.1.1	NEDC TUH Seizure Corpus	33

## Chapter 2. Literature Review on Health-Related Artificial Intelligence Applications

---

2.5.1.2	EPILEPSIAE . . . . .	35
2.5.2	Existing works on seizures types recognition . . . . .	37
2.6	Conclusion . . . . .	38

---

### 2.1 Introduction

Health-related Artificial Intelligence marks an evolution in the healthcare systems. The ability of these applications to mimic the human processing for problem resolution gives them the strength to make approximate conclusions based solely on input data.

Such applications are expansively used for diagnosis and data analysis, thus supporting the decision of clinicians and experts.

Algorithms based on machine learning and deep learning are able to give very high precision for detecting abnormalities, classifying disorders, highlighting differences between multi-states, etc.

Meanwhile, these techniques are important despite presenting few drawbacks, among which, the huge amount of data needed, some of these techniques are black boxes and give few ways to interpret the obtained results and explain the high level of recognition that they offer.

From the claimed necessity for automatic recognition and analysis systems, another need appears aiming to improve the quality of life of people suffering from brain disorders, emotion disturbance like stress and state anxiety, and even epileptic patients. An important request is reported expressing the need of self-monitoring systems.

One of the most used tools for diagnosing multiple disorders is the electroencephalography. This tool provides the ability to reflect the inner state of a person, to present brain activity on several brain regions. It is the first exam to carry out for epileptic patients and have a high importance for dementia diagnosis.

Furthermore, many researches have demonstrated the high correlation between EEGs and anxiety types by identifying same relevant bio-marks.

In this chapter, we describe the background of Artificial Intelligence in Healthcare, related researches and available benchmarks for the research community. Section 2.2 introduces some preliminaries on Anxiety state, Epilepsy and Electroencephalography, which is the common

## **Chapter 2. Literature Review on Health-Related Artificial Intelligence Applications**

---

tool used in the automatic analysis of both brain disorders. Section 2.3 gives an overview of the research about EEG-based anxiety detection as well as epileptic seizure prediction, and seizures types recognition are given in Section 2.4 and 2.5 respectively. Finally, Section 2.6 concludes the chapter.

## **2.2 Health-Related Artificial Intelligence Applications**

### **2.2.1 Electroencephalography**

Hans Berger discovered EEG in 1924, and defined it as the recording of the electrical fields generated in the brain and emitted by a group of neurons oriented perpendicularly to the surface of the head [Kropotov, 2010]. The electrical activity needs approximately 106 neurons with the same orientation to make it observable on the scalp [Nunez and Srinivasan, 2006]. The EEG signals are present and can be recorded in non-natal brain (pre-birth) and will stay present until brain death. Since it was discovered, EEG has been one of the most used tools in diagnosing various neurological disorders. Compared to fMRI or PET, EEG is simpler and cheaper. However, EEG is a complex combination of rhythms, reflecting the activity simultaneously in different parts of the brain. The brain activity is in correlation with any human body activity performed, from muscular to cognitive tasks.

Early EEG-based studies were stuck with visual interpretation and handcrafted measurements due to the lack of technology thereof. Following the uprising of technology, it became possible to automatically analyse and investigate EEG recordings leading to intelligent systems for healthcare field.

Some of the reasons explaining the expansive use of EEG [Kropotov, 2010]:

1. No other neuroimaging technique can achieve the high temporal resolution produced by EEG. It provides a resolution of few milliseconds, while PET and fMRI are bound to a few seconds.
2. The knowledge of the mechanism that generates spontaneous EEG activity has risen.
3. fMRI and PET scans are atrociously more expensive than EEG recording systems.

## **Chapter 2. Literature Review on Health-Related Artificial Intelligence Applications**

---

4. A number of methods like Blind Source Separation (BSS) or time-frequency analysis (i.e. wavelet analysis) emerged for the EEG analysis.
5. EEG signals have been investigated using machine learning and Deep learning approaches and the obtained results are promising.
6. It can be used in many environment (e.g., walking, driving, sleeping, physical activity, meditation and also for marketing)

For these reasons, EEG is a helpful tool in clinical neuroscience. Particularly, the low cost extending its wide use. Consequently, several research centers and hospitals currently opt for EEG recording system that has been used in different neuroscience clinical applications.

### **2.2.1.1 EEG rhythms**

EEG rhythms vary depending on the subject task since EEG is remarkably sensitive of the subject's state. Nonetheless, five primary types of continuous rhythmic EEG activities are identified in the recordings. They are split into distinctive frequency bands. Said waves are originated in the brain, then amplified and displayed using a computer or other convenient equipment. It consists of a wave varying in time, resembling a sound or speech sign wave. Five EEG signal spectral sub-bands are largely of clinical interest: Delta (0 - 4 Hz), Theta (4 - 8 Hz), Alpha (8 - 16 Hz), Beta (16 - 32 Hz) and Gamma waves (>32 Hz). These EEG rhythms are described below.

- $\delta$  rhythms are the slowest compare to all existing rhythms. Yet, they demonstrate the highest amplitude of all these rhythms. Said rhythms are evident when the subject is sleeping. The higher value is produced when the subject is in deep sleep.
- $\theta$  rhythms are correlated with adolescence, childhood, young adulthood and drowsiness. They are also present during critical-thinking, e.g. mathematical problems. These rhythms are located in the prefrontal cortex.
- $\alpha$  rhythms are correlated with untroubled states. These were the first rhythms to be identified, since they are discernible in almost the entire world population. They appear

## Chapter 2. Literature Review on Health-Related Artificial Intelligence Applications

---

in different parts of the cortex, but are distinctly visible in the occipital part, with a higher amplitude compared to other rhythms [Sanei and Chambers, 2013]. Distinctive  $\alpha$  rhythms are originated in the human cortex:  $\mu$  rhythm,  $\alpha$  occipital rhythm and  $\alpha$  parietal rhythm [Sanei and Chambers, 2013].

- $\beta$  rhythms show low amplitude with multiple and changing frequencies, apparent at different parts in the cortex. They are generally correlated with anxious, busy or active thinking and active focusing states. Different types of  $\beta$  rhythms exist, such as  $\beta$  Rolandic rhythms and  $\beta$  frontal rhythms [Sanei and Chambers, 2013].
- $\gamma$  rhythms: Originally,  $\gamma$  rhythms were not studied, since outdated EEG recording systems were not able to record signals above 25 Hz. Prior to the use of digital recordings systems, these rhythms were undiscovered. One of the first articles illustrating these rhythms appeared in 1964.  $\gamma$  rhythms seem to appear in advanced mental activity, including fear, perception, consciousness and problem solving [Sanei and Chambers, 2013].

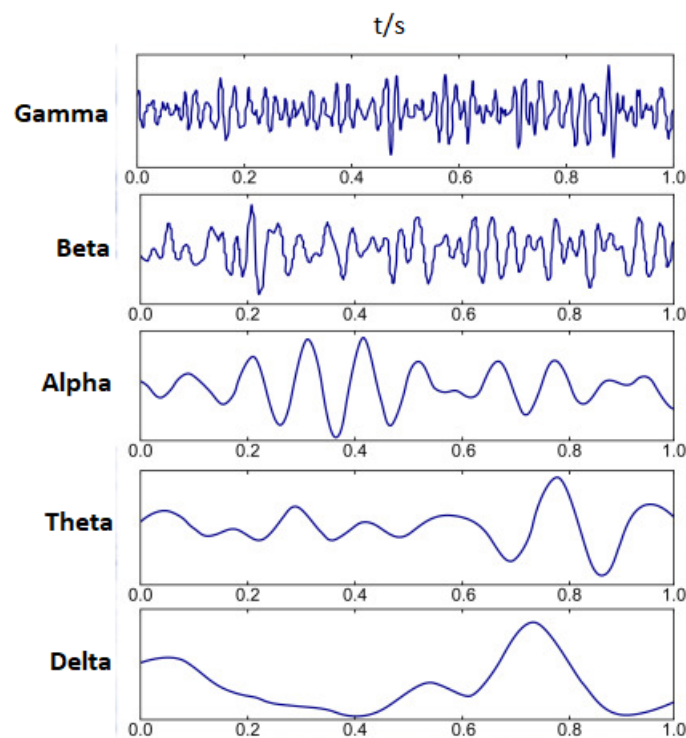


Figure 2.1: EEG rhythms (Gamma, Beta, Alpha, Theta, Delta)

## Chapter 2. Literature Review on Health-Related Artificial Intelligence Applications

### 2.2.1.2 10-20 system

The 10-20 system is one of various standardized electrode locations sets on the skull. Said system is used as a viewpoint to determine a convenient electrode placement in different tests. The skull sizes vary from a person to another, hence why this system utilizes distances as percentages taken from a couple of fixed points on the head.

The system is established based on the link between the electrode location and the underlying area of the cerebral cortex. The numbers "10" and "20" refer to notion that the actual distances between adjacent electrodes are either 10% or 20% of the total front–back or right–left distance of the skull.

To make this textual explanation a little less abstract, refer to Figure 2.2 for a visual representation.

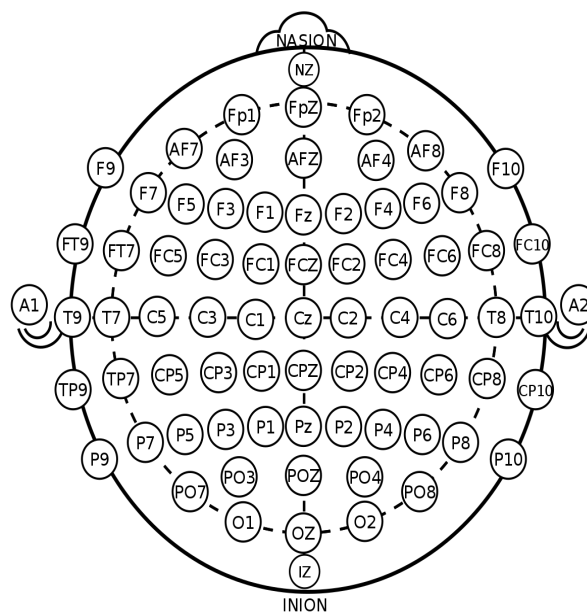


Figure 2.2: The international 10-20 system of electrodes placement

### 2.2.1.3 EEG artifacts

Different forms of artifacts can contaminate an EEG recording, having various types and sources. Artifacts can be internal or external. Internal artifact sources are due to the subject's physiological activities (e.g. ECG, EMG/muscle artifacts, EOG) and movement. External artifacts can be caused by environment-generated interference, recording equipment, electrode

## Chapter 2. Literature Review on Health-Related Artificial Intelligence Applications

pop-up and cable movement. Artifacts can contaminate several channels or just located in single channel. An example of artifact-contamination is illustrated in Figure 2.3.

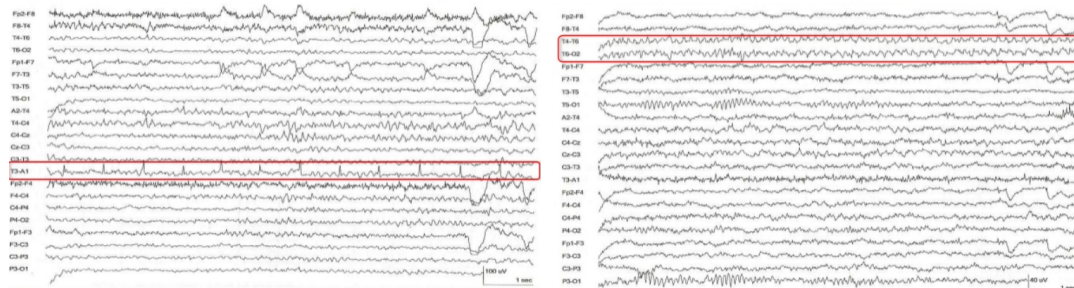


Figure 2.3: An example of artifact-contamination, Left: ECG is identified by its fixed period and morphology and is limited to T3-A1 channel, Right: The focal slowing in the T4-T6 and T6-O2 channels has no fields beyond T6 electrode and has the oscillation typical of rhythmic electrode movement

### 2.2.2 Anxiety state

#### 2.2.2.1 Anxiety state definition

“State anxiety” is defined as a temporary reaction to conflicting events. It is a deep, transitory intense emotional state, associated with a short-term increased affectionate nervous system activity, with no specific pathological conditions [Spielberger, 2013].

Webster’s College Dictionary, 4<sup>th</sup> edition (2000) defines anxiety as:

- A state of being uneasy, apprehensive or worried about what might happen; concern about a possible future event.
- Such an abnormal state, outlined by a feeling of powerlessness and inability to cope with overwhelming events (generally imaginary) along with physical tension, demonstrated by sweating, trembling, etc.

#### 2.2.2.2 Changes on EEG waves

EEG reflects the inner state of a person and it correlates with human tasks. Many researches proved the high correlation between EEG signals and the state anxiety. For instance, given a rather clear anxiety-related behavioral state, or considering one or more specific EEG/QEEG

## **Chapter 2. Literature Review on Health-Related Artificial Intelligence Applications**

---

pattern, attention to increasing posterior alpha power and/or decreasing beta power in frontal or temporal locations is a commonly reported method.

Brain researchers studying epilepsy, anxiety and other brain disorders turned to EEG spectral analysis measures for correlations within various disorders.

Costa et al. (1965), in a 72 first-year medical students study, found a notable negative correlation between alpha amplitude and scores on Welsh's "A" (anxiety) test.

The EEG demonstrated a lower alpha rhythm band frequency and amplitude during the insurance claim examination. This discovery appears to be similar in terms of EEG activity to an earlier study by Cohn (1946), in which he reported that anxiety related to particular life situations, presented an intermittent low magnitude alpha that would manifest itself within 20 seconds of the deep breathing initiation.

In various therapeutic approaches, the patients are asked to utilize the alpha feedback in order to bring themselves back to a high-percent-alpha-state, thus decreasing their anxiety.

It was largely understood that anxiety inhibited alpha.

### **2.2.3 Epilepsy disorder**

Epilepsy is a chronic disorder, characterized by unprovoked, recurrent seizures. A person is diagnosed with epilepsy if they go through two unprovoked seizures (or one unprovoked seizure with the probability of having more) that were the consequence of a medical condition like extremely low blood sugar or alcohol withdrawal.

The seizures may be linked to a family medical history or brain injury, but the cause is often completely unknown. The word "epilepsy" does not indicate anything about the cause of the person's seizures or their severity.

On a global scale, the incidence of the disease is about 50 to 100 cases per 100,000 population. Epilepsy is the fourth most common neurological disease after migraines, stroke, and Alzheimer's.

Worldwide, a quarter of all newly diagnosed cases of epilepsy are found in children.

Epilepsy is most commonly diagnosed below the age of 20 or above the age of 65, and the rate of new cases increases after the age of 55 when people are more likely to develop strokes, tumors, and Alzheimer's disease.

## Chapter 2. Literature Review on Health-Related Artificial Intelligence Applications

---

Seizures can cause a range of symptoms, from momentarily staring blankly to loss of awareness and uncontrollable twitching. Some seizures can be milder than others, but even minor seizures can be dangerous if they occur during activities like swimming or driving.

Overall, the average life span of an epileptic patient is slightly lower than that of the general population, mainly because of the risk of accidental death during a crisis (drowning, falling, accident) [Pellegrino, 2014]

### 2.2.3.1 Epilepsy definitions

Over the years, the definition and the classification of epilepsy were revised and updated following new discoveries and researches. The International League Against Epilepsy (ILAE) defined Epilepsy in 2005 as a brain disorder identified by an enduring predisposition to generate epileptic seizures, as well as the cognitive, neurobiologic, psychological and social consequences of this condition.

Epilepsy's definition requires the occurrence of at least one epileptic seizure [Fisher et al., 2014]. ILAE defined an epileptic seizure as a transient occurrence of signs and/or symptoms due to synchronous neuronal or abnormal excessive activity in the brain [Fisher et al., 2014]. In 2017, The ILAE presented a revised operational classification of seizure types [Fisher et al., 2017].

Table 2.1: EEG frequency bands signification for diseases causing mental disorders

Disease	Earlier age	Advanced age
Epilepsy	EEG in partial seizure may be normal, or show quite usually high amplitude and is localized or lateralized Abnormal rhythmic activity	Rhythmic activity have diffused. The EEG signature of absence epilepsy is the generalised 3 Hz spike-wave discharge EEG during a myclonic seizure typically shows a poly-spike and-slow-wave discharge

### 2.2.3.2 Prediction vs detection of epileptic seizures

The seizure detection main problem relies with its complexity because of the not-so clear definition of the seizures and spikes morphologies. Detecting seizures manually by an expert

## **Chapter 2. Literature Review on Health-Related Artificial Intelligence Applications**

---

is a tedious and time-consuming task, therefore, automatic detection methods can be of great assistance during long-term monitoring of epileptic EEG since they save a lot of time in the long recordings interpretation. Human validation remain essential for every developed method and system.

We can present two different problems: Seizure prediction and seizure detection systems. Prediction mean to anticipate the seizure few minutes before it occurs. These systems are trained using only the preictal and interictal data, ictal data containing the real seizure are discarded from the learning process.

In the first method, a preictal duration is pre-selected to classify EEG signals into preictal and interictal states and a binary classifier is trained to exploit differences between the two states.

The second method can be achieved using threshold-based methodologies where the analysis is focusing on identifying increasing and/or decreasing trends in the values over some features during the preictal state. An alarm is raised to declare an incoming seizure when the value of the examined feature exceeds the activation threshold. Recently Deep learning is applied for the seizure detection problem and demonstrated a high ability in classifying a segment into seizure or not seizure classes.

### **2.2.3.3 Seizures types**

In 2017, the International League Against Epilepsy [Scheffer et al., 2017] published a revised version of the official report of seizures classification. Adding a new group to the two primary ones, and applying a change based on three key features of seizures: where seizures begin in the brain, level of awareness during a seizure and other seizures features.

Seizure types are: focal, generalised and unknown onsets [Scheffer et al., 2017].

**Focal seizures** Focal or partial seizures originate in neuronal networks but are limited to part of one cerebral hemisphere.

Focal seizures account for about 60% of all epileptic seizures. They last one to two minutes and have milder symptoms that someone may be able to work through.

Symptoms:

- Motor, sensory, and even psychic abnormalities

## **Chapter 2. Literature Review on Health-Related Artificial Intelligence Applications**

---

- Sudden, inexplicable feelings of joy, anger, sadness, or nausea
- Automatism like repetitive blinking, twitching, smacking, chewing, swallowing
- Auras, or a sense of warning or awareness of an oncoming seizure

**Generalised seizures** Generalised seizures originate in bilateral distributed neuronal networks. They can start as focal, then become generalised. These seizures can cause a loss of consciousness, falling and severe muscle contractions. More than 30% of people with epilepsy experience generalised seizures.

They can be identified more specifically by these subcategories [Scheffer et al., 2017]:

- **Tonic.** This type is characterized by stiffening muscles primarily in the arms, legs, and back.
- **Clonic.** Clonic seizures involve repetitive jerking movements across both sides of the body.
- **Myoclonic.** In this type, jerking or twitching movements occur in the arms, legs, or upper body.
- **Atonic.** Atonic seizures involve a loss of muscle tone and definition, ultimately leading to falls or inability to hold the head up.
- **Tonic-clonic.** Tonic-clonic seizures are sometimes called grand mal seizures. They can include a combination of these varied symptoms.

**Unknown seizures** The origin of these seizures is unknown. They manifest by sudden extension or flexion of the extremities. Moreover, they can reoccur in clusters.

Up to 20% of people with epilepsy experience non-epileptic seizures (NES), which appear like epileptic seizures, but are not associated with the typical electrical discharge found in the brain.

### **2.2.3.4 Seizures vs Artifacts**

Artifact is present in virtually every EEG. It is an essential component for routine visual analysis, yet it may beguile the interpreter into falsely identifying waveforms that simulate

## **Chapter 2. Literature Review on Health-Related Artificial Intelligence Applications**

---

### Epileptiform Discharges (ED)

The principal importance of artifact is represented by the frequency of its occurrence in contrast to the limited frequency of normal variants that may imitate pathological ED.

Some types of artifacts can look like a seizure. For example, the tremor, which is a muscular artifact, have different characteristic movements and can appear suddenly and periodically.

Neurologists [Tatum, 2013] assume that the ability to distinguish artifacts from pathological ED requires a human element in order to provide the essential identification of an abnormal EEG.

On the other hand, researches in the field of seizures detection have showed greater results with a negligible false alarm rate, thanks to the methods and approaches robustness including artifacts removal techniques.

## **2.3 Review of EEG-based approaches for anxiety detection**

### **2.3.1 Available benchmarks**

Anxiety affects human capabilities and behavior as much as it affects productivity and quality of life. It is considered to be the main cause of depression and suicide. Anxious states are detectable by specialists by virtue of their acquired cognition and skills. There is a need for non-invasive reliable techniques to perform the complex task of anxiety detection. Several works [García-Martínez et al., 2017], [Arsalan et al., 2019], and [Zhang et al., 2020a] were proposed to recognize anxious states. There is no consensus about the elicitation of anxious states nor about the labels, making existing works very different and difficult to compare.

Recently, we released a new dataset known as "DASPS" for anxiety levels recognition [Baghdadi et al., 2020a] from a low-cost 14-channels portable EEG device (EMOTIV-EPOC, <https://www.emotiv.com/epoc/>). The EEG recordings were taken from 23 participants. DASPS is characterized by a therapeutic elicitation that triggers different levels of anxiety in participants by self-recalling stressful situations. To accord labels to two and four levels, Hamilton score was taken from a questionnaire filled before and after experiment.

In the same context, Arsalen *et al.* [Arsalan et al., 2019] carried out a psychological exper-

## **Chapter 2. Literature Review on Health-Related Artificial Intelligence Applications**

---

iment on 28 participants by recording EEG signals using a low-cost 4-channels portable EEG device (MUSE). Preparing oral presentation is used as stressful activity to trigger perceived mental stress. Three sessions were recorded: the pre-activity is when participants are in a resting position, activity is when they prepare the presentation and post-activity is for the public oral presentation. Arsalen *et al.* showed that only pre-activity EEG recordings are well correlated to two and three stress levels, respectively. In the classification task, only pre-activity EEG signals are considered.

Anxiety disorder is recognized through the Healthy Brain Network (HBN) dataset [Alexander et al., 2017] launched by the American Institute of Child Psychology and includes data collected from children and adolescents (ages 5 to 17) in New York City. HBN was proposed to diagnose and intervene in the mental health of minors. The dataset also contains eye movements and large EEG recordings.

### **2.3.2 Existing works on anxiety levels recognition**

Studies conducted for stress/anxiety detection based on EEG signals analysis are scarce in comparison to researches done for emotion recognition surveyed in [Baghdadi et al., 2016]. The majority of the proposed works for EEG-based emotion recognition in ([Fourati et al., 2017a]; [Fourati et al., 2020b]) were verified using DEAP dataset [Koelstra et al., 2012]. In their work, Giorgos *et al.* [Giannakakis et al., 2015] extracted two trials subdatasets from the DEAP dataset following predefined conditions for two emotional states: calm and stress. The main goal is to define the thresholds for arousal and valence, and to only extract trials that respect the aforementioned condition. Ergo, the previous step lead to a 18-subjects subset in conformity with the adequate norm. The authors extracted non-linear, temporal and spectral EEG features in order to represent the investigated states.

Alternatively, other researchers opted to conduct a relevant experimentation in order to collect their proper EEG signals. In the work of Vanita *et al.* [Vanitha and Krishnan, 2016], the authors studied the stress levels of students and designated their proper experimental protocol to collect EEG signals during a stress stimulation session. Consequently, data was pre-processed for noise and ocular artifact removal. The features were then extracted using time-frequency analysis and classification was performed by a hierarchical Support Vector Machines

## **Chapter 2. Literature Review on Health-Related Artificial Intelligence Applications**

---

producing an accuracy of 89.07%. In order to investigate the real-time issue, Lahane *et al.* [Prashant Lahane, 2016] proposed a stress detection system based on EEG. They utilized an android application for the purpose of collecting EEG data. As a feature, the Relative Energy Ratio (RER) was calculated for each frequency band.

Single channel EEG signal was collected from 25 students from the Sunway University for a Stress Detection System proposed by [Lim and Chia, 2015]. Utilizing the NeuroSky Mindwave headset, the data was recorded and stored for additional analysis. Students' stress was evoked for 60 seconds with the help of a Stroop color word test preceded by 30 seconds of one-screen instruction reading. Following an interview with the subjects who proclaimed that the instruction reading was the most demanding part of the experiment, it was deduced that solely the first 30 seconds of the collected data were preprocessed and processed for stress classification. The results reveal that k-NN, reaching 72%, outperforms LDA(60%) and ANN(44%) in stress classification.

Khosrowabadi *et al.* [Khosrowabadi et al., 2011], recognized that the examination period is the most demanding part for students. Consequently, they conducted their experiment during and after the examination period. For which, they collected EEG signals from 26 students (15 of which were during examination period and the remaining 11 two weeks after). The data was preprocessed for noise removal with an elliptic band-pass filter (2-32 Hz). Three different features were investigated in this work: Gaussian mixtures of EEG spectrogram, Higuchi's Fractal Dimension (HFD) and Magnitude Square Coherence Estimation (MSCE). Classification was carried out using k-NN and SVM classifiers. Thereby, MSCE gives the best accuracy with up to 90% in classifying chronic mental stress.

As demonstrated in Table 2.2, the majority of the previous works depended on audio-visual stimulus from the international IAPS, IADS databases [Oude, 2007]. Despite that, others followed the path of arithmetic tasks as shown in [Jun and Smitha, 2016], where the stress level is presumed to increase when the tasks hardness level increases. As of late, Arsalan *et al.* [Arsalan et al., 2019] utilized a public speaking test as a stress stimulus. The stress level was calculated using the Perceived Stress Scale PSS before and after public speaking. The muse headset was used to collect EEG signals and the gathered data was labeled following the collected PSS scores of each participant. Which presents a novel method for feature selection

## **Chapter 2. Literature Review on Health-Related Artificial Intelligence Applications**

---

established following the EEG frequency bands classification accuracy. Said work achieved an accuracy of 89.30% for the binary classification task. However, this accuracy degrades for the classification of three stress levels (60.91%).

Zhang *et al.* [Zhang et al., 2020a] selected 92 subjects (where 45 children are considered as anxious and 47 children as normal) to conduct experiments according to the Screen for Child Anxiety Related Disorders (SCARED) scale. Zhang *et al.* He extracted PSD features from Gamma band and transform them using a new proposed Group Sparse Canonical Correlation Analysis (GSCCA) to achieve 82.70% with SVM classifier.

## **2.4 Review on EEG-based approaches for epileptic seizures prediction**

### **2.4.1 Available benchmarks**

#### **2.4.1.1 Bonn dataset**

This dataset is freely shared by the University of Bonn <https://www.upf.edu/web/mdm-dtic/-/1st-test-dataset?inheritRedirect=true#.YV64AbhKhPY>. The EEG recordings in this database are divided into five sets (A-E). Each set consists of 100 segments of artifact-free single channel EEG recorded for 23.6 s durations. Sets A and B are scalp EEG recorded from five healthy volunteers where A is recorded with 'eyes open' and B is recorded with 'eyes closed' conditions. Sets C, D, and E consist of intracranial EEG (iEEG) recordings obtained for pre-surgical evaluation from five patients with temporal lobe epilepsy. Set D consists of EEG from the epileptogenic zone and set C from the hippocampal formation of the opposite hemisphere. EEG of both C and D are recorded in inter-ictal intervals. EEG in set E are recorded at seizure activities from all recording sites showing ictal activity. All the recordings are digitized and amplified using a 128 channel system with the average common reference method. The original sampling rate for all EEG in this dataset is 173.61 Hz.

Table 2.2: Previous works on EEG-based anxiety detection

Reference	Stimulus	#Participants	#Channels	Method	Affective states	Accuracy (%)
[Fourati et al., 2020b]	Audio-Visual	32	32	ESN with band power features	Stress and Calm	76.15
[García-Martínez et al., 2017]	Audio-Visual	32	32	SVM with Entropy features	Stress and Calm	81.31
[Katsigiannis and Ramzan, 2018]	Audio-Visual	23	14	PSD with SVM	Valence, Arousal and Dominance	62.49
[Giannakakis et al., 2015]	Audio-Visual	18	32	Asymmetry Index, Coherence, Brain Load Index and Spectral Centroid Frequency	Stress and Relax	
[Vanitha and Krishnan, 2016]	Mathematical tasks	6	14	Hilbert-Huang Transform with SVM	Neutral, Stress-low, Stress-medium and Stress-high	89.07
[Patil et al., 2017]	—	13	8	k-means clustering with stress indice	Stress and Relax	—
[Lim and Chia, 2015]	Stroop Word test	25	1	ANN, k-NN, LDA with DCT coefficient	Non-stressed and Stressed	72.00
[Khostrowabadi et al., 2011]	Examination period	26	8	k-NN and SVM with Higuchi FD, GM and MSCE	Stress and Stress-free	90.00

## Chapter 2. Literature Review on Health-Related Artificial Intelligence Applications

---

### 2.4.1.2 CHB-MIT dataset

The CHB-MIT scalp long-term EEG dataset [Shoeb, 2009] was recorded from pediatric patients (males with ages varying between 3 and 22 and females with ages varying between 3 and 19) with intractable seizures at Boston Children's Hospital. Table 2.3 presents the properties of seizure records (i.e., records with at least one seizure event) in this dataset. The total duration of the EEG data is 8756 min (146 h) within which the total duration of the seizure segments is only around 165 min (<3 h). So even with the seizure record selection, the seizure segments cover only 1.88% of the EEG dataset, presenting a highly imbalanced data distribution, which makes the classification highly challenging. The sampling frequency of all recorded signals was 256 Hz with 16-bit resolution and each frame is annotated whether it is seizure or non-seizure. International 10–20 system for electrode positioning was used. The 18 processed channels are: FP1–F7, F7–T7, T7–P7, P7–O1, FP1–F3, F3–C3, C3–P3, P3–O1, FP2–F4, F4–C4, C4–P4, P4–O2, FP2–F8, F8–T8, T8–P8, P8–O2, FZ–CZ and CZ–PZ. Each case (chb01, chb02, etc.) contains between 9 and 42 continuous .edf files from a single subject.

In all, these records include 198 seizures (182 in the original set of 23 cases); the beginning (I) and end (J) of each seizure is annotated in the .seizure annotation files that accompany each of the files listed in the file 'records-with-seizures'.

The files named chbnn-summary.txt contain information about the montage used for each recording, and the elapsed time in seconds from the beginning of each .edf file to the beginning and end of each seizure contained in it.

In order to manipulate data from the CHB-MIT database, we used the toolbox EEGLAB. EEGLAB is an interactive Matlab toolbox for processing continuous and event-related EEG, MEG and other electrophysiological data incorporating independent component analysis (ICA), time/frequency analysis, artifact rejection, event-related statistics, and several useful modes of visualization of the averaged and single-trial data.

### 2.4.2 Existing works on epileptic seizures detection and prediction

Many different approaches have been experimented in order to produce EEG features specific to seizure and perform well in capturing the majority of the latter. Seizure prediction has

## Chapter 2. Literature Review on Health-Related Artificial Intelligence Applications

Table 2.3: Details of all 24 cases included in the CHB-MIT database

Case	Gender	Age (years)	# of seizures	Seizure duration (mm:ss)	EEG duration (hh:mm)
1	F	11	7	07:20	40:30
2	M	11	3	02:52	35:00
3	F	14	7	06:42	38:00
4	M	22	4	06:18	156:00
5	F	7	5	09:18	39:00
6	F	105	10	02:33	66:30
7	F	14.5	3	05:25	67:00
8	M	3.5	5	15:19	20:00
9	F	10	4	04:35	68:00
10	M	3	7	07:27	50:00
11	F	12	3	13:26	35:00
12	F	2	27	17:36	21:00
13	F	3	12	08:55	33:00
14	F	9	8	02:49	26:00
15	M	16	20	26:55	40:00
16	F	7	10	01:24	19:00
17	F	12	3	04:53	21:00
18	F	18	6	05:17	35:30
19	F	19	3	03:56	30:00
20	F	6	8	03:49	27:30
21	F	13	4	03:19	33:00
22	F	9	3	03:24	26:30
23	F	6	7	05:30	26:30
24	-	-	16	08:31	21:00

been approached as a machine-learning problem. The main steps of this problem are: extracting relevant features corresponding to the pre-ictal state and designing an adequate classifier. In this section, we resume approaches used by most of the recent researches in the field of epileptic seizure detection and prediction.

Pre-treatment of EEG signals (suppression of noise and artifacts): According to M. K. Islam et al [Islam et al., 2016] the pre-treatment phase of EEG signals in the case of detection of seizures is very important and sensitive. Since 'Seizure' attacks are very similar in shape (amplitude, frequency, distribution) to artifacts (movement of the eyes, hands, external noises, etc.), it is imperative to differentiate between the crises and the artifacts in the pre-treatment phase in order to suppress artifacts and leave the crises. They proposed a wavelet-based system (SWT) and tested it on 3 different sets of data: real EEG signals from the CHB MIT database,

## **Chapter 2. Literature Review on Health-Related Artificial Intelligence Applications**

---

semi-synthesized data and fully synthesized data as shown in the following figure.

Bhattacharyya and Pachori [Bhattacharyya and Pachori, 2017] proposed a multivariate approach for patient specific EEG seizure detection. They employed a multivariate extension of the Empirical Wavelet Transform (EMD). The proposed architecture consists of selecting only 5 channels from the 23 ones of the CHB MIT database in order to reduce the computation cost. The channel with the least standard deviation was regarded as reference to calculate the Mutual Information of other channels. The four channels with the highest MI are selected with the reference channel. Then EMD was applied to the 5 selected channels and instantaneous amplitudes and frequencies were calculated for each MODE. The three features extracted are: Mean, Mean monotonic absolute AM and Variance monotonic absolute AM. Synthetic minority over-sampling technique (SMOTE) was used to resolve the problem of imbalanced data. In order to evaluate performances of the proposed system, authors used three classifiers : RF, linear Naive Bayes and K-NN. The proposed method has achieved maximum average sensitivity of 97.91% and maximum average specificity of 99.57% using RF classifier with five adaptively selected EEG channels.

Lasitha et al. both used Bonn and CHB MIT databases to evaluate their work aiming to detect seizure onsets based on Harmonic Wavelet Packet Transform (HWPT) and Fractal Dimension (FD). Energy features from HWPT and FD are extracted for all channels and epochs to construct the feature vector passed to a Relevance Vector Machine (RVM) to achieve classification. This work [Sharma and Pachori, 2017] presents a new approach for the detection of epileptic seizures based on the Fractal Dimension features extracted for each sub-band obtained after the application of Tunable-Q wavelet transform (TQWT) to obtain the tempo-frequency representation of the EEG signal. TQWT offers the possibility to adjust the Q factor differently to the DWT, which provides a low Q factor, whereas in oscillatory signal analysis, a high Q factor is recommended. 8 classification tasks were predefined by the authors (CT1: A vs E, CT2: B vs E, CT3: C vs E, CT4: D vs E, CT5: AB vs E, CT6: CD vs E, CT7: AB vs CD and CT8: ABCD vs E). TQWT is applied to each resulting CT at 17 sub-bands. Then FD is calculated for each sub-band obtained. Mean and STD of all FDs of each CT are subsequently passed to LS-SVM for the classification task. The authors compared the results obtained by their approach to several other approaches in the literature. An accuracy of 100% is obtained

## **Chapter 2. Literature Review on Health-Related Artificial Intelligence Applications**

---

for CTs 1, 2, 3 and 5, 99.5% for CT4, 99.67% for CT6, 98.5% for CT7 and 99.6% for CT8.

In this paper [Patidar and Panigrahi, 2017], the author proposed the combination of a TQWT and kraskov Entropy as a new method for detecting epileptic seizures using EEG signals from the Bonn database. The system performance in terms of accuracy, sensitivity, specificity and Matthew's correlation coefficient (MCC) are: 97.75%, 97.00%, 99.00% and 96.00% respectively for a window sized 1000. According to the analyzes elaborated in this research, the calculated values of the Entropy are higher for the segments with crisis and are identifiable even without classifier. This paper focuses on the effectiveness of using a single feature for detecting seizures, unlike other researches that investigates several types of features to improve performance.

In [Bhattacharyya et al., 2017], the authors analyze the complexity and non-linearity of electroencephalogram (EEG) signals by calculating a new multi-scale entropy measurement for the classification of normal and ictal EEGs. Q-based entropy (QEn) is calculated by decomposing the signal with the (TQWT) in number of sub-bands and cumulatively estimating the entropy of the K-nearest neighbors (K-NN) of various sub-bands. The optimal selection of Q and the redundancy (R) parameter of TQWT showed better robustness for the calculation. The extracted features are passed to the SVM classifier. The proposed method yielded 100% accuracy for classification of normal EEG signals (A and B) and epileptic seizures, 99.5% for the classification of EEG signals without seizure (C and D) and 98% for the classification of EEG signals without seizure (E).

In [Qiu et al., 2018], the authors presented a new method for automatic detection of seizures based on DSAE (Denoising Sparse AutoEncoder). DSAE is a deep neural network designed on SAE and DAE. The application of parsimony constraints allows the expression of the higher level of the EEG signal, which makes the distinction between normal and critical cases more obvious. The corruption operation adds noise to the input signal. The authors evaluated their method using Bonn database. They also classified 3 types of problems (2 classes, 3 classes and 5 classes) and reached 100% accuracy in the first 2 cases and 92% in the last 2 cases. Classification was done using logistic regression.

In [Samiee et al., 2015], the authors present a new tempo-frequency method for feature extraction. Discrete Short Time Fourier Transform (DSTFT), which is based on a set of rational

## **Chapter 2. Literature Review on Health-Related Artificial Intelligence Applications**

---

functions. The authors explain transformations applied to the simple STFT by a series of equations. They evaluated the impact of the system parameters. Each time they test a combination and see the results until they reach the optimal configuration they call "Optimal Pole". Based on this optimal pole, they compared the results obtained by their system and the other results obtained in the literature, certainly by referring to the same database "Bonn database". The characteristics extracted are: the absolute values of the 32 coefficients of DSTFT and 5 other statistical measures (absolute average value, absolute median value, absolute standard deviation, absolute maximum value, absolute minimum value of the coefficients). Different binary classifications were performed to evaluate the robustness of the proposed technique: (E vs A, E vs B, E vs C, E vs D, E vs A, C and E vs A, B, C, D) . As a classifier, the authors chose MLP (configuration:  $N + 5$  neurons in the first layer,  $N + 6/2$  in the hidden layer and 2 neurons in the output layer,  $N$  is the number of coefficients). The best precision obtained is 98.3% for a window sized 256 and 32 coefficients.

The work of [Yuan et al., 2018] presents a new approach to the detection of epileptic seizures based on the attentive representation of the different channels of an EEG signal. The authors assume that, in the field of epileptic seizure detection from multiple-channel signals, several channels are unimportant and do not give any information about the activities, but they add a lot of noise to the signal, thus generating degradation of the detection system's performance. Based on these facts, they proposed a multi-view deep learning model that can accurately detect the onset of epileptic seizures from multiple-path EEG signals. They introduced two attention mechanisms, taking into account the pathways, to dynamically calculate the scores of each channel and obtain a light selection of the channels.

A deep convolutional neural network is proposed by the authors in this paper. Comprised of 13 layers (5-convolutional layer, 5-max-pooling and 3-fully connected). The work of [Acharya et al., 2018] proposes the implementation of deep learning for the detection of normal, predictive and epileptic EEG signals (normal, interictal, ictal), without extraction or selection of characteristics. The system automatically learns and discovers the characteristics necessary for classification from input data processing through multiple layers. System performance is validated by the Bonn database, achieving 88.67% accuracy, 95.00% sensitivity and 90.00% specificity.

Antoniades et al. in their work [Antoniades et al., 2017] proposed a system to detect interic-

## **Chapter 2. Literature Review on Health-Related Artificial Intelligence Applications**

---

tal discharges from intracranial EEG signal. 18 subjects assessed for temporal lobe epilepsy at King's College Hospital, London were included in this study. 13 EEG traces were entirely recorded during wakefulness and the remaining included periods of slow wave sleep (Subjects S2, S9, S10, S13, S15). 32-channels telemetry system was employed during the recording under general anesthesia and data was digitized at 200Hz. 20 min of scalp EEG recording was used for each patient. Score attributed for each trial of 325ms can be 0-4. This action was performed by an expert epileptologist. Filters in each layer of the proposed CNN are used to capture the temporal information of the EEG, and this by combining each electrode signal with a 1-d filter and adding a bias term to generate the feature map. The output of the hidden layer of this CNN is passed to a logistic regression model to classify intracranial EEG features into non-IED, IED1, IED2 and IED3 classes. To resolve the problem of unbalanced data, authors employed the undersampling method for the non-IED class. Best accuracy obtained in this study is 89% achieved by the CNN multi-class approach.

Cerebral connectivity refers to a set of anatomical links ("anatomical connectivity"), statistical dependencies ("functional connectivity") or causal interactions ("effective connectivity") between distinct units of the nervous system. The units correspond to individual neurons, neuronal populations or anatomically separated brain regions. The connectivity model is formed by structural links such as synapses or fiber paths, or it represents statistical or causal relationships measured as cross-correlations, coherence, or information flows. Neuronal activity and, by extension, neuronal codes, are limited by connectivity. Brain connectivity is therefore crucial to elucidate the way neurons and neural networks process information.

Based on this fact, Wang et al. [Wang et al., 2018] asserts that brain connectivity during seizures is certainly different to that between seizures, making it possible to differentiate between 'crisis' and 'non-crisis' by estimating brain connectivity for each segment of the seizure. He therefore proposes to use Directed Transfer Function (DTF) to estimate cerebral connectivity. The DTF is a measure of the dynamic causal relationship in the frequency domain, which can be estimated by the MVAR model coefficients. Functional brain connectivity based on DTF can characterize the intensity and direction of the link between the different EEG channels. For each segment of the EEG signal, DTF is calculated for each pair of electrodes, resulting in a 19x19 matrix (since it used a 19-channels EEG headset). Each 19x1 line is considered a feature

## **Chapter 2. Literature Review on Health-Related Artificial Intelligence Applications**

---

vector.

A time-frequency analytic algorithm, denoted LMD for Local Mean Decomposition was applied to EEG signal in order to detect seizure activity in [Zhang and Chen, 2017]. LMD decomposes the EEG signal into several Product Functions (PFs). Maximal amplitude, minimal amplitude, average absolute value are three time-domain features. Maximum, skewness, kurtosis of PF's power spectral density are three frequency-domain features. Fractal Dimension, Renyi Entropy and Hurst Component are also extracted for the first five PFs. Features are passed to different types of classifiers: including back propagation neural network (BPNN), K-nearest neighbor (KNN), linear discriminant analysis (LDA), unoptimized support vector machine (SVM) and SVM optimized by genetic algorithm (GA-SVM). Authors performed five classification cases of the Bonn epilepsy dataset and presented obtained accuracy of all classifiers. Classification accuracy of the presented approach are equal to or higher than 98.10% in all the five cases. Based on the statistical analysis elaborated in this work, it is showed that Set E is easily distinguishable from other sets regarding the difference of the mean values of statistics features.

Different to other studies, Page et al. in [Page et al., 2015] proposed a flexible hardware system for feature extraction and classification with five seizure detection processors fully placed and routed on a Virtex-5 FPGA. Statistics features are extracted from raw EEG signals for each channel and for 1 second epoch with 50% overlapping. Authors compared all classifiers in term of latency, complexity, memory and energy. Logistic regression had the best average F1 score of 91% and occupies less resource and memory, and consumes less energy than the other classifiers processors .

The transition between the preictal and seizure is still not well understood by neuroscientists. The nature and specificity of epileptic seizures are patient dependent. Handcrafted characteristics show limitations for some patients compared to others. Cook showed that building a such predictive system is not impossible, and that the key instruction is the use of a long term EEG data recorded over years for some patients [Cook et al., 2013]. The proposed implantable system records continuous iEEG data for specific patient setting. Cook showed the feasibility of seizures prediction, his findings encourage researches for more clinical investigation and accentuate the need for new technologies to be tested for this issue. As the cook trial is based

## **Chapter 2. Literature Review on Health-Related Artificial Intelligence Applications**

---

on a predefined set of features, the system was not suitable for all patients, thus presenting its major limitation. The proposed system cannot generalise for all preictal patterns. This limitation makes researches deviate from the use of handcrafted predefined sets of features to a more generalised high level characteristics. The task is challenging with a high level of requirement that can only be handled by novel computational techniques. These days, many databases for continuous long-term EEG data are provided by clinical partners in order to help researchers validate their algorithms. The availability of big data has cemented the usefulness of deep learning for a diverse range of problems [LeCun et al., 2015]. The basis of deep learning models is to train deep network with a large amount of data in order to accomplish a task of classification. Nowadays, deep learning is expansively used in medical imaging, early diagnosis and prevention of neuro-degenerative disorders [Kiral-Kornek et al., 2018].

The availability of open access competitions for seizures prediction offered the possibility for developers to improve their algorithms and to demonstrate the capabilities of machine learning techniques.

Seizures prediction competitions have enabled the validation and comparison of algorithms performances using a common set of data.

Competitions started in 2007 in the International Workshop of Seizure Prediction IWSP3 <https://iwsp8.umn.edu/>, rendering long-term intracranial EEG data available for only three patients. Data was structured into training and testing sets, enabling the assessment of entered algorithms. Results for the first time competition does not exceed the above-chance rate of prediction.

In 2014, an international prediction competition (American Epilepsy Society Seizure Prediction Challenge) ran on a combination of short-term human EEG data and long-term dog EEG data. All provided data was intracranial EEG recorded over multiple days (>500 days in humans and >1,500 days in dogs) [Howbert et al., 2014][Brinkmann et al., 2016].

Sets provided to participants contained a 10 min segments of discontinuous data labelled into interictal and preictal classes. Furthermore, a set of unlabelled data was provided for testing the participant's system.

The second large-scale competition was in 2016, organized by the Melbourne University (Melbourne University AES/MathWorks/NIH Seizure Prediction) aiming to predict seizures in long-

term human intracranial EEG recordings. 1,139 seizures were recorded during a period of 1,326 days from three persons with intractable seizures.

In the both competitions, the evaluation of seizure prediction algorithms require the use of the Area Under Curve (AUC) metric. Similar performances were provided by both top-performing algorithms, producing an AUC value of 0.84 [Brinkmann et al., 2016] and 0.81 [Kuhlmann et al., 2018] respectively.

## **2.5 Review of EEG-based approaches for seizures types recognition**

### **2.5.1 Available benchmarks**

#### **2.5.1.1 NEDC TUH Seizure Corpus**

The full TUH EEG corpus is the world's largest publicly available corpus of clinical EEG data ([https://www.isip.piconepress.com/projects/tuh\\_eeg/html/downloads.shtml](https://www.isip.piconepress.com/projects/tuh_eeg/html/downloads.shtml)). The corpus contains 15,757 hours (56,726,510 secs) of EEG recordings from 13,539 patients. It represents the collective output from Temple University Hospital's Department of Neurology since 2002. EEG signals were recorded using several generations of Natus Medical Incorporated's Nicolet™ EEG recording technology. The raw signals obtained from the studies consist of recordings that vary between 20 and 128 channels sampled at 250 Hz minimum using a 16-bit A/D converter. The data is stored in a proprietary format that has been exported to EDF with the use of NicVue v5.71.4.2530. These EDF files contain a header with important metadata information distributed in 24 unique field that contain the patient's information and the signal's condition. There are additional fields that describe signal conditions, such as the signals maximum amplitude, which are stored for every channel.

The TUH EEG Seizure Corpus, which is a subset of the TUH corpus has been manually annotated and separated into training and test sets, as well as split up into sessions with and without seizures. The full training set contains 592 patients, 202 of which have seizures, for a total of 2370 seizures categorised into 9 types. The duration of all the seizures is 46.7 hours

Table 2.4: Previous works on EEG-based seizure prediction

Ref	Technique				Results			
	Features	Classifier	Dataset	#Patient	#Channel	Spec	Sen	Acc
[Wang et al., 2018]	Features extracted from the Direct transfer Function (DTF)	SVM	Private database	10	19	—	93.36	—
[Qiu et al., 2018]	—	DSE based on SAE ans DAE	Bonn	5	1	—	—	100
[Yuan et al., 2018]	—	Deep learning	CHB MIT	9	23	—	—	96.00
[Acharya et al., 2018]	CNN	Softmax	Bonn	5	1	90.00	95.00	88.67
[Zhang and Chen, 2017]	Temporel, static and non linear features extracted after LMD decomposition	—	Bonn	5	1	—	—	98.1
[Sharma and Pachori, 2017]	FD extracted after TQWT	LS-SVM	Bonn	5	—	—	—	100
[Patidar and Panigrahi, 2017]	Kraskov Entropy extracted after TQWT	LS-SVM	Bpnn	5	1	99.00	97.00	97.75
[Bhattacharyya et al., 2017]	Entropy extracted after TQWT	SVM	Bonn	5	1	—	—	100
[Mohammad et al., 2017]	WPE	K-NN	CHB MIT	9	23	—	—	97.60
[Zabihli et al., 2016]	—	—	CHB MIT	23	23	—	—	93.1
[Samiee et al., 2015]	N Coefficients of DSTFT and 5 statistic features	MLP	Bonn	5	1	—	98.8	98.3
[Supratak et al., 2014]	—	SAE	CHB MIT	6	—	—	—	100
[Kiranyaz et al., 2014]	Temporel, frequency ans tempo-frequency features	—	CHB MIT	21	18	—	—	89.1

## Chapter 2. Literature Review on Health-Related Artificial Intelligence Applications

---

Table 2.5: Summary of TUH dataset

Dataset Features	TUH	EPILEPSIAE
No. of patients	314	278
No. of seizure recordings	2012	2702
No. of seizure classes	8	4

(168,139.2295 secs) out of the full 752.3 hours (2,708,284 secs) of available EEG data. The test data is also large, with a total of 50 patients, 39 with seizures, 685 seizures (16.95hrs; 61,036.8393 secs) and 170.34 hours (613,232 secs) of data.

### 2.5.1.2 EPILEPSIAE

Long-term EEG recordings from 278 epilepsy patients (149 males (53.8%); age range, 2–67 years; mean age: 34.3 years) suffering from medically intractable partial epilepsy were analyzed. Data was recorded in three different epilepsy units in a total of almost 2,031 days (48,742 h) of EEG including 2,702 seizures. 68% of the patients had temporal lobe epilepsy. Concerning lateralization 42% present epilepsies in the left side of the brain, 41% in the right side, 8% in both sides (bilateral), and for 0.7% it was impossible to define a lateralization. In 227 patients, EEG was recorded using 22–37 scalp electrodes; the average recording period was 162 h. In 42 patients, intracranial EEG with 14–124 recording sites was recorded using stereotactically implanted depth electrodes, subdural grids and/or strips; the average recording period was 253 h. Nine “mixed” patients were subjected to both intracranial and scalp EEG recordings. In the mixed patients, the number of electrodes vary between 54 and 113, being the average recording time of 140 h. EEG data were recorded using Nicolet, Micromed, Compumedics, or Neurofile NT digital video EEG systems at sampling rates of 250 Hz, 256 Hz, 400 Hz, 512 Hz, 1024 Hz, 2048 Hz or 2500 Hz. In all the acquisition systems, data was recorded relative to a common electrical reference.

\*: Since the Epilepsiae is not an open access database, we do not have the exact number of samples for each class.

## Chapter 2. Literature Review on Health-Related Artificial Intelligence Applications

Dataset	Seizure Type	No. of seizures events	Total recording time (mins)
TUH	Focal Non-specific	992	1224
	Generalised Non-Specific	415	567
	Simple Partial	44	26
	Complex Partial	342	540
	Absence	99	14
	Tonic	67	21
	Tonic Clonic	502	80
	Myonic	3	22
	Total	2012	2494
EPILEPSIAE	Complex Partial	*	*
	Unclassified	*	*
	Simple Partial	*	*
	Secondarily Generalised	*	*
	Total	2702	*

Table 2.6: Previous works on EEG-based seizure types classification

Ref	Method	Dataset	Seizure types	Performance
[Asif et al., 2020]	Saliency-Encoded Spectrograms+ Ensemble CNN's	TUH	As above	F1: 95.00%
[Saputro et al., 2019]	Support Vector Machine	TUH	(3) focal non-specific, generalised non-specific, tonic-clonic	Accuracy: 91.4%
[Roy et al., 2019]	K-Nearest Neighbors	TUH	(7) focal non-specific, generalised non-specific, simple-partial, complex-partial, absence, tonic, tonic-clonic	F1: 90.10%
[Ahmedt-Aristizabal et al., 2019]	CNN	TUH	(8) focal non-specific, generalised non-specific, simple-partial, complex-partial, absence, tonic, tonic-clonic, myoclonic	Accuracy: 84.06%
[Sriram et al., 2019]	Neural Memory Network Hybrid Bilinear	TUH TUH Epilepsiae	As above As above unclassified, simple partial, complex partial, secondarily generalised	F1:94.50% F1:97.40% F1:97.00%

### 2.5.2 Existing works on seizures types recognition

Table 2.6 describes a benchmark of recent seizure classification approaches. In some cases, it is challenging to compare different approaches as each method is tested on a different dataset with differing number of seizure classes.

In the domain of deep learning based methods, the authors in [Asif et al., 2020] achieved an average F1-score of 98.4% on an ensemble of three DenseNet-based CNN's trained on the TUH dataset. This proposed architecture contains 45.94 million parameters, compared to 1.2 million parameters in the hybrid bilinear structure proposed in the study of [Liu et al., 2020]. This work also omitted myoclonic seizures from the classification task due to the low numbers of samples of myoclonic class in the TUH dataset.

Both [Ahmedt-Aristizabal et al., 2019] and [Sriraam et al., 2019] proposed solutions to the 8-class classification problem on the TUH dataset, achieving 84.06% and 94.05%. As can be seen from Table 2.6, the bilinear models proposed by [Liu et al., 2020] achieved better performance on the 8-class classification problem. Non-deep learning methods, including the KNN proposed by [Roy et al., 2019] and the Support Vector Machine proposed in [Saputro et al., 2019], demonstrate reasonable performance (90.7% and 91.4%) but were achieved through extensive feature engineering that is not desirable.

Often in seizure detection, models trained on a single patient perform better than general models trained on multiple patients data. This is partly because there is a large variation between human brains, and partly because there is not necessarily any correspondence between device channels across patients.

In [Cisotto et al., 2020], the author has discussed the difference between Machine Learning techniques and Deep Learning approach in distinguishing patients taking either anticonvulsant and those taking no medications; as well as between the two anticonvulsants. The techniques was validated on the TUH-Corpus database since it is the largest available dataset [Nahmias et al., 2020]. The comparison invoked in this paper shows that a small difference exists between the used ML techniques and Deep model in achieving a moderate accuracy rate for medication use detection and that Deep models are less time consuming than ML techniques.

### 2.6 Conclusion

Health-related applications are expansively used for diagnosis and data analysis, thus supporting the decision of clinicians and experts.

In this chapter, we detailed several concepts on the EEG-based systems for state anxiety and epilepsy recognition. We described the EEG signal specificities and we presented related definitions. Surveys of existing works on anxiety levels recognition, epileptic seizures prediction and seizures types classification were provided.

In the next chapter, a novel psychological stimulation experiment for anxiety levels recognition will be detailed. We will present the feature-based and the LSTM Autoencoder-based approaches that achieved both promising results for anxiety levels recognition. The second approach makes the system convenient for a real-time framework since it does not require neither feature extraction nor feature selection steps.

# EEG-based anxiety levels recognition using a psychological stimulation

---

## Contents

---

<b>3.1</b>	<b>Introduction</b>	<b>40</b>
<b>3.2</b>	<b>DASPS: a new database for anxiety levels detection based on a psychological stimulation</b>	<b>41</b>
3.2.1	Anxiety stimulation	41
3.2.2	Psychological evaluation	42
3.2.2.1	Self Assesement Manikin	43
3.2.2.2	Hamilton anxiety rating scale	44
3.2.3	Subjects	44
3.2.4	EEG recording	45
3.2.5	Experiment protocol	46
3.2.6	Data analysis	48
3.2.7	Artifacts removal	51
<b>3.3</b>	<b>Feature-based Machine Learning Approach for anxiety levels recognition</b>	<b>52</b>
3.3.1	Time Domain Features	53
3.3.1.1	Hjorth features	53
3.3.1.2	Fractal dimension	54
3.3.2	Frequency domain features	55
3.3.3	Time-frequency domain features	55
3.3.3.1	Hilbert-Huang spectrum	55
3.3.3.2	Band power and RMS using DWT	56
3.3.4	Other features	57
3.3.4.1	Quantitative features	57
3.3.4.2	Differential asymmetry	57
<b>3.4</b>	<b>Anxiety detection results and discussion</b>	<b>58</b>
3.4.1	SAM-based results	58

## Chapter 3. EEG-based anxiety levels recognition using a psychological stimulation

---

3.4.2	HAM-based improved results . . . . .	63
<b>3.5</b>	<b>A mobile application for anxiety level recognition based on deep LSTM model</b>	<b>66</b>
3.5.1	Broader impact and overview . . . . .	67
3.5.2	Evaluation of LSTM architectures . . . . .	68
3.5.3	Overview of the application . . . . .	69
<b>3.6</b>	<b>Conclusion . . . . .</b>	<b>71</b>

---

### 3.1 Introduction

Anxiety is a mental health issue that has physical consequences on our bodies. However, it can affect the immune system, and unfortunately, there is evidence that too much anxiety can actually weaken the immune system dramatically [Felman, 2018]. Anxiety is essentially a long term stress, in such a way the stress hormone is liberated by our bodies in huge quantities which correlates with body performance degradation. This invisible disability can greatly affect academic performance as well. Anxiety impacts memory capacities, leading to difficulties in learning and retraining information.

One in eight children suffers from anxiety disorders according to the Anxiety Disorders Association of America reports [ADAA, 2018]. Nevertheless, it presents a risk for poor performance, diminished learning and social/behavioral problems in school. Since anxiety disorders in children are difficult to identify, it is an imperative task to learn how to detect them in early stages in order to help them. It may manifest by signs such as increased inflexibility, overreactivity and emotional intensity.

Besides, effective anxiety and stress management can help balance stress in your life, while keeping high productivity and enjoying life. The intention is to find harmony between work, relationships and self-awareness, and to learn how to deal with anxiety states to confront challenges. But anxiety management is not one-size-fits-all, so we need to detect when anxiety is present, how it manifests in our bodies and how our neurological system reacts to such situations.

Anxiety detection is an underlying part of affect recognition. Another area that could significantly benefit from progress in affect recognition is the video game industry. New trends

## **Chapter 3. EEG-based anxiety levels recognition using a psychological stimulation**

---

of therapeutic environments for rehabilitation of patients with serious mental disorders, implement an affect detection algorithms. Biofeedback systems can help children, adolescent and adults control and manage their levels of anxiety, and facilitate real life challenges.

This chapter is organized into 4 sections. In section 2, we detail the implemented experimental protocol and the analysis of the collected data in terms of variability and coherence. The followed steps for data recording and preprocessing as well as the general architecture of the proposed system are also included. A variety of features are presented in Section 4. An analysis and discussion of the obtained results are carried out in section 5. Finally, the last section summarizes our chapter and outlines future work.

### **3.2 DASPS: a new database for anxiety levels detection based on a psychological stimulation**

Due to the lack of public benchmarks on anxiety levels recognition, we propose to design a new database characterized by the following advantages:

1. Elicitation of four anxiety levels based on real life situations.
2. Use of comfortable EEG headset which it is wireless and has dry electrodes.
3. Interaction with the psychotherapist ensures that the subject feels more comfortable in a safe place.

DASPS is available in IEEE Dataport <https://iee-dataport.org/open-access/dasps-database>. It contains edf files of the raw EEG signals collected from a 23 volunteers. Raw data and preprocessed data are stored under .mat format and also provided with the database.

#### **3.2.1 Anxiety stimulation**

Carrying out mental states related research, usually means it is necessary to provoke the desired response on the subject at the required moment. Before the experiment, we selected real

### Chapter 3. EEG-based anxiety levels recognition using a psychological stimulation

---

life situations to induce a stressed mental state. Actually, anxiety mainly arises due to three factors, namely external, internal and interpersonal. Table 3.1 shows anxiety categories and their stimuli from real life situations. To select the situations with the highest anxiety levels, a survey was carried out and broadcasted to all volunteers who wanted to participate in our experiment. In accordance with survey answers, we selected 6 situations where participants experienced the highest anxiety levels as portrayed hereinafter: Loss (68%), Family issues (64%), Financial issues (54%), Deadline (46%), Witnessing deadly accident (45%) and Mistreating (40%).

Table 3.1: Anxiety triggers categories and stimuli

Category	Stimuli
External	Witnessing a deadly accident Familial instability / Financial instability / Maltreatment / Abuse Deadlines / Insecurity / Routine
Interpersonal	Relationship with the supervisor / manager Lack of confidence towards spouse Being in an embarrassing situation
Internal	Fear of getting cheated on / Fear of losing someone close Fear of children's failure / Feeling guilty permanently Recalling a bad memory Health (Fear of getting sick and missing on an important event) Health (Fear of being diagnosed with a serious illness)

The experiment was performed in an isolated environment to avoid distracting noises and to guarantee a subject's full concentration. The anxiety stimulation is accomplished by face-to-face psychological elicitation performed in a professional manner by our psychotherapist.

#### 3.2.2 Psychological evaluation

As mentioned, the experiment lasts almost 6 minutes divided into 6 different situations. The first 30 seconds of each trial are considered and the 15 seconds of SAM are removed which results in 6 trials of 30 seconds per each participant. According to the experiment protocol, after each 30 seconds of stimulation the participant is asked to fill in the SAM survey to express

## **Chapter 3. EEG-based anxiety levels recognition using a psychological stimulation**

---

in terms of excitement (Arousal) and feeling (Valence) his emotions during the stimulation.

Data were labeled with respect to arousal and valence values to handle two classification problems which are "Anxious/ Normal" and "Normal/ Light/ Moderate/ Severe anxiety". We have applied a matlab script to label all trials based on thresholds. By applying the labeling algorithm, we get: 156 'Normal' trials, 90 'Severe' trials, 10 trials 'Moderate' and 20 'Light' trials.

In order to increase the number of samples per participant, we follow previous work [Zheng et al., 2017] by constructing two additional sub-datasets for 5 seconds and 1 second trials extracted as sample from the main EEG signal. After segmentation, we obtained more trials in each sub-dataset. The 5 seconds segmentation results: 468 'Normal', 270 'Severe', 30 'Moderate', and 60 'Light'. Sub-dataset of 1 second contains 2340 'Normal', 1350 'Severe', 150 'Moderate', and 300 'Light' trials.

The script for HAM-A-based labelling respects the basis of the test. Trials with a HAM-A score  $\leq 12$  are labeled as normal anxiety. If the score is between [12-20], the anxiety level is considered light. And it is moderate if the score is between [20-25]. Finally, for severe states, the score should be above 25.

### **3.2.2.1 Self Assesement Manikin**

In emotion-related studies the Self Assessment Manikin (SAM) [Bradley and Lang, 1994] is widely used. It consists of a picture-oriented questionnaire, shown in Figure 3.1, containing five images for each of the three affective dimensions: valence (ranging from unpleasant/ stressed to happy/ relaxed); perceived arousal (from uninterested/ bored to excited/ alert); and perceptions of dominance/control. The participants rate their experience on a scale, normally with 9 points. In most cases, only the valence and arousal scales are used, since the concept of dominance is harder to be understood and expressed. In our experiment, we collected SAM ratings for Valence and Arousal dimensions after each presented "situation", i. e. the stimuli.

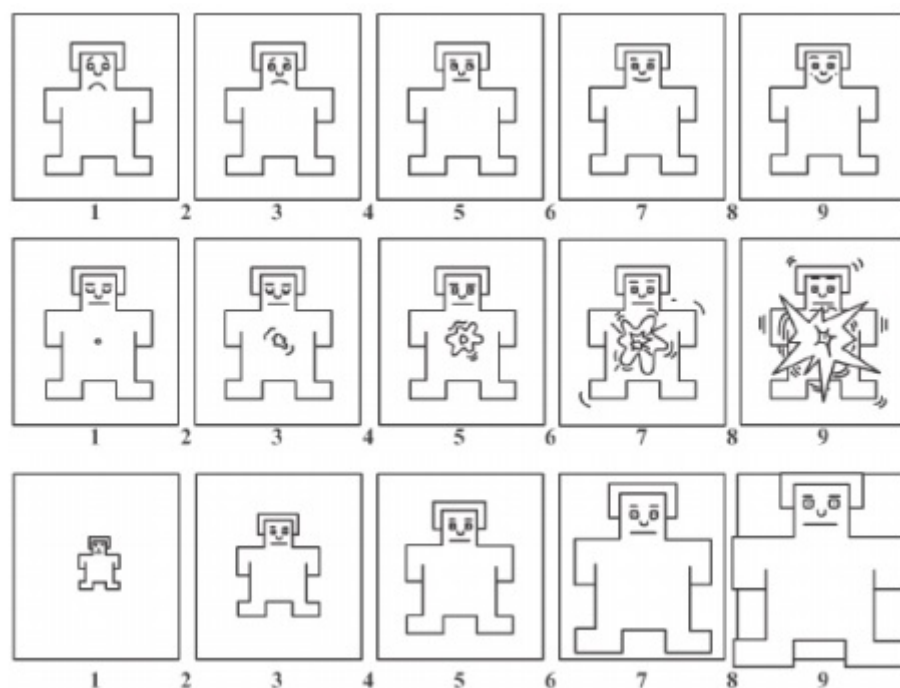


Figure 3.1: Self-Assessment Manikin (SAM) proposed by Bradley and Lang (1994). Self-evaluation scales for the dimensions of valence (top row), arousal (middle row), and dominance (bottom row) in a 9-point scale.

### 3.2.2.2 Hamilton anxiety rating scale

Hamilton Anxiety Rating Scale (HAM-A) is a multi-point survey that allows psychologists to take a complete view of the body metrics related to an anxious state as depicted in Figure 3.2. It provides 14 items, each one contains a number of symptoms that can be rated on a scale of zero to four in order to measure the severity of participants' anxiety. The HAM-A scores were calculated before and after the entire experiment, to assess the impact of the psychological stimulation. While, the SAM rating were used to measure the intensity of each situation.

### 3.2.3 Subjects

The experiment was performed on 23 healthy subjects who do not suffer from psychological diseases. 13 women and 10 men with an average age of 30 years old were selected. The experiment involves Tunisian subjects, therefore the Arabic language was used to communicate. The purpose was clearly explained to each participant before starting the experiment. Items of

## Chapter 3. EEG-based anxiety levels recognition using a psychological stimulation

### Hamilton Anxiety Rating Scale (HAM-A)

Below is a list of phrases that describe certain feeling that people have. Rate the patients by finding the answer which best describes the extent to which he/she has these conditions. Select one of the five responses for each of the fourteen questions.

0 = Not present,                      1 = Mild,                      2 = Moderate,                      3 = Severe,                      4 = Very severe.

<p><b>1 Anxious mood</b>                      <input type="checkbox"/> 0 <input type="checkbox"/> 1 <input type="checkbox"/> 2 <input type="checkbox"/> 3 <input type="checkbox"/> 4</p> <p>Worries, anticipation of the worst, fearful anticipation, irritability.</p>	<p><b>8 Somatic (sensory)</b>                      <input type="checkbox"/> 0 <input type="checkbox"/> 1 <input type="checkbox"/> 2 <input type="checkbox"/> 3 <input type="checkbox"/> 4</p> <p>Tinnitus, blurring of vision, hot and cold flushes, feelings of weakness, pricking sensation.</p>
<p><b>2 Tension</b>                      <input type="checkbox"/> 0 <input type="checkbox"/> 1 <input type="checkbox"/> 2 <input type="checkbox"/> 3 <input type="checkbox"/> 4</p> <p>Feelings of tension, fatigability, startle response, moved to tears easily, trembling, feelings of restlessness, inability to relax.</p>	<p><b>9 Cardiovascular symptoms</b>                      <input type="checkbox"/> 0 <input type="checkbox"/> 1 <input type="checkbox"/> 2 <input type="checkbox"/> 3 <input type="checkbox"/> 4</p> <p>Tachycardia, palpitations, pain in chest, throbbing of vessels, fainting feelings, missing beat.</p>
<p><b>3 Fears</b>                      <input type="checkbox"/> 0 <input type="checkbox"/> 1 <input type="checkbox"/> 2 <input type="checkbox"/> 3 <input type="checkbox"/> 4</p> <p>Of dark, of strangers, of being left alone, of animals, of traffic, of crowds.</p>	<p><b>10 Respiratory symptoms</b>                      <input type="checkbox"/> 0 <input type="checkbox"/> 1 <input type="checkbox"/> 2 <input type="checkbox"/> 3 <input type="checkbox"/> 4</p> <p>Pressure or constriction in chest, choking feelings, sighing, dyspnea.</p>
<p><b>4 Insomnia</b>                      <input type="checkbox"/> 0 <input type="checkbox"/> 1 <input type="checkbox"/> 2 <input type="checkbox"/> 3 <input type="checkbox"/> 4</p> <p>Difficulty in falling asleep, broken sleep, unsatisfying sleep and fatigue on waking, dreams, nightmares, night terrors.</p>	<p><b>11 Gastrointestinal symptoms</b>                      <input type="checkbox"/> 0 <input type="checkbox"/> 1 <input type="checkbox"/> 2 <input type="checkbox"/> 3 <input type="checkbox"/> 4</p> <p>Difficulty in swallowing, wind abdominal pain, burning sensations, abdominal fullness, nausea, vomiting, borborygmi, looseness of bowels, loss of weight, constipation.</p>
<p><b>5 Intellectual</b>                      <input type="checkbox"/> 0 <input type="checkbox"/> 1 <input type="checkbox"/> 2 <input type="checkbox"/> 3 <input type="checkbox"/> 4</p> <p>Difficulty in concentration, poor memory.</p>	<p><b>12 Genitourinary symptoms</b>                      <input type="checkbox"/> 0 <input type="checkbox"/> 1 <input type="checkbox"/> 2 <input type="checkbox"/> 3 <input type="checkbox"/> 4</p> <p>Frequency of micturition, urgency of micturition, amenorrhoea, menorrhagia, development of frigidity, premature ejaculation, loss of libido, impotence.</p>
<p><b>6 Depressed mood</b>                      <input type="checkbox"/> 0 <input type="checkbox"/> 1 <input type="checkbox"/> 2 <input type="checkbox"/> 3 <input type="checkbox"/> 4</p> <p>Loss of interest, lack of pleasure in hobbies, depression, early waking, diurnal swing.</p>	<p><b>13 Autonomic symptoms</b>                      <input type="checkbox"/> 0 <input type="checkbox"/> 1 <input type="checkbox"/> 2 <input type="checkbox"/> 3 <input type="checkbox"/> 4</p> <p>Dry mouth, flushing, pallor, tendency to sweat, giddiness, tension headache, raising of hair.</p>
<p><b>7 Somatic (muscular)</b>                      <input type="checkbox"/> 0 <input type="checkbox"/> 1 <input type="checkbox"/> 2 <input type="checkbox"/> 3 <input type="checkbox"/> 4</p> <p>Pains and aches, twitching, stiffness, myoclonic jerks, grinding of teeth, unsteady voice, increased muscular tone.</p>	<p><b>14 Behavior at interview</b>                      <input type="checkbox"/> 0 <input type="checkbox"/> 1 <input type="checkbox"/> 2 <input type="checkbox"/> 3 <input type="checkbox"/> 4</p> <p>Fidgeting, restlessness or pacing, tremor of hands, furrowed brow, strained face, sighing or rapid respiration, facial pallor, swallowing, etc.</p>

Figure 3.2: Hamilton anxiety rating scale (HAM-A) proposed by [Hamilton, 1959] [Maier et al., 1988]. 14 questions about feelings and thoughts during the last month in a 4-point scale.

the HAM-A questionnaire are highlighted to avoid misunderstanding each question.

### 3.2.4 EEG recording

EEG signals were recorded using a wireless EEG headset, the Emotiv EPOC with 14 channels and 2 mastoids [Ekanayake, 2010] were placed according to the international 10-20 system. The electrodes were attached to the scalp at position AF3, F7, F3, FC5, T7, P7, O1, O2,

### Chapter 3. EEG-based anxiety levels recognition using a psychological stimulation

---

P8, T8, FC6, F4, F8 and AF4. A picture of the electrodes placement and the Emotiv Epoc+ is shown in Figure 3.3.

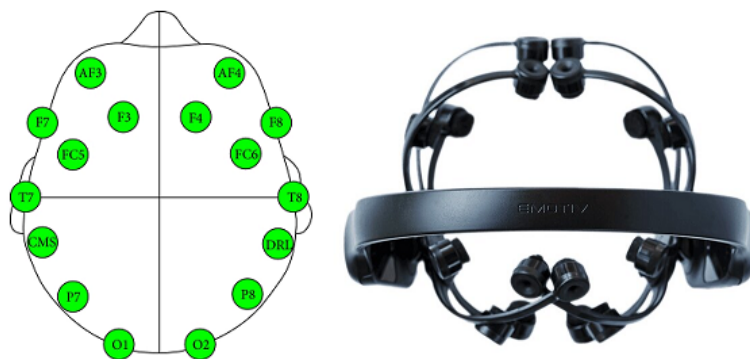


Figure 3.3: The Emotiv EPOC EEG headset with 14 channels

Emotiv Epoc neuro headset is used in this work owing to it's easiness of use. It offers comfort to users and mainly it is a wireless equipment and don't require an intricate set up like with clinical EEG material. In addition, it shows efficiency while used for emotion recognition systems like proved by [Jatupaiboon et al., 2013] [Anh et al., 2012] [Coan and Allen, 2003] and more recently by [Katsigiannis and Ramzan, 2018] [Benitez et al., 2016].

The recording was performed through Emotiv Epoc Software for EEG raw data recording. It allows us to view and save data for all channels or just customised the ones we need. The produced raw data have ".Edf" extension that is convertible using matlab script to ".mat" for further processing. The recording started before carrying out the first situation and ended after finishing the sixth one. The acquired EEG signals were processed at 128 Hz and impedance was kept as low as 7 k $\Omega$ .

#### 3.2.5 Experiment protocol

The experimental protocol was designed carefully with a psychotherapist, who recommended the use of exposure therapy. The latter is a form of the well known Cognitive Behavioral Therapy (CBT). Exposure therapy involves starting with items and situations that cause anxiety, but anxiety that you feel able to tolerate [Eraldi-Gackiere and Graziani, 2007]. There are different forms of exposure, such as Imaginal Exposure, virtual reality exposure, and in-vivo exposure. In the experimental protocol, we used the Flooding as in-vivo exposure therapy

### Chapter 3. EEG-based anxiety levels recognition using a psychological stimulation

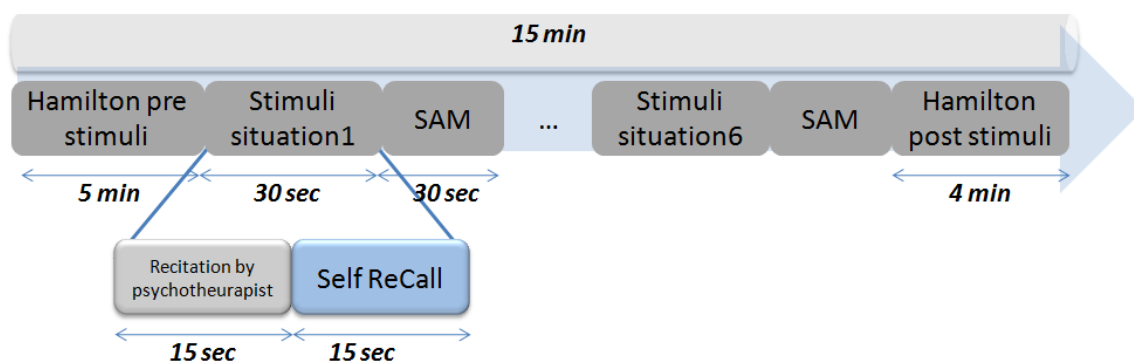


Figure 3.4: The experimental protocol of anxiety stimulation

[Eftekhari et al., 2006], actual exposure to the feared stimulus. The subject is confronted with a situation in which the stimulus that provoked the original trauma is present. Regarding the conditions of our experimentation, we used Flooding since it is quick and usually effective.

The fixed protocol is as depicted in Figure 3.4. Each participant is asked to sign a consent before starting the experiment. The anxiety level is calculated before stimulation according to the HAM-A score [Hamilton, 1959] [Maier et al., 1988] to examine the current state of the participant (some participants are already in a routine related anxious state, but their score increases after the experiment, while others start with a low level of anxiety and migrate to a severe level after the experiment). This tool provides 14 items, each one contains a number of symptoms that can be rated on a scale of zero to four. The HAM-A test, widely used for anxiety, allows the detection of the anxiety levels by the mean of its wide variety of items and can handle the variability of people's reactions. The psychic factor was represented by anxious mood, tension, fearfulness, insomnia, intellectual-cognitive function, depressed mood, and behavior-at-interview items, whereas the somatic factor consisted of the somatic-muscular, somatic-sensory, cardiovascular, respiratory, gastrointestinal, genitourinary, and autonomic items [Dr. Aaron T, 1991].

Our psychotherapist inquires the participant about the degree of severity of each symptom and its rate on the scale, with four being the most severe. This acquired data is used to compute an overarching score that indicates a person's anxiety severity. After that, the participant is prepared to start the experiment, with closed eyes and minimizing gesture and speech. The psychotherapist starts by reciting the first situation and helps the subject to imagine it. This

### **Chapter 3. EEG-based anxiety levels recognition using a psychological stimulation**

---

phase is divided into two stages: recitation by the psychotherapist for the first 15 sec and Recall by the subject for the last 15 sec.

When time is over, the subject open his eyes to rate how he felt during stimulation using SAM scales. Rating feeling using SAM is one of the most used evaluation technique in the field of affective computing. For instance, it is used in emotion recognition [Katsigiannis and Ramzan, 2018][Koelstra et al., 2012] [Shukla et al., 2019]), anxiety detection [Giannakakis et al., 2015] [Murdoch et al., 2019], and game assessment [Xie et al., 2020] [Hvass et al., 2017]. It has two rows for rating: Valence ranging from negative to positive and Arousal ranging from calm to excited. Each row contains nine items for rating. In order to evaluate the current emotion, each volunteer has to tick items that are suitable for emotion on only two dimensions (Arousal, valence). This trial is repeated until the sixth situation. At the end of the experiment, some items from HAM-A are re-evaluated by the psychotherapist to adjust the participant's anxiety level.

#### **3.2.6 Data analysis**

Before the processing phase, the data were evaluated to eliminate those with large difference between expected and real rating. Russell defines anxiety as [Russell, 1980] : Low Valence and High Arousal (LVHA). As a matter of fact, trials having this condition and belonging to LVHA quadrant are the main focus of our work as shown in Figure 3.5. To analyze data across all participants, we opt to measure the relative variability by computing the Coefficient of Variation (CV) for all participants' ratings for all stimuli situations. The mean CV between the participants' assessments was 0.58 for valence and 0.42 for arousal, which can be considered as low variability. Note that this value is higher than expected. In most cases, this variability is due to the lack of comprehension of SAM scales leading to no objective rating. The mean rating across all study participants for each stimuli case in terms of valence and arousal are shown in Table 3.2.

### Chapter 3. EEG-based anxiety levels recognition using a psychological stimulation

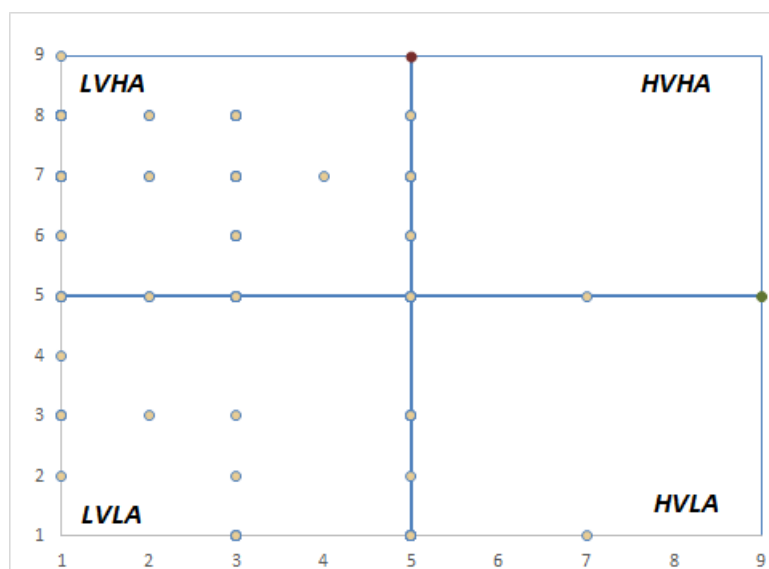


Figure 3.5: Presentation of participant rating in two-dimensional space

Table 3.2: Mean rating and Standard Deviation across all participants for each situation

Stimulus	Valence	Arousal
Situation 1	2.13 ± 1.68	6.13 ± 2.63
Situation 2	3.43 ± 1.44	5.13 ± 2.68
Situation 3	1.86 ± 1.25	6.04 ± 1.69
Situation 4	3.86 ± 1.79	4.30 ± 2.47
Situation 5	3.30 ± 1.63	5.95 ± 2.24
Situation 6	2.26 ± 1.54	6.30 ± 2.18
Mean CV	0.58	0.42

For each situation, the participant rating can be presented in 2D plan corresponding to the valence and arousal values. This plan can be divided into four quadrants according to the possible combinations of valence and arousal scales. The four quadrants as shown in Figure 3.5 are: Low Valence and Low Arousal (LVLA), High Valence and Low Arousal (HVLA), Low Valence and High Arousal (LVHA), and High Valence and High Arousal (HVHA). A summary of the subjective classification into the four Valence-Arousal quadrants from participants' ratings is presented in Table 3.3.

### Chapter 3. EEG-based anxiety levels recognition using a psychological stimulation

---

Table 3.3: Participants Number in each quadrant according to SAM ratings

Stimulus	LVLA	HVLA	LVHA	HVHA
Situation 1	7	0	16	0
Situation 2	12	0	11	0
Situation 3	9	0	14	0
Situation 4	14	0	7	0
Situation 5	8	0	15	0
Situation 6	7	0	16	0

As shown in Figure 3.5, samples are focused on LVHA and LVLA quadrants, which proves that the employed situations successfully worked in eliciting anxiety with most participants. HAM-A score was calculated before and after the EEG recordings. According to HAM-A score, it is possible to know the anxiety level of the participant. Table 3.4 presents the number of participants with their corresponding anxiety level based on Hamilton score before and after the experiment. It can be seen that the number of participants before the experiment with Normal, Light, and Moderate levels is decreased in favour of an increasing in the number of the participants after the experiment with Severe level from 7 to 13. This is another proof that anxiety elicitation in our experiment was successful.

Table 3.4: Participants number by anxiety levels according to Hamilton scores

Anxiety level	Normal	Light	Moderate	Severe
Before Experiment	4	6	6	7
After Experiment	2	5	3	13

Before processing the collected data, we elaborated a study on the correlation between each anxiety level and all EEG bands. Data were sorted by anxiety level resulting in 4 groups with variable number of samples N. The mean relative power per group was calculated and the EEG topographic maps were assembled in the Figure 3.6. The latter highlights the negative correlation between the anxiety and the right hemisphere. The alpha bands (Alpha1, Alpha2) are more present in the groups (G1: Normal, G2: Light), which are the closest from a calm state [Larson, 2019].

The Beta band spreads into all brain regions for G4: Severe. It is well known that Beat increases

## Chapter 3. EEG-based anxiety levels recognition using a psychological stimulation

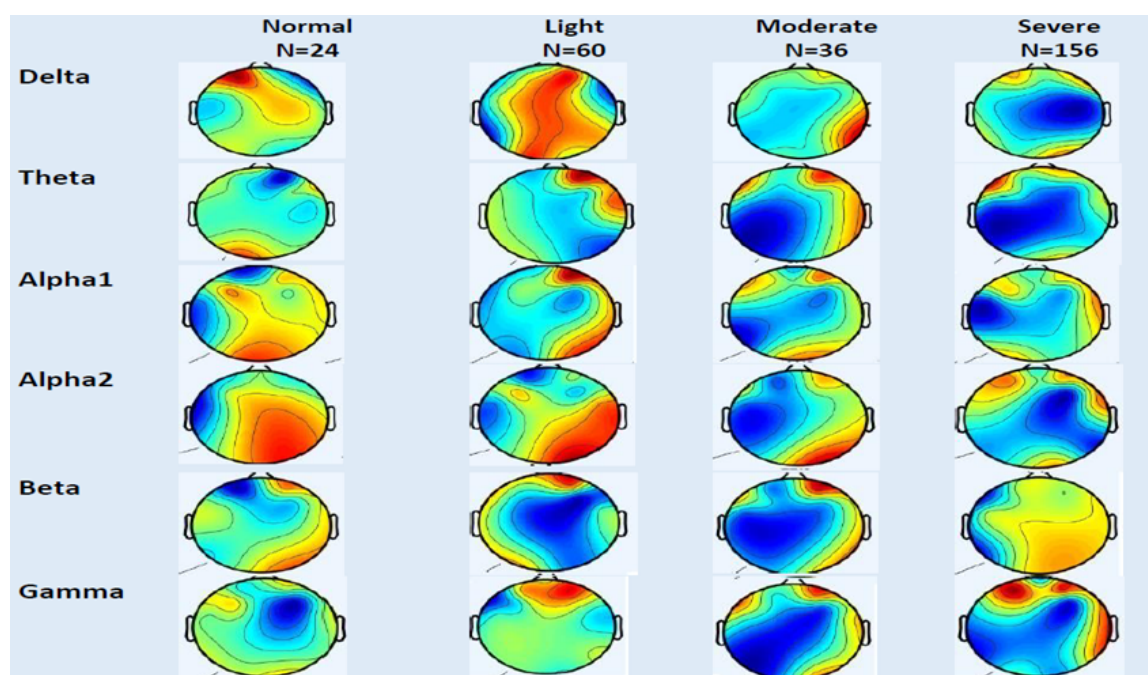


Figure 3.6: Head plots of the distribution of mean power per frequency band. The warmer colors indicate higher relative power (scaled from minimum to maximum values of the total group)

when the person is in a complex thinking state.

These findings validate the consistency of the collected EEG data.

### 3.2.7 Artifacts removal

In biomedical signal processing, the determination of noise and artifacts in the acquired signal is necessary to move to the feature extraction phase with a clean signal and achieve good classification results. Physiological artifacts are generated by a source different than the brain, such as electroculogram (EOG) artifacts under 4 Hz, muscle artifacts (EMG) with frequency exceeding 30 Hz, and heart rate (electrocardiogram: EMG) of about 1.2 Hz. They can also be extra physiological, unrelated to the human body and are in the 50 Hz range. This may be caused by the environment or related to EEG acquisition parameters [Oude, 2007] [McEvoy et al., 2015] .

For the aim of denoising our set of signals, we have applied an EEGLab script serving to cut relevant sub-band of EEG signals, removing baseline and removing Ocular and Muscular artifacts. A 4-45 Hz Finite impulse response (FIR) pass-band filter was applied to the raw data.

## **Chapter 3. EEG-based anxiety levels recognition using a psychological stimulation**

---

The Automatic Artifact Removal (AAR) in EEGLAB toolbox [Delorme and Makeig, 2004] was used to remove EOG and EMG artifacts. This toolbox implements several algorithms for EMG and EOG artifacts removal. We used the implementation of BSSCCA Canonical Correlation Analysis (CCA) which projects the observed EEG data into maximally auto-correlated components [De Clercq et al., 2006]. We chose the criterion `emg_psd` that considers the components whose average power ratio in the typical EEG and EMG bands is below certain threshold to be EMG-related. In order to estimate the power in the EEG and EMG bands, the default estimator used is a Hamming-windowed Welch periodogram with segment length equal to the analysis window length.

By default, the toolbox uses a combination of `iWASOBI` which is an asymptotically optimal Blind Source Separation (BSS) algorithm for autoregressive (AR) sources [Tichavský et al., 2006], and the criterion `eog_fd` to automatically correct EOG artifacts in the EEG. `Eog_fd` marks as artifactual the components with smaller fractal dimension. Conceptually, components with low fractal dimensions are those that are composed of few low-frequency components [Gómez-Herrero et al., 2006]. This is often the case of ocular activity and therefore it is a suitable criteria for detecting ocular (EOG) components.

### **3.3 Feature-based Machine Learning Approach for anxiety levels recognition**

This work covers all stages needed to create a robust EEG-based anxiety detection system, starting from the elaboration of an anxiety stimulation experimental protocol to the classification of anxiety levels. The general architecture of the proposed system is depicted in Figure 3.7. Generally, we can classify EEG features into three main classes according to the domain, namely, time-domain features, frequency-domain features and time-frequency-domain features. Other features can be extracted from a combination of electrodes, we mention one of them in this section.

## Chapter 3. EEG-based anxiety levels recognition using a psychological stimulation

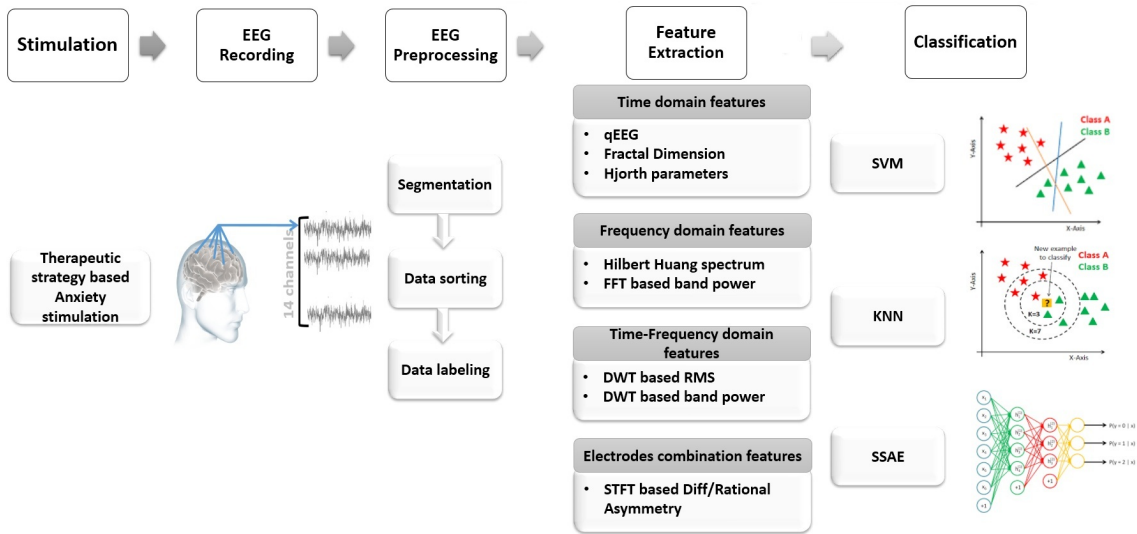


Figure 3.7: Architecture of the proposed system for anxiety levels detection

### 3.3.1 Time Domain Features

Time-domain features are results of an exploration of signal characteristics that differ between emotional states. Many approaches were employed in the researches to extract this type of features. In our work, we have extracted Hjorth features and FD features:

#### 3.3.1.1 Hjorth features

Hjorth parameters [Hjorth, 1970] are: Activity, Mobility, and Complexity. The variance of a time series represents the activity parameter. The mobility parameter is represented by the mean frequency, or the standard deviation proportion of the power spectrum. Finally The complexity parameter represents the variation in frequency. Besides, it indicates the deviation of the slope.

Assume that  $dx_i = x_{i+1} - x_i, (i = 1, \dots, n - 1), ddx = dx_{i+1} - d_i, (i = 1, \dots, n - 1)$ .

The expressions of Hjorth parameters are:

$$Activity = \frac{1}{n} \sum_{i=1}^n x_i^2 \quad (3.1)$$

### Chapter 3. EEG-based anxiety levels recognition using a psychological stimulation

---

$$Mobility = \frac{\frac{1}{n-1} \sum_{i=1}^{n-1} dx_i^2}{\frac{1}{n} \sum_{i=1}^n x_i^2} \quad (3.2)$$

$$Complexity = \sqrt{\frac{\frac{1}{n-2} \sum_{i=1}^{n-2} ddx_i^2}{\frac{1}{n-1} \sum_{i=1}^{n-1} dx_i^2} - \frac{\frac{1}{n-1} \sum_{i=1}^{n-1} dx_i^2}{\frac{1}{n} \sum_{i=1}^n x_i^2}} \quad (3.3)$$

Hjorth were used in many EEG studies such as in [Hjorth, 1970] [Horlings et al., 2008]. In our work, we calculated Hjorth parameters for all EEG channels, that produce a size Feature Vector of 42x1 for each trial.

#### 3.3.1.2 Fractal dimension

The Higuchi algorithm calculates fractal dimension value of time-series data.  $X(1), X(2), \dots, X(N)$  is a finite set of time series samples. Then, the newly constructed time series is defined as follows:

$$X_k^m : X(m), X(m+k), \dots, X\left(m + \left\lceil \frac{N-m}{k} \right\rceil .k\right) \quad (3.4)$$

(  $m=1,2,\dots,k$  )

where  $m$  is the initial time and  $k$  is the interval time.  $k$  sets of  $L_m(k)$  are calculated as follows:

$$L_m(k) = \frac{\left\{ \left( \sum_{i=1}^{\left\lceil \frac{N-m}{k} \right\rceil} |X(m+ik) - X(m+(i-1).k)| \right) \frac{N-1}{\left\lceil \frac{N-m}{k} \right\rceil .k} \right\}}{k} \quad (3.5)$$

where  $L(k)$  denotes the average value of  $L_m(k)$ , and a relationship exists as follows:

$$\langle L(k) \rangle \propto k^{-D} \quad (3.6)$$

Then, the fractal dimension can be obtained by logarithmic plotting between different  $k$  and its associated  $L(k)$ .

### 3.3.2 Frequency domain features

**Band Power** Power bands features are the most popular features in the context of EEG-based emotion recognition. The definition of EEG frequency bands differs slightly between studies. Commonly, they are defined as following:  $\delta$  (1-4 Hz),  $\theta$  (4-8 Hz),  $\alpha$  (8-13 Hz),  $\beta$  (13-32 Hz) and  $\Gamma$  (32-64 Hz).

The decomposition of the overall power in the EEG signal into individual bands is commonly achieved through Fourier transforms and related methods for spectral analysis as stated in [Jenke et al., 2014]. Otherwise, short-time fourier transform (STFT) is the most commonly used alternatives, or the estimation of power spectra density (PSD) using Welch's method [Koelstra et al., 2012]. We use the STFT with a Hamming window of 1s with no overlapping.

### 3.3.3 Time-frequency domain features

#### 3.3.3.1 Hilbert-Huang spectrum

The Empirical Mode Decomposition (EMD) along with the Hilbert-Huang Spectrum (HHS) are considered as a new way to extract necessary information from EEG signal since it defines amplitude and instantaneous frequency for each sample [Panoulas et al., 2008]. EMD decomposes the EEG signal into a set of Intrinsic Mode Function (IMF) through an automatic shifting process. Each IMF represents different frequency components of original signals. EMD acts as an adaptive high-pass filter. It shifts out the fastest changing component first and as the level of IMF increases, the oscillation of the latter becomes smoother. Each component is band-limited, which can reflect the characteristic of instantaneous frequency [Zhuang et al., 2017].  $x(t)$  is then represented as a sum of IMFs and the residual.

$$x(t) = \sum_{i=1}^K c_i(t) + r_K(t) \quad (3.7)$$

where  $C_i(t)$  indicate the  $i^{\text{th}}$  extracted Empirical Mode,  $r_K(t)$  indicate the residual, and  $K$  is the total number of IMFs.

In this work, we computed HHS for each signal using the EMD to obtain a set of IMFs representing the original signal. Extracted features are Hilbert Spectrum (HS) and instantaneous

### Chapter 3. EEG-based anxiety levels recognition using a psychological stimulation

---

energy density (IED) level. The decomposition into IMFs resulted in 10 IMFs per each channel.

#### 3.3.3.2 Band power and RMS using DWT

Discrete wavelet transform (DWT) is a technique of signal processing, that proceeds by the decomposition of the signal into different levels of approximation and detail corresponding to different frequency bands. It also keeps the temporal information of the signal. Compromise is done by downsampling the signal for each level.

Correspondence of frequency bands and wavelet decomposition levels depends on the sampling frequency. In our case, the correspondent decomposition is given in the last column of Table 3.5 for  $f_s=128$  Hz.

Table 3.5: EEG signal frequency bands and decomposition levels at  $f_s=128$  Hz

Bandwidth (Hz)	Frequency Band	Decomposition Level
1-4 Hz	Delta $\delta$	A4
4-8 Hz	Theta $\theta$	D4
8-13 Hz	Alpha $\alpha$	D3 (8-16 Hz)
13-32 Hz	Beta $\beta$	D2 (16-32 Hz)
32-64 Hz	Gamma $\Gamma$	D1 (32-64 Hz)

In our approach, in addition to the Band Power, the statistical feature Root Mean Square (RMS) derived from a wavelet decomposition with the function 'db5' for 4 levels, is extracted for each frequency band.

$$RMS(j) = \sqrt{\frac{\sum_{i=1}^j \sum_{n_i} D_i(n)^2}{\sum_{i=1}^j n_i}} \quad (3.8)$$

where  $D_i$  are the detail coefficients,  $n_i$  the number of  $D_i$  at the  $i$ 'th decomposition level, and  $j$  denotes the number of levels [Murugappan et al., 2010].

### 3.3.4 Other features

#### 3.3.4.1 Quantitative features

In addition to the aforementioned features, we adopted the set of features used in [Toole and Boylan, 2017], which include a variation of commonly used EEG features. However, for some features we use all channels and bands unlike in [Toole and Boylan, 2017] in which, a reduction of features was applied by averaging outputs. Details of the feature set are depicted in the Table 3.6.

The column FB indicate if features are generated for each frequency band or not.

A feature vector resulting from this step containing a fusion of all qEEG features, constructed for ulterior classification.

Table 3.6: EEG quantitative features

<b>Feature Description</b>	<b>FB</b>
Absolute and relative(normalised to total spectral power) spectral power	Yes
Spectral entropy: Wiener (measure of spectral flatness)	Yes
Difference between consecutive short-time spectral estimates	Yes
Cut-off frequency: 95% of spectral power contained between 0.5 and fc Hz	No
Amplitude: Time-domain signal: total power and standard deviation	Yes
Amplitude: Skewness and of time-domain signal	Yes
Amplitude: Envelope mean value and standard deviation (SD)	Yes
Connectivity: Brain Symmetry Index	Yes
Connectivity: Correlation between envelopes of hemisphere-paired channels	Yes
Connectivity: lag of maximum correlation coefficient between hemisphere-paired channels	Yes
Connectivity: coherence: mean, maximum and frequency of maximum values	Yes
Range EEG: mean, median, standard deviation and coefficient of deviation	Yes
Range EEG: measure of skew about median	Yes
Range EEG: lower margin (5th percentile) and upper margin (95th percentile)	Yes
Range EEG: upper margin - lower margin	Yes

#### 3.3.4.2 Differential asymmetry

Frontal asymmetry (the relative difference in power between two signals in different hemispheres) has been suggested as biomarker for anxiety [Demerdzieva and Pop-Jordanova, 2015]. Due to the inverse relationship between alpha power and cortical activity, decreased alpha power reflects increased anxiety [Demerdzieva and Pop-Jordanova, 2015].

## Chapter 3. EEG-based anxiety levels recognition using a psychological stimulation

---

Frontal asymmetry within the alpha band can be inversely related to stress/anxiety. The feature was calculated using alpha band power. The natural logarithm of left side channels were subtracted from the right ones (L-R).

$$AsymmetryIndex = \ln(\alpha) \Big|_{LChannel} - \ln(\alpha) \Big|_{RChannel} \quad (3.9)$$

To calculate the asymmetry index, the continuous signal must be broken into small parts. Scientific studies recommend overlapping epochs with each limited to a duration of 1-2 seconds [Zheng et al., 2017].

### 3.4 Anxiety detection results and discussion

#### 3.4.1 SAM-based results

The main aim of the current work is to provide a new database for EEG-based anxiety detection. Therefore, to validate the proposed methodology three experiments basing on trial duration were conducted. As a preliminary step, data were labeled by applying an algorithm based on arousal and valence values to handle two classification problems which are anxiety two levels detection and anxiety four levels detection. The number of trials for each class resulting from this step is presented in Figure 3.8 in term of distribution percentage leading to unbalanced classes.

We believe that unbalanced data in the case of 4 anxiety levels affects the classification results. So, we propose in order to obtain a balanced data, to regroup classes two-by-two: normal and light in the first class and moderate and severe in the second class. The dataset becomes slightly unbalanced, with samples amounting to 36% and 64% in average for the first class (labeled light) and the second class (labeled severe) respectively. Figure 3.8 shows the overall class distribution throughout the whole dataset for the two-class rating scale. Classification was performed using a SVM classifier with Radial Basis Function (RBF) kernel. It was trained and tested in Matlab. Furthermore, a 5-fold cross validation technique was used in order to validate the classification performance. It must be noted that k-NN was also evaluated using the same procedure, and happened in some cases to produce a more significant results than SVM. We

### Chapter 3. EEG-based anxiety levels recognition using a psychological stimulation

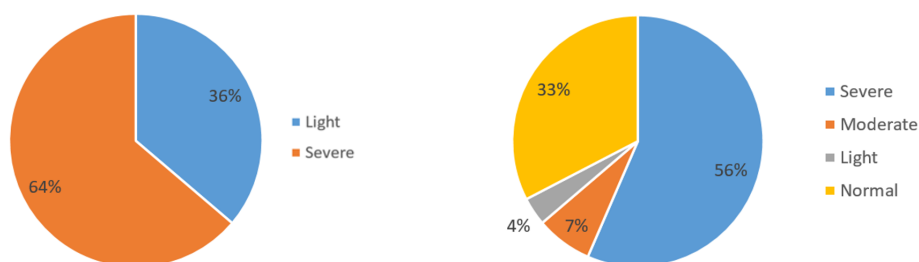


Figure 3.8: Overall class distribution across all participants for two and four anxiety levels.

Table 3.7: Anxiety detection results of 4 and 2 levels

Trial duration	Feature	#Features	Accuracy(%)			
			4 levels		2 levels	
			SVM	k-NN	SVM	k-NN
15s	Hjorth	42	56.20	56.50	66.30	63.80
	qEEG	25	56.50	56.50	64.10	63.80
	HHT	10	57.00	56.80	64.10	64.10
	Power	56	58.30	<b>57.60</b>	<b>66.30</b>	66.30
	RMS	56	<b>59.10</b>	56.50	<b>66.30</b>	<b>67.00</b>
5s	Hjorth	42	57.40	58.80	72.90	64.90
	qEEG	25	56.80	56.40	64.00	63.60
	HHT	9	56.90	56.30	64.00	64.10
	Power	56	62.00	63.20	<b>73.10</b>	70.50
	RMS	56	<b>65.30</b>	<b>64.30</b>	72.90	<b>73.40</b>
1s	Hjorth	42	60.10	57.00	67.40	<b>81.40</b>
	qEEG	25	58.30	56.40	64.00	63.50
	HHT	7	56.60	56.30	64.00	63.60
	Power	56	64.40	68.00	76.00	74.90
	RMS	56	<b>70.20</b>	<b>73.60</b>	<b>77.40</b>	80.30

highlight that the task here is subject-independent that means the training and test samples does not belongs to the same subject. Anxiety detection results for two and four levels are presented in Table 3.7. We report results obtained from different kind of features. We remark that DWT-based RMS features with SVM achieve the best results 59.10% and 65.30% for 15s and 5s trial duration respectively. When the trial length is 1s, the result is increased with k-NN classifier

### Chapter 3. EEG-based anxiety levels recognition using a psychological stimulation

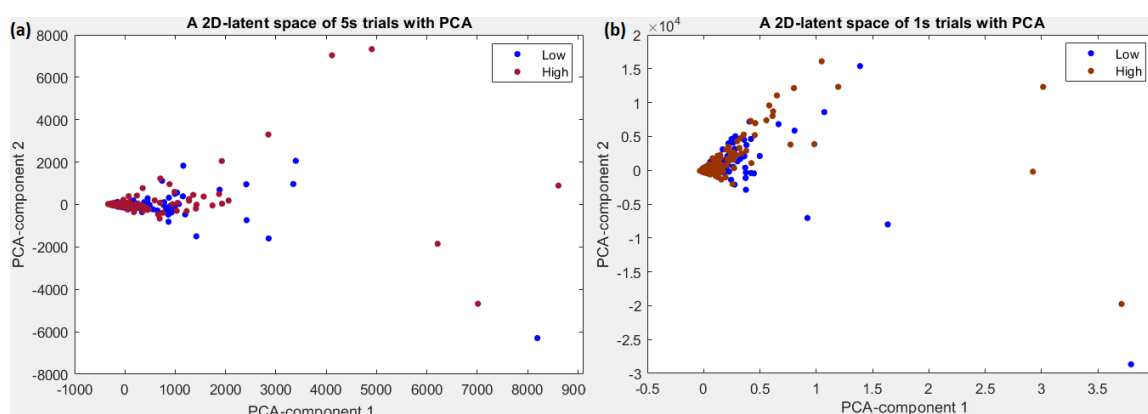


Figure 3.9: PCA score plot of PC1 and PC2 for (a) 5s trial duration and (b) 1s trial duration again with DWT-based RMS features to reach 73.60%.

Power and RMS features obtained after a DWT for the 15s EEG signals in the case of the binary classification give a significant rates 66.30%, 67.00% with SVM and k-NN classifiers, respectively. For 5s Trial duration, 73.40% is achieved with DWT based RMS features and k-NN classifier which slightly outperforms the result 73.10% obtained with Power features and SVM classifier. Classification accuracy reached 81.40% using Hjorth parameters and k-NN classifier against 77.40% with DWT based RMS features and SVM for 1s trial duration.

In this work, we varied the trial duration to verify the anxiety manifestation. To make the comparison fair, we used the same classifiers and the same features. As depicted in Table 3.7, for Hjorth features it is remarkable that SVM accuracy decreases from 72.90% (5s) to 67.40% (1s) and k-NN accuracy is increased from 64.90% (5s) to 81.40% (1s). Two key ingredients are behind this accuracy variation, to know, the dataset size and the data projection in the space. Theoretically, with more samples the training phase is more efficient and the classifier is prevented from overfitting. In practice, k-NN improved the performance results while SVM decreased the accuracy results. To further analyze such variation, a 2D Principal Component Analysis (PCA) for data projection of trials with 5s and 1s, respectively is handled as shown in Figure 3.9. Low anxiety level (Blue dots) data are more overlapped with High anxiety level (dark red dots) in Figure 3.9.b with 1s than in Figure 3.9.a with 5s. This overlapping is responsible for the obtained results with SVM, it means that the Hjorth features for 1s are less discriminative than those with 5s and SVM was not able to find a hyperplane to discriminate between the two levels.

### **Chapter 3. EEG-based anxiety levels recognition using a psychological stimulation**

---

Through the aforementioned results, it is clear that detection from one second trial length is more accurate and this is related to the anxiety as an emotion. It can be evoked in 1s, but 5s or 15s are too long and may contain more than one emotion. To add, we can notice that the best rates are related to time-frequency features obtained after a wavelet transform which was also proved by [Zhao et al., 2018]. The latter showed that the frequency-domain features are more prominent for EEG signals regarding the time-varying and non-stationary nature. Regardless of the trials' duration, features produced from a Hilbert Hung Transform and the set of quantitative EEG features do not lead to a great accuracy, despite proving that this approach outperform rates in many researches. Knowing this, Hjorth parameters are the most simple features to extract from an EEG signal, yet they produce a significant accuracy throughout all types of datasets.

For further study the impact of feature type on the performance of the proposed system, Feature vectors from 1s trial are grouped by type and then passed to SSAE. SSAE is a well-known neural network proposed for data compression. In our work, SSAE is used for feature selection step. SSAE with one hidden layer is first considered and then a deeper SSAE with two hidden layers is tested. The activation of the last hidden layer is extracted and it is known as the latent representation. It is worthy to note that the sparsity constraint on the latent vector is very important in finding the most relative features. Actually, the sparsity on the activation allows to preserve only the most expressive (non-sparse) neurons that handle the pattern matched with the input. Once having the latent vector, it is passed to a softmax layer which is responsible for the classification step. Since the input of SSAE is a handcrafted feature vector, there is no feature learning process in our work. The latter consists in extracting automatically the relevant features from raw data which is not our case.

As the role of SSAE is the selection of the most relevant features, we specified the size of both hidden layers to be lower than the input size. Note that, a softmax layer is added to perform the classification task. Table 3.8 depicts the results obtained for Time, Frequency, Time-Frequency and All Features. Frequency features outperform other types with 82% and 71.20% for 2 and 4 anxiety levels, respectively. The highest accuracy is obtained with the combination of all features to reach 83.50% for 2 anxiety levels and 74.60% for 4 anxiety levels.

### Chapter 3. EEG-based anxiety levels recognition using a psychological stimulation

Table 3.8: Anxiety detection results using SSAE

	#Features	L1-L2 sizes	Accuracy(%)	
			2 Levels	4 levels
Time	67	44-33	<b>67.90</b>	57.80
		33-16	67.60	<b>59.90</b>
Frequency	154	102-77	<b>82.00</b>	<b>71.20</b>
		77-38	78.70	68.80
Time-Frequency	112	74-56	<b>67.10</b>	<b>59.70</b>
		56-28	<b>67.10</b>	59.50
All	277	184-138	<b>83.50</b>	<b>74.60</b>
		138-70	81.60	72.60

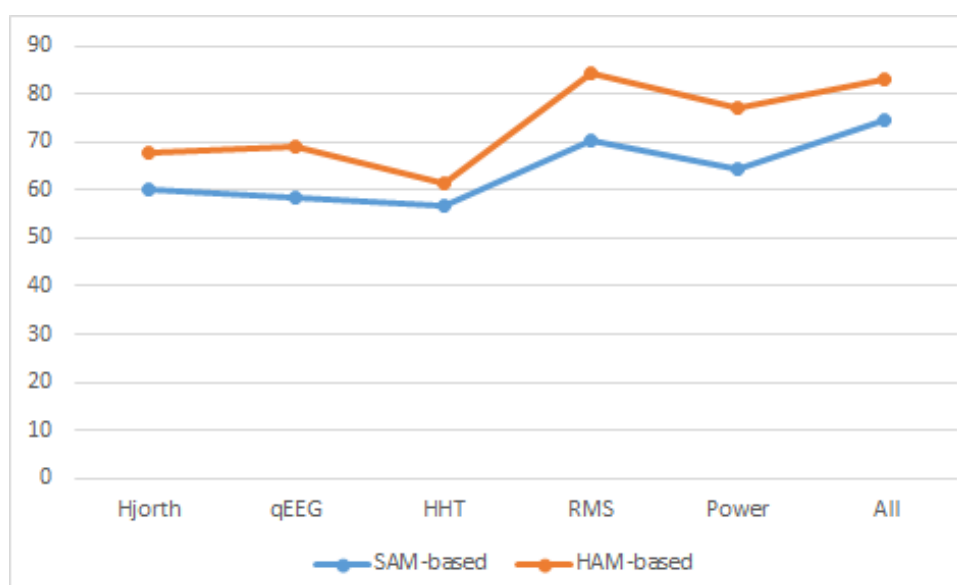


Figure 3.10: Improved results across all features extracted from the SAM-based and HAM-based databases

While, the combination of features allows to provide rich information, the representation generated by SSAE proved their effectiveness in handling more discriminative aspect. The result of 2 levels is higher than the 4 levels and this is mainly to the increase of complexity aspect in the classification task.

### Chapter 3. EEG-based anxiety levels recognition using a psychological stimulation

Table 3.9: Performance comparison of the proposed work with the state-of-the-art methods

Reference	#Subjects	#Channels	Classifier	#Classes	Accuracy(%)
[Saeed et al., 2015]	28	01	SVM	2	71.42
[Saeed et al., 2017]	28	01	Naive Bayes	2	71.40
[Secerbegovic et al., 2017]	09	01	SVM	2	83.33
[Subhani et al., 2017]	22	128	Naive Bayes	Multiple	83.40
[Saeed et al., 2018]	23	01	SVM	2	78.57
[Arsalan et al., 2019]	28	04	MLP	2	89.30
	28	04	MLP	3	60.91
[Zanetti et al., 2019]	17	14	LR-RF	3	84.60
<b>[Baghdadi et al., 2020a]</b>	<b>23</b>	<b>14</b>	<b>SSAE</b>	<b>4</b>	<b>86.70</b>

#### 3.4.2 HAM-based improved results

In order to evaluate the HAM-A test efficiency in the data labelling process, we keep the most relevant features and redo the classification on the HAM-based dataset. Best results were obtained for 1s duration trials with RMS features for 4 levels detection, and with all features combination with a SSAE classifier. In this section, we will discuss only the improved results for 4 levels detection.

As shown in Figure 3.10, better detection accuracies are obtained across all features using the HAM-A scores labeled dataset. Since SAM rates are related on the level of participant comprehension, a lack of comprehension of these scales may lead to a confusing rating. On the other hand, the HAM-A test was performed with the complete psychologist's assistance. The calculated scores are most accurate and informative.

Table 3.9 presents the performance comparison of our proposed work with recent studies conducted for the classification of human stress. The mentioned methods were compared with our proposed scheme on the basis of the number of participants, number of channels, classifier, number of classes and achieved accuracy. For multi-level stress classification, an accuracy of 83.40% was achieved using 128 electrodes [Subhani et al., 2017]. Whereas our proposed methodology achieved an accuracy of 86.70% for multi-level classification with only 14 electrodes.

The multi-modal system proposed by Zanetti *et al.* [Zanetti et al., 2019] achieved an accuracy of 84.60% in the classification of 3 mental stress levels using multiple physiological

### Chapter 3. EEG-based anxiety levels recognition using a psychological stimulation

---

signals. When reducing the number of signals, the accuracy had decreased down to 76.50%. Whereas, we proposed a less complicated single-modal approach and achieved a higher performance. Arsalan *et al.* [Arsalan et al., 2019] tried to classify three levels of stress (non-stressed, mildly stressed and stressed) and proposed a feature selection algorithm in order to enhance the classification accuracy. Further, they didn't perform this task since the obtained accuracy is outstandingly lower than for binary classification (60.91%).

We performed a feature selection with deep SSAE and we obtained the highest state-of-the-art results for multiple-label classification problem using SSAE with HAM-based labels (86.70%) as shown in Table 3.10. As for SAM-based results in Table 3.10, k-NN achieved higher accuracy (81.40%) in comparison to SVM classifier with RBF kernel (79.00%). This is not surprising, it is confirmed with previous findings in [Piho and Tjahjadi, 2018] for EEG-based emotion recognition task. SSAE handle an improvement up to 5% in comparison with k-NN. In general, neural networks reach better performance than SVM or k-NN especially in the case of big dataset. Furthermore, SSAE due to its compression capability it performs better in case of dataset with large feature vector.

Table 3.10: Anxiety detection improved results for 4 levels

Trial duration	Feature	Classifier	Accuracy (%)
1s	RMS	SVM	79.00
		KNN	81.40
	All Features	SSAE	<b>86.70</b>

The confusion matrix of the three classifiers on trials with 1s duration labeled with HAM scores is shown in Figure 3.11, which shows the details of strength and weakness of each classifier. The row refer to the target class and the column indicates the predicted class. The element  $(i, j)$  in a confusion matrix is the percentage of samples in class  $i$  that was classified as class  $j$ . As observed in Figure 3.11.a, SVM with RMS features slightly confuses normal level when classifying severe level. It highly confuses severe and moderate levels with light level. K-NN classifier confuses highly severe level when classifying moderate level. For both SVM and k-NN, the highest confusion is made with severe level for light level classification task. SSAE does not confuse normal level when classifying severe, moderate, and light levels.

### Chapter 3. EEG-based anxiety levels recognition using a psychological stimulation

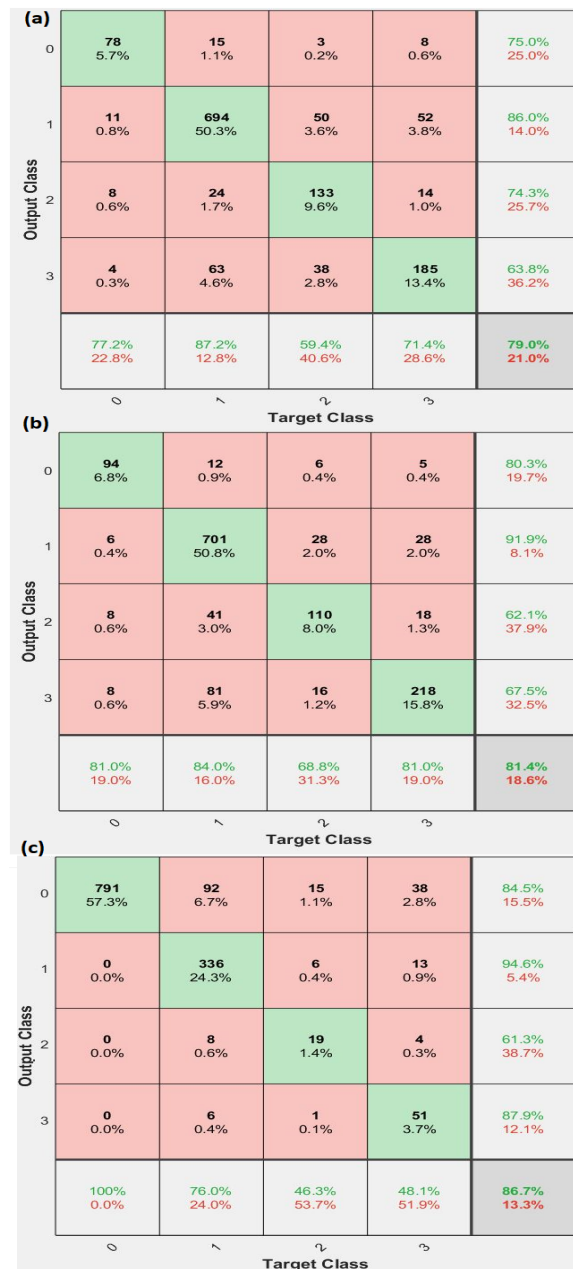


Figure 3.11: Confusion matrix for (a) SVM, (b)k-NN and (c) SSAE summarizing the targeted (y-axis) and predicted (x-axis) anxiety level, where 0: Normal, 1: Severe, 2: Moderate and 3: Light

While k-NN and SSAE handle lower accuracy for the prediction of moderate level, the lowest accuracy of SVM classifier exists for the prediction of light level. All classifiers predict severe level very well in comparison with other levels and this is mainly due to the high number of trials in such class.

Receiver Operating Characteristic (ROC) curve shows classifier performance as a trade off

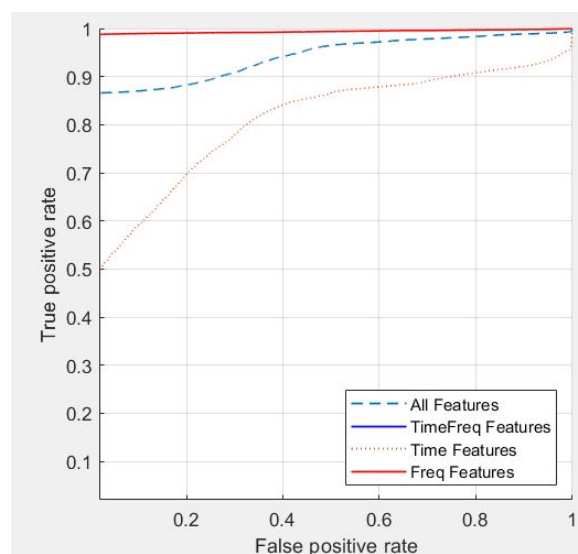


Figure 3.12: ROC curve of 2-levels anxiety using SSAE with 4 types of features.

between specificity and sensitivity, giving a good estimate on how well the classifiers separate the classes. Figure 3.12 of SSAE with HAM-based labels shows that frequency features separate anxiety two levels better than the other kind of features. Time frequency features curve is superimposed upon Frequency features curve, that means they separate similarly. Time features do not separate well between anxiety two levels.

From the aforementioned results, HAM-based labels are more expressive and reflective than SAM-based labels which means that Hamilton score is well related to anxiety elicitation than simple SAM ratings. Among different features, RMS features are the most discriminative for SVM and k-NN classifiers. Thanks to the segmentation into 1s trials, classification problem is more realistic. In such case, SSAE is more powerful than SVM and k-NN since it is able to perform both feature selection step and the classification step when linked to a softmax layer.

### 3.5 A mobile application for anxiety level recognition based on deep LSTM model

Mobile applications are massively used, regardless of their utility in event prediction and making decision. In health domain, this application can present an improvement if only their effectiveness is validated in term of sensitivity and specificity improvement for diseases pre-

## Chapter 3. EEG-based anxiety levels recognition using a psychological stimulation

vention, diagnosis and prognostics.

[Espinoza and Paredes, 2020] elaborated a study to prove that the use of mobile applications supports the diagnosis of anxiety by improving the performances.

In this work, the author determined that the use of a mobile application improved the anxiety diagnosis sensitivity at the psychological service. The results of the study showed an improvement in sensitivity (from 33.3% to 83.3%) and a decrease in specificity (from 94.1% to 82.3%) of the preliminary diagnosis of this disorder.

The development of a mobile application will assist the psychotherapists and reduce the time of consultation and thus reduce costs and improve the clinician availability. To demonstrate the advantages of an EEG-based mobile application for anxiety levels recognition. we have elaborated a business canvas of the proposed framework Figure3.13.

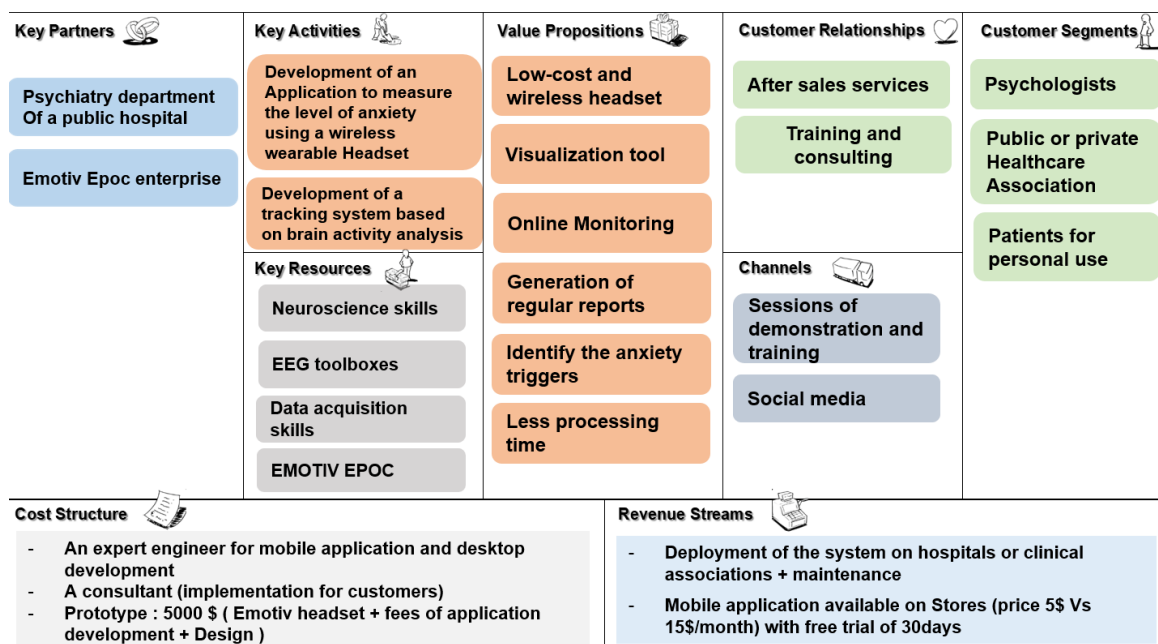


Figure 3.13: Business model canvas of an EEG-based mobile application for anxiety levels recognition

### 3.5.1 Broader impact and overview

Broader impacts refers to the potential for a research project to benefit society or advance desired societal outcomes. In our case, those outcomes include:

- Using a wearable wireless EEG headset; this application will allow users to track their

## Chapter 3. EEG-based anxiety levels recognition using a psychological stimulation

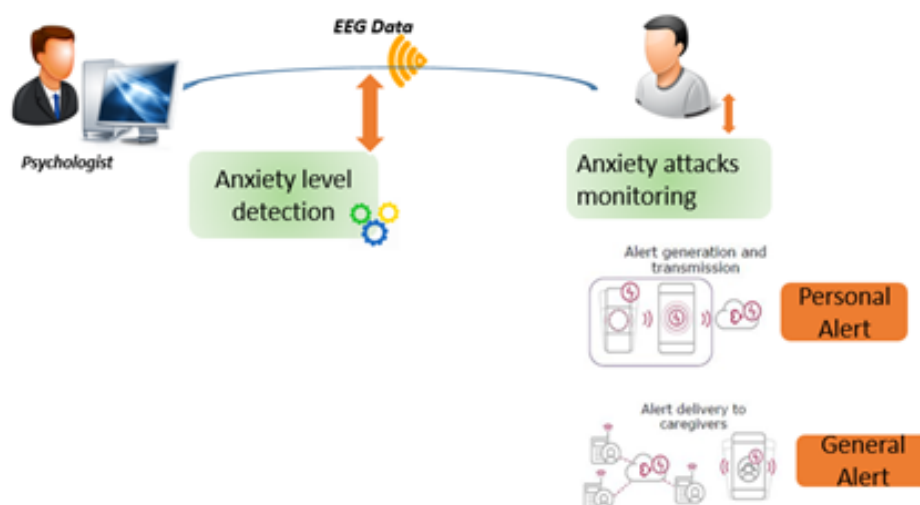


Figure 3.14: The process of an anxiety levels recognition application with all implicated parts

anxiety and guarantee their safety by notifying nearby caregivers

- The proposed system is attractive to many application fields: Marketing, coaching, medical monitoring...

Our application presents the following advantages:

- Our application analyzes the brain activity that reflects the inner state of a person.
- Application implements an AI algorithm
- Deep learning is implemented to train the model aimed to improve the performances of anxiety detection, assess a high level of generalization, fast training and processing and adaptability to real time applications

### 3.5.2 Evaluation of LSTM architectures

We conceived a deep LSTM model adequate to our input data with parameters tuned to meet the best performances for anxiety levels detection.

While tuning the LSTM architectures, we used the whole amount of EEG data of our dataset DASPS described in section 3.2 of this chapter. The total classification accuracy for assigning

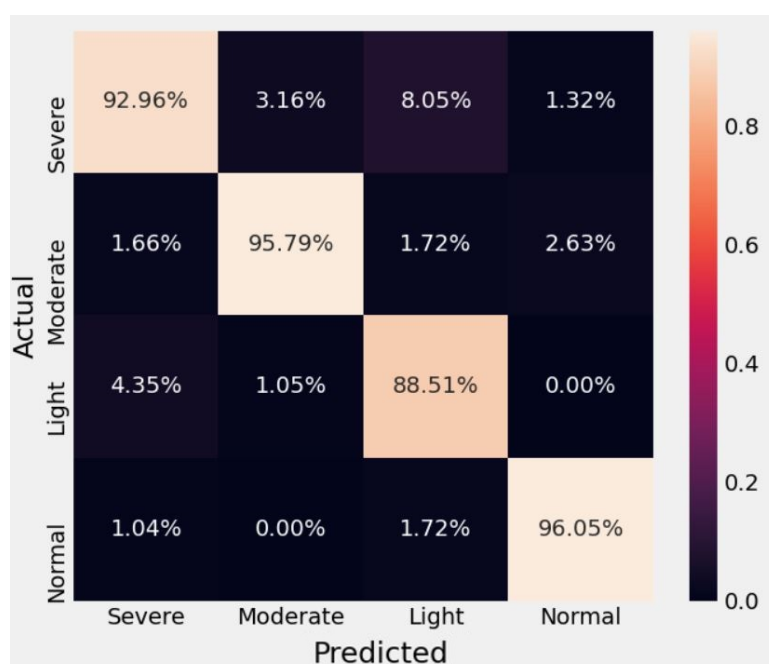


Figure 3.15: Confusion matrix of anxiety levels recognition for the LSTM model evaluated with a test set from DASPS

the EEG segments into 4 classes is estimated using the complete duration of all the available EEG recordings. The impact of the LSTM input size is further assessed through the testing of 3 different numbers of EEG segments as input, ranging from an input sequence consisting of 10 EEG segments, with an LSTM input size of 128x14 channels and up to 30 EEG segments. Also, the number of LSTM layers, number of units per layer and the probability of the dropout layer are evaluated.

### 3.5.3 Overview of the application

In order to visualize the recognized anxiety level, we implemented our algorithm with Tkinter [2]. The Api Pycharm was used to implement Tkinter wrappers and run the application. Data Acquisition: An Emotiv headset set at 128 Hz is used to collect EEG data. Emotiv Software Development Kit was also used to collect raw data from the device. For the anxiety level recognition step, a 1-second multi-channel segment was fed into the trained model. A data flow from the Emotiv headset is stored in a buffer. All the samples in the buffer are deleted and the buffer is cleared, every time a read command is prompted. Accordingly, the amount of data obtainable at a certain time depends on the length of samples accumulated in the buffer. The data

### Chapter 3. EEG-based anxiety levels recognition using a psychological stimulation

to be fed into the model must be in a batch of the dimension  $128 \times 14$ . Accordingly, a queue is used in order to buffer the data from Emotiv's buffer into the model. Every time the read command is prompted, the queue is refreshed by the current number of samples in Emotiv's buffer. We created four images to indicate the recognized level in order to define four levels. These levels are: light, normal, moderate and severe. The aforementioned levels can be identified by the suggested anxiety level recognition model specified in section 3.5.2. Screenshots of the two major functionalities of the application implemented with Tkinter are shown in Figure 3.16.

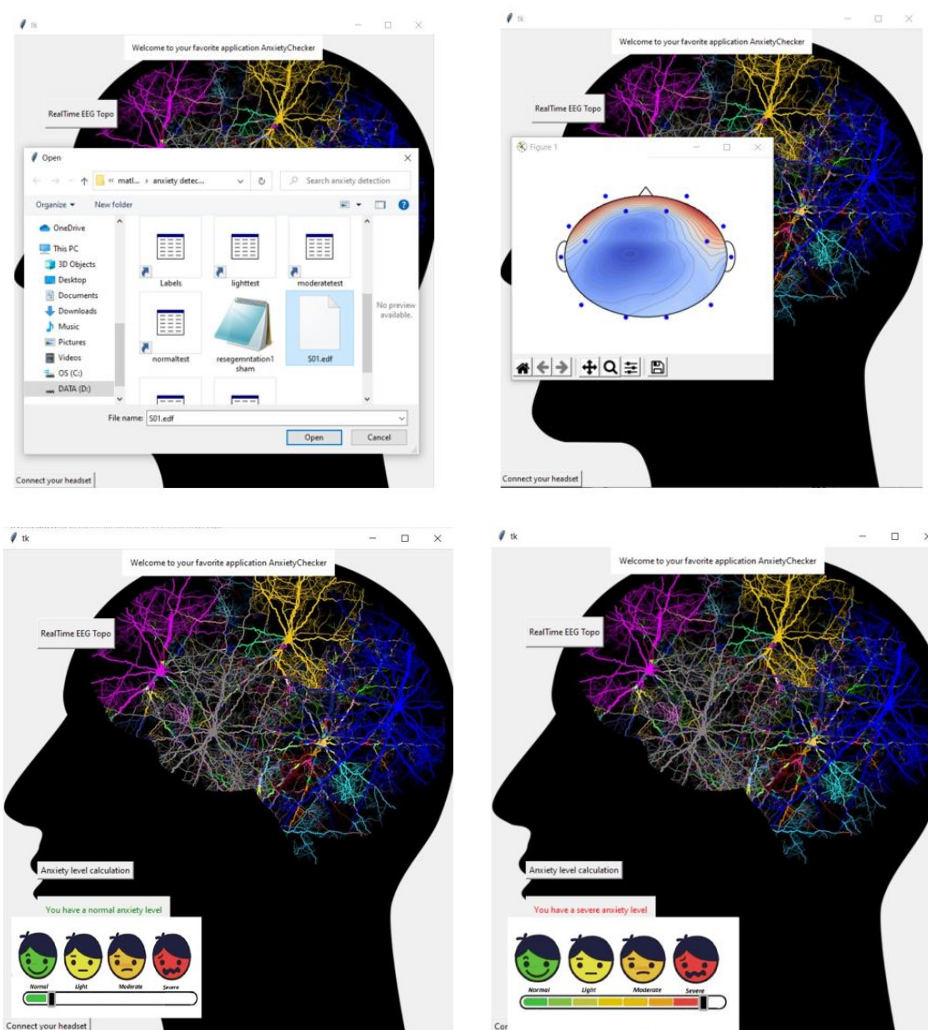


Figure 3.16: ScreenShots of the anxiety checker application, Top: Topographic map option, Bottom: Anxiety level recognition

### 3.6 Conclusion

A novel approach to anxiety elicitation based on a face-to-face psychological stimulation has been presented in this chapter. A dataset was constructed containing EEG data gathered during the experimentation. We present insights to analyze acquired data showing the efficiency of the followed strategy. The approach showed success in inducing anxiety levels, which was validated by HAM-A Test Scores calculated before and after the experiment. A various sets of emotion recognition features and in particular anxiety/stress, based on EEG signal, are reviewed and applied in this chapter. We presented the most popular feature extraction techniques from the wide range used in the literature. Some methods perform slightly better than others. We also investigated which trial duration are most promising and which features are most effective for it.

To the best of our knowledge, there are no available databases that contain EEG data recorded with a portable device for anxiety detection. The headset Emotiv Epoc used in our work is available for the public and is easy to install and use. Patients can use it at the comfort of their homes, and check their stress levels without the need to consult an expert. Many clinical applications can be derived from this work, improving life quality and reducing cognitive disabilities. Raw and preprocessed data were made available to the scientific community on IEEE DataPort (<https://iee-dataport.org/open-access/dasps-database>).

# A novel region-aware attention with deep LSTM for EEG epileptic seizure classification

## Contents

<b>4.1 Introduction</b> . . . . .	<b>73</b>
<b>4.2 A region-aware attention mechanism for seizure types classification from raw EEG signals</b> . . . . .	<b>75</b>
4.2.1 Attention mechanism for multi-channel epileptic signals . . . . .	75
4.2.2 LSTM model with an attention mechanism . . . . .	78
<b>4.3 Experiment results for seizure detection and seizure type classification</b> . . . .	<b>80</b>
4.3.1 Experiment design . . . . .	80
4.3.1.1 Data preparation . . . . .	80
4.3.1.2 Training and evaluation . . . . .	80
4.3.1.3 Hyper-parameters fitting . . . . .	81
4.3.2 Experimental results . . . . .	82
4.3.2.1 Evaluation on TUSZ for seizure detection and type classification	83
4.3.2.2 Evaluation on CHB-MIT for seizure vs normal classification .	85
<b>4.4 Cases study</b> . . . . .	<b>91</b>
4.4.1 Myoclonic seizure . . . . .	91
4.4.2 Tonic-clonic seizure . . . . .	93
4.4.3 Complex partial seizure . . . . .	95
<b>4.5 Conclusion</b> . . . . .	<b>97</b>

### 4.1 Introduction

Epilepsy is a neurological disease that manifests with irregular and sudden discharges of neurons in the brain. Affecting almost 1% of the worldwide population, it negatively impacts the quality of life for these persons.

Epileptologists use medications to control seizures. While it might work for some, this method might not have the same effect for a patient with uncontrolled seizures.

Seizures manifest in different forms and each type need a specific treatment. The initialisation of the treatment procedure rely to the correct identification of seizures type. Seizure types are classified by the ILAE based-on the manifestation symptoms. Epileptologists perform the identification process using electroencephalography recording combined with EEG-videos. Thanks to their expertise, a correct identification of the seizure attack is usually lead. The correct seizure type diagnosis is a critical step in selecting the appropriate drug therapy and to provide information regarding the prognosis. However, it remains challenging, labor-intensive, and time-consuming. It usually involves the monitoring of several real-time seizures of a patient, needing a continuous EEG recording [Goldenberg, 2010].

Similar clinical features are the main contributing elements in inaccurately distinguishing characteristics, as focal and generalized seizure disorders show overlap of both clinical and EEG symptoms [Panayiotopoulos, 2005a]. Recently, many studies have demonstrated that focal and generalized epilepsy are regularly troublesome to distinguish by experienced neurologists [Panayiotopoulos, 2005b]. Since the manifestation of the same epilepsy classes might be somewhat variable between different patients, and even for a single patient over time [Panayiotopoulos, 2005a], this variable epilepsy interpretation further complicates the clinical diagnosis.

EEG artifacts must be detected over the entire recording and this complicates the task of seizure bio-markers identification.

The time-consuming nature of clinical EEG diagnosis and its variability could be greatly improved with an automated seizure classification/detection system that assists professionals.

A robust Neural network model can handle the task of feature learning and classification using its embedded layers.

## **Chapter 4. A novel region-aware attention with deep LSTM for EEG epileptic seizure classification**

---

The choice of the neural network to implement for any automatic recognition system depends on the nature of the input data and the complexity of the task.

Since artificial neural networks are inspired from the natural neural networks which have a complex structure including recurrent synaptic connections, Recurrent Neural Networks (RNNs) are the most representative and suitable for dynamical systems modeling. An NN consider that all segments are independents, however this dependency on time is achieved by the recurrent connection of an RNN, on which the prediction at time  $t$  depends on the previous state at time  $t-1$ .

LSTM (Long Short-term Memory) is an improvement over traditional RNN characterized by the long memory. Based on its cell states mechanism, LSTMs can select the information to remember or forget. LSTM as a special RNN structure has proven stable and powerful for modeling long-range dependencies in various previous studies [Xingjian et al., 2015]

As EEG have a complex nature with temporal dependencies, LSTMs are suitable RNN for the task of EEG-based seizure detection and type classification.

Regarding the clinical importance of the recognition of the most relevant channels of each seizure type and based on a clinical need for more investigation about the most contributed brain region per epilepsy type, we have proposed the novel channel-wise attention mechanism to address the current requests.

In our methodology we implement an attention-based Deep LSTM model to learn the temporal representation of the EEG signals while analysing the level of contribution of each channels.

Our main contributions presented in this chapter are:

- The use of EEG raw data as input to our model resulting in a gain of the pre-processing and feature extracting time. Also, to allow our model with high level of abstraction to learn more discriminative features.
- The integration of an attention layer that learns channel-wise weights from multi-channel raw EEG signal. To the best of our knowledge, this is the first application of a Raw-based channel-wise attention mechanism applied to seizure types classification.
- The analysis of the resulting attention scores of a case study to measure the correlation

## Chapter 4. A novel region-aware attention with deep LSTM for EEG epileptic seizure classification

---

between the seizure type and the localization of the highest weights.

The three main phases of the proposed method are depicted in the Figure 4.1. This chapter is composed of 6 sections. Sections 4.2.1 and 4.2.2 detail the proposed channel-wise attention mechanism and the LSTM model respectively. Section 4.3 summarizes the model parameters and the environment settings. Section 4.3.2 illustrates the experimental results and discussion. Section 4.4 presents many case studies analyzing the correlation between the channels contribution and the scientific findings.

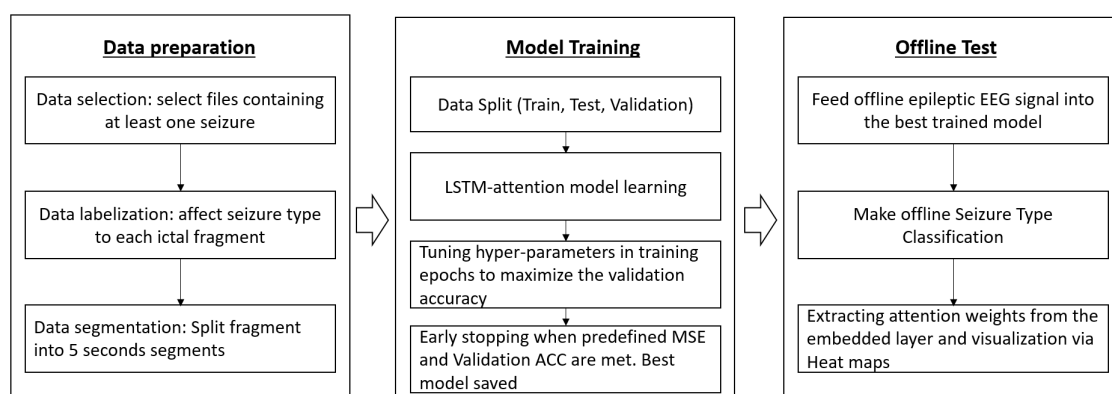


Figure 4.1: The overall workflow of our proposed method including the three main phases

## 4.2 A region-aware attention mechanism for seizure types classification from raw EEG signals

### 4.2.1 Attention mechanism for multi-channel epileptic signals

Attention mechanism was first introduced by [Bahdanau et al., 2015] in Encoder/Decoder based on LSTM units for textual sequence translation. They suggest that relative importance should be given to each input words, as well as taking into account the context vector. In a follow up work [Chen et al., 2017], channel-wise attention-based CNN demonstrates superior performance in image captioning because it has the ability to change different channels' weight in order to explore feature map information. More specifically, it has the ability to gather additional important information about channels.

## Chapter 4. A novel region-aware attention with deep LSTM for EEG epileptic seizure classification

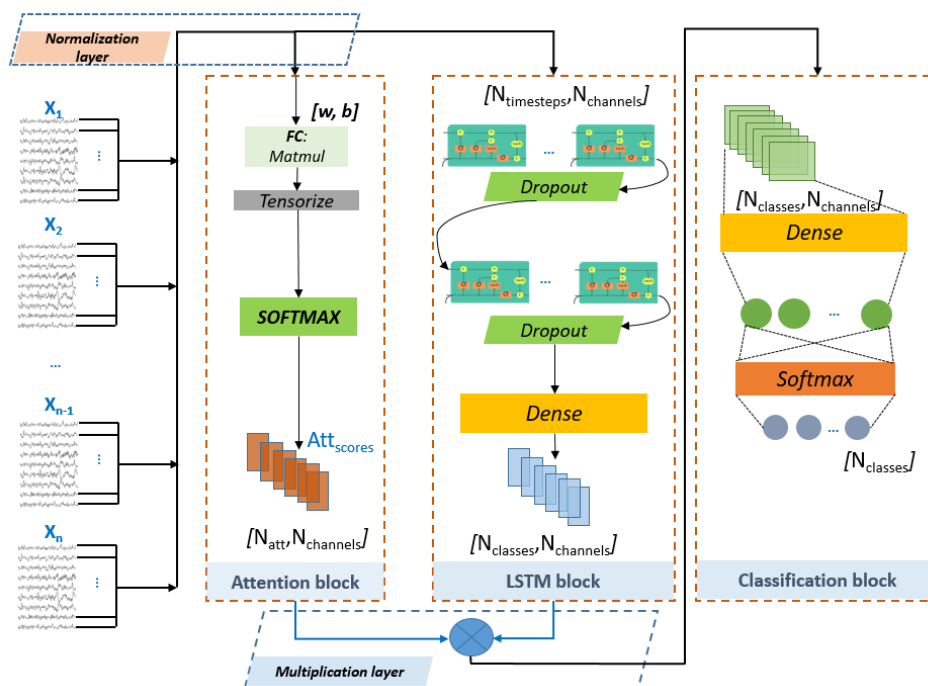


Figure 4.2: The structure diagram of our attention-based LSTM model

on the other side, the contribution of different EEG channels varies in seizure diagnosis [Temko et al., 2011]. Thus, an attention mechanism is introduced for channel importance learning and to pay different attention to various brain lobes. As abovementioned, the attention mechanism allows modeling of dependencies among EEG channels [Zhang et al., 2020b] and has shown success in some research topics [Cisotto et al., 2020] [Hu et al., 2020] [Eom et al., 2020].

Meanwhile, the excellent temporal feature learning ability of Recurrent Neural Networks (RNNs) has been extensively used in research areas such as speech recognition [Miao et al., 2015], language modeling [Yin et al., 2017], diseases prediction [Tsiouris et al., 2018] and many others. Thus, we propose an attention-based LSTM model to automatically extract discriminative information from the received temporal multi-channel EEG data. The Figure 4.2 depicted all block of the proposed method. First, to explore the importance among the different channels of EEG signal, a channel-wise attention-based mechanism is employed as shown in the left block of the structure diagram of Figure 4.2. In the case of seizure detection or seizure type classification, some channels may not contribute to the final decision and thus add redundant information and demean the method capabilities.

#### Chapter 4. A novel region-aware attention with deep LSTM for EEG epileptic seizure classification

---

The adapted channel-wise mechanism takes into consideration the information of all channels and assigns weights to different channels based on their importance. This mechanism will allow to explain the contribution of each channel to the final decision. Consider that,  $X = [X_1, X_2, \dots, X_n]$  represents EEG samples, and  $X_i = [x_1, x_2, \dots, x_k]$  where  $x_k$  represents the  $k^{th}$  channel of EEG sample  $X_i$ , and  $k$  is the total number of channels of each sample. In this model, the attention scores are directly learnt from the EEG sample. The attention layer, shown in Figure 4.2, is used to generate attention weights for each channel and then executes an element-wise multiplication with the output of the dense layer of the LSTM block. In the attention block, the original data are inputted into a fully connected layer where the parameters  $W$  and  $b$  are initialised for all channels. The attention matrix is element-wisely multiplied by the original inputs. The outputs of the attention block are multiplied by the output of the dense layer of the LSTM block. Then, the attention-based temporel features are passed to a dense layer with the suitable activation respecting the classification task, i. e. sigmoid for seizure detection or softmax for seizure type classification to get the label of the EEG sample.

The attention layer is computed using the following equations:

$$Y_1 = f_{nor}(X_0) \quad (4.1)$$

$$Y_2 = w_{al} * Y_1 + b_{al} \quad (4.2)$$

$$Y_3 = f_{tens}(X_2) \quad (4.3)$$

$$Y_4 = \sigma(Y_3) \quad (4.4)$$

Here,  $X_0$  denotes an input of size  $(N_{samples}, N_{timesteps}, N_{channels})$ . Symbols  $(N_{samples}, N_{timesteps}$  and  $N_{channels})$  represent the number of samples, the number of time steps, and the number of EEG channels, respectively.  $Y_1$  is a normalized matrix of  $X_0$  size.  $W_{al}$  a weight of size  $(N_{channels}, N_{channels})$ , a bias  $b_{al}$  of  $(N_{samples}, N_{timesteps}$  and  $N_{channels})$ , and  $Y_2$  have the same size as  $Y_1$ . A symbol  $\sigma(\cdot)$  represents a nonlinear activation function, which transforms the importance of channels to probability distribution, like softmax(.) and sigmoid(.).  $Y_2$  is a tensorized matrix of  $Y_2$ .

## Chapter 4. A novel region-aware attention with deep LSTM for EEG epileptic seizure classification

---

Functions  $f_{nor}(\cdot)$  and  $f_{tens}(\cdot)$  are to normalize and tensorize a matrix.

$$att_{scores} = Y_3 = [att_1; att_2; \dots; att_k] \quad (4.5)$$

The middle block of the Figure 4.2 shows the temporal feature learning module, which comprises a two-layer LSTM. The LSTM network can learn the context information of the sequence thanks to its recurrent structure [Hochreiter and Schmidhuber, 1997]. The predicted seizure class  $Y_5$  is related to the last dense layer (D2) and the learnt attention scores:

$$Y_5 = Dense_{out} \odot att_{scores} \quad (4.6)$$

The symbol  $\odot$  means an element-wise multiplication between tensors.

### 4.2.2 LSTM model with an attention mechanism

Over the last years, deep learning networks were used for EEG classification tasks, including seizure detection [Li et al., 2019], emotion recognition [Fourati et al., 2020b] [Fourati et al., 2020a] [Fourati et al., 2017b], and classification of motor (imagery) tasks. Various studies showed that LSTMs outperform other models like decision trees, support vector machines used in our previous work [Baghdadi et al., 2020a], logistic regressions, random forest classifiers, naïve Bayes, feedforward neural networks, deep belief networks, and even CNNs for some tasks [Yao et al., 2021]. The superior performance of LSTMs' EEG classification over other models is likely due to their ability to account for time dependencies. As EEG is a time-series data, preserving temporal characteristics might significantly improve the model's accuracy.

The LSTM architecture like an RNN network contains 3 main layers. The strength of LSTM came from its hidden layer. This latter contains special blocks called memory blocks. The input and output gates of these blocks perform the control by the activation functions. The revised version of LSTM added a forget gate to the memory blocks. An LSTM network finds the mapping from input sequence  $x = (x_1, x_2, \dots, x_T)$  to the output sequence  $y = (y_1, y_2, \dots, y_T)$  by figuring out the network unit activations using the following equations:

#### Chapter 4. A novel region-aware attention with deep LSTM for EEG epileptic seizure classification

---

$$i_t = \sigma(W_{ix}x_t + W_{im}m_{t-1} + W_{ic}c_{t-1} + b_i) \quad (4.7)$$

$$f_t = \sigma(W_{fx}x_t + W_{fm}m_{t-1} + W_{fc}c_{t-1} + b_f) \quad (4.8)$$

$$c_t = f_t \odot c_{t-1} + i_t \odot g(W_{cx}x_t + W_{cm}m_{t-1} + b_c) \quad (4.9)$$

$$o_t = \sigma(W_{ox}x_t + W_{om}m_{t-1} + W_{oc}c_{t-1} + b_o) \quad (4.10)$$

$$m_t = o_t \odot hc_t \quad (4.11)$$

$$y_t = \phi(W_{ym}m_t + b_y) \quad (4.12)$$

In the above equations,  $W$  represents the weight and  $W_{ix}$  is the maximum weight of the input gate to the input.  $W_{ic}$ ,  $W_{fc}$  and  $W_{oc}$  are the diagonal weights of peepholes connections. The majority of the architectures consisted of one or two LSTM layers, followed by one or two fully connected layers. Input to the LSTM comprised mostly features extracted from EEG signals. However, the signal itself and EEG images (spectrograms) were also used [Craik et al., 2019].

Several EEG-based studies compared the use of handcrafted features to the raw EEG signal as input for the LSTM model. Usage of the signal itself is consistently and massively under-performed in these comparisons [Kaushik et al., 2018], [Tsiouris et al., 2018], and [Abbasi et al., 2019]. These studies reported an accuracy rate of  $50.00\% \pm 1.50$  when applying their methods on raw EEG data, while using artifact removal techniques to reduce noise slightly improved the performances. Our work shows that even with raw EEG data and without any pre-processing, our LSTM-att is able to achieve our objective in classifying epileptic seizures. Figure 4.2 detailed all blocks of the proposed system discussed in the two previous sections.

## **4.3 Experiment results for seizure detection and seizure type classification**

### **4.3.1 Experiment design**

#### **4.3.1.1 Data preparation**

Since the TUSZ data contains numerous sampling rates and to ensure constant input dimension to the neural network, we used the 250 Hz re-sampled version of the dataset. Twenty-two common channels were selected and readjusted based on the 10–20 international system of scalp EEG placements. In this study, we keep the re-sampled EEG data unchanged. The data is structured into an adequate shape to be fed into the proposed model. The sample duration is fixed to 5-seconds. More specifically, the dimension of each sample becomes [22x1250] where 22 is the number of EEG channels and 1250 is the number of time steps.

In the case of CHB-MIT dataset, recordings are 23-channels signals with almost 18 common channels to be used in this work: FP1, T7, P7, O1, F3, C3, P3, FP2, F4, C4, P4, O2, F8, T8, P8, FZ, CZ and PZ. To the aim of seizure detection task, we extracted ictal and interictal segments from all patients. Then, we shuffled the obtained vectors and we selected a balanced amount of data to be used for the model training and evaluation. A total of 18,320 segments is used with a dimension of [18x1280].

#### **4.3.1.2 Training and evaluation**

In order to extensively evaluate the proposed model performance, a stratified five-fold cross validation is used. We randomly split the dataset into five-folds, where each fold maintains the proportional distribution of classes. Adam optimizer is chosen for the LSTM training with batch size value 20 and for 100 epochs. The TUSZ dataset have an unbalanced class distribution as shown in Table 2.5. The minor class, absence seizures, has 6 minutes of recording. In this case, accuracy by itself is unlikely to evaluate the model. The Precision, Recall and F1-score are thus added as metrics to evaluate the performance of our proposed model. As a regularization technique, we employed the Early stopping mechanism. Hence, we avoided an over-fitting

## Chapter 4. A novel region-aware attention with deep LSTM for EEG epileptic seizure classification

---

during the training process. This technique consists on the monitoring of the validation loss, if the latter does not improve within 10 epochs, the training process is stopped.

### 4.3.1.3 Hyper-parameters fitting

In our work, a grid search for all parameters was adopted as depicted in Table 4.1.

Table 4.1: Proposed LSTM architecture parameters

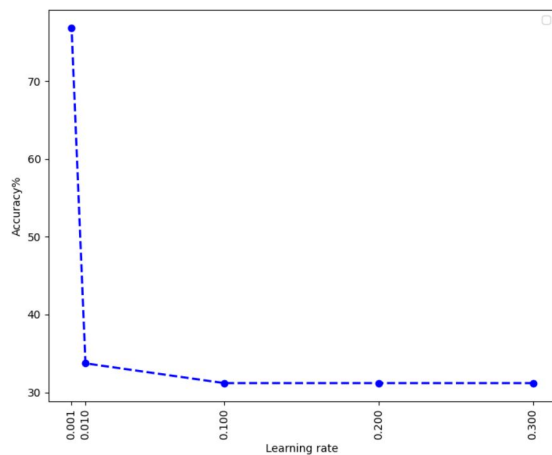
Parameters	Range	Best Value
LSTM Layers	[1-2]	2
Dropout Layers	[0-2]	0
Learning rate	[0.001,0.002,0.005, 0.01,0.1,0.2,0.3]	0.001
Memory units	[50,100,150,200,250]	250
Dropout probability	[0.2,0.3]	None
Dense activation	['softmax', 'relu', 'tanh', 'sigmoid', 'linear']	Softmax
Optimizer	None	Adam
Epochs	[20, 50, 100]	100
Batch size	[10,20,50]	20

This technique prompted the best accuracy for all possible combination of parameters. It is a time consuming step, but it insures that better fitting is used for the final model. Next, we report the hyper-parameter settings in detail. The input EEG sample has a shape of  $[N_{timesteps}; N_{channels}]$ . The number of units on the first and second LSTM layers was tuned to a range of [50,100,150,200,250]. Dropout probability of each layer tested to be between [0.0,0.2,0.5]. The two FC layers have  $N_{features}$  and  $N_{classes}$  hidden neurons respectively, and several activation functions were tested ['softmax', 'relu', 'tanh', 'sigmoid', 'linear']. The attention layer has  $N_{channels}$  hidden neurons corresponding to the input channels.

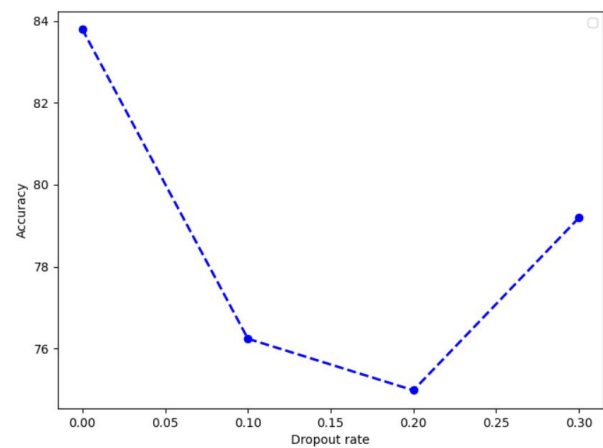
A categorical cross-entropy loss function is used in our model for multi-class classification, while binary cross-entropy is used for seizure detection. Considering the limited computational resources available in this study, we chose to use the Adam optimizer and omit other optimizers in the gridsearch parameters.

We tested our method for two classification problems on two datasets: TUSZ and CHB-MIT. Our model was implemented using Python 3.7.9 and Keras 2.3 with the Tensorflow-gpu 2.1.0.

## Chapter 4. A novel region-aware attention with deep LSTM for EEG epileptic seizure classification

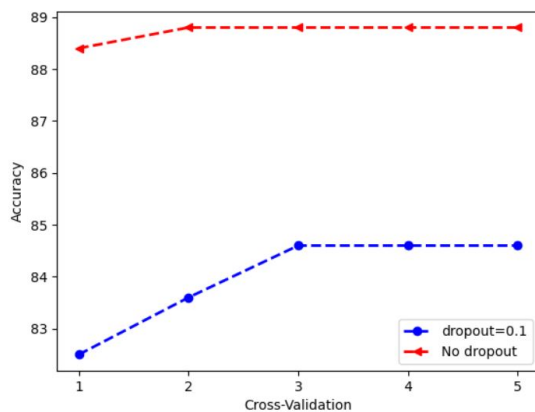


(a) Validation accuracy trends in five learning rates

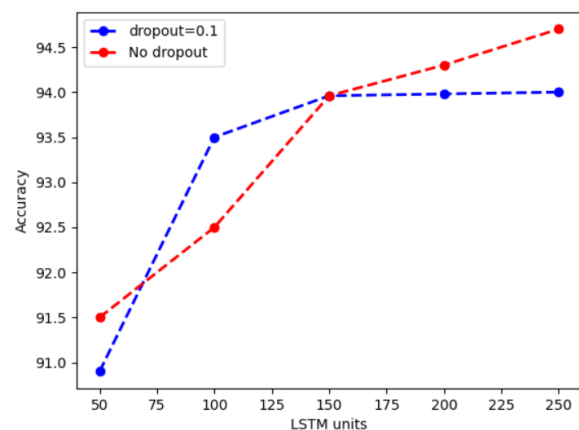


(b) Validation accuracy trends in four dropout rates

The model was run on a NVIDIA GEFORCE GTX 960M. The average Accuracy, Precision, Recall and F1-scores were reported. AUC scores are reported only for seizure detection on CHB-MIT dataset.



(a) Validation accuracy trends in five cross-validation iterations with and without a dropout layer



(b) Validation accuracy trends in five units number with and without a dropout layer

### 4.3.2 Experimental results

In this section, we will discuss the performance results of the proposed model based-on raw EEG data: attention-based deep LSTM, as described in section 4.2.1 and the basic deep LSTM model section 4.2.2. Two different classification problems based-on EEG signals are addressed to evaluate whether the integration of the proposed channel-wise attention mechanism

## Chapter 4. A novel region-aware attention with deep LSTM for EEG epileptic seizure classification

Table 4.2: Results on TUSZ dataset for seizure detection

Class	LSTM				LSTM-att			
	Accuracy	Precision	Recall	F1-score	Accuracy	Precision	Recall	F1-score
Seizure	88.40	88.40	88.45	88.42	97.01	97.01	96.39	96.69
Normal	86.25	86.25	86.72	86.48	96.56	96.56	97.24	96.89
Mean	87.32	87.08	87.39	87.59	<b>96.78</b>	<b>96.86</b>	<b>96.50</b>	<b>96.60</b>
Std	0.14	0.63	0.78	0.44	0.21	0.64	0.60	0.54
	AUC=0.913				AUC=0.976			

Table 4.3: Results on TUSZ dataset for seizure classification

Class	LSTM				LSTM-att			
	Accuracy	Precision	Recall	F1-score	Accuracy	Precision	Recall	F1-score
GNSZ	96.00	96.00	84.56	<b>89.91</b>	98.48	98.48	98.57	98.52
FNSZ	83.01	83.01	93.14	87.78	98.11	98.11	98.86	98.48
CPSZ	83.78	83.78	<b>94.57</b>	88.85	98.95	98.95	98.38	98.66
ABSZ	81.25	81.25	87.00	84.14	93.75	93.75	<b>100.00</b>	96.77
SPSZ	84.85	84.85	38.36	52.83	97.30	97.30	98.63	97.96
TCSZ	<b>100.00</b>	<b>100.00</b>	53.85	70.00	98.11	98.11	<b>100.00</b>	<b>99.05</b>
TNSZ	80.21	80.21	87.64	83.76	<b>100.00</b>	<b>100.00</b>	87.50	93.33
MYSZ	<b>100.00</b>	<b>100.00</b>	43.42	60.55	95.83	95.83	90.79	93.24
Mean	88.32	88.32	72.14	77.55	<b>98.41</b>	<b>97.86</b>	<b>96.02</b>	<b>96.87</b>
Std	0.26	0.26	1.30	0.96	0.18	0.90	1.06	0.78

is attractive for either method performance improvement and results explainability. Since the considered datasets are imbalanced in their nature, Accuracy, Precision, Recall and F1-score, the average and the standard deviation are used as evaluation metrics.

### 4.3.2.1 Evaluation on TUSZ for seizure detection and type classification

In seizure detection problem, the LSTM-att achieves an accuracy of  $96.78 \pm 0.21\%$  which outperforms the basic LSTM model of approximately 9.46% for the TUSZ dataset as illustrated in Table 4.2. To add, our LSTM-att reached a value 0.976 for AUC metric. Note that, the higher the AUC, the better the model is at distinguishing between patients with the seizure and no seizure. According to the training and validation loss curves depicted in Figure 4.5, the LSTM-att model does not suffer from overfitting problem.

For seizure type classification, the imbalanced issue is more highlighted than the seizure

## Chapter 4. A novel region-aware attention with deep LSTM for EEG epileptic seizure classification

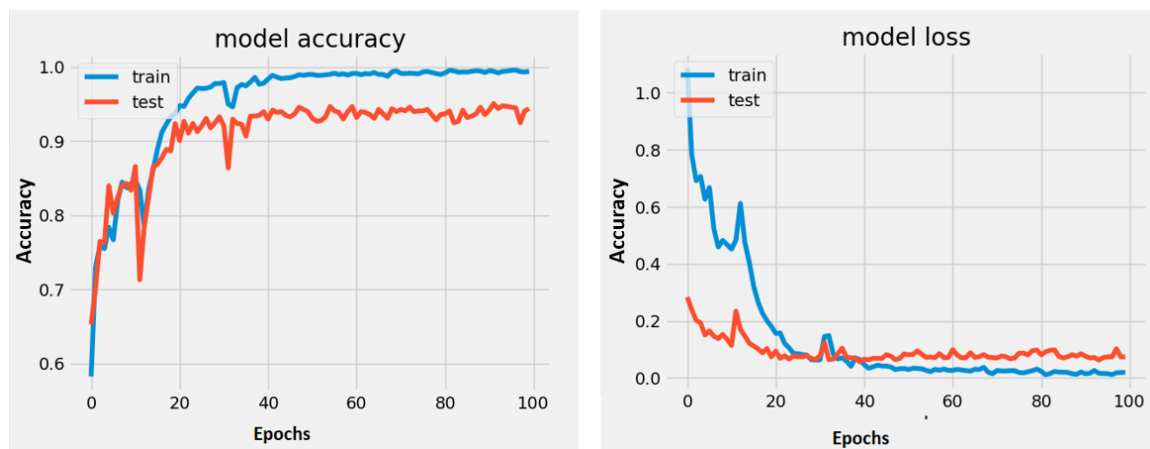


Figure 4.5: LSTM-att model performance in term of accuracy and loss for seizure detection with TUSZ dataset

detection. In this case, comparison is made using F1-score which is the harmonic mean of Precision and Recall and gives a better measure of the incorrectly classified cases than the accuracy metric. For instance, the LSTM model achieves 77.55% as F-score value while the LSTM-att model improved it by 19.32% as shown in Table 4.3.

The confusion matrix in Fig 4.6 highlights the classification performance of the LSTM-att model on 8 seizure types from TUSZ dataset. For example, MYoclonic Seizure (MYSZ) is confused with Focal Non-specific Seizure (FNSZ) and Complex Partial Seizure (CPSZ) with 1.39% and 2.78%, respectively. The highest accuracy achieved is with the Tonic seizure (TNSZ) class. However, the lowest accuracy is obtained for ABSZ class. The low count of absence seizures in the TUH dataset can account for this comparability, with just six recording minutes for the model to learn from..

According to the aforementioned results, it was shown that the model trained using learnt feature in combination with calculated weights generated by the attention layer produced higher accuracy compared to the basic LSTM model. For instance, these improvements show that the channel weights representing their contribution scores compliment the learnt features in better discriminating seizure classes.

In comparison with state-of-the art methods as illustrated in Table 4.4, our LSTM-att is the first work to consider seizure detection and type classification on TUSZ dataset using the channel-wise attention mechanism and LSTM model directly fed with EEG raw data. For seizure detection, our proposed model improved the AUC scores and accuracy with 2.68% and

## Chapter 4. A novel region-aware attention with deep LSTM for EEG epileptic seizure classification

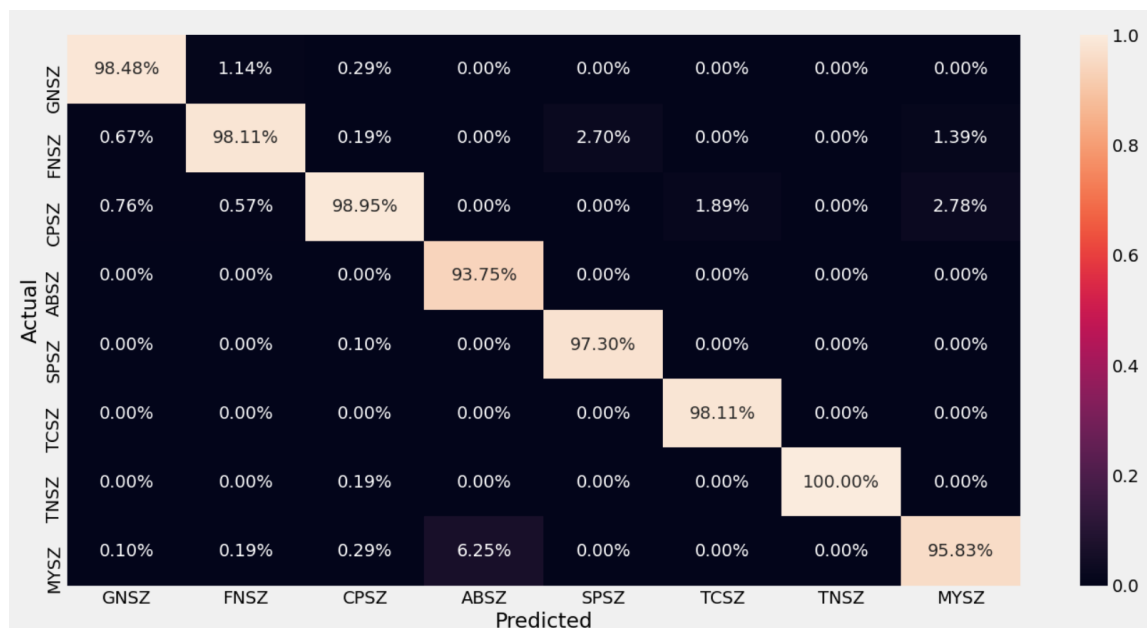


Figure 4.6: Confusion matrix of our LSTM-att model validated on TUSZ

16.28% compared to CNN fed raw data [Zhang et al., 2020b]. In the literature, there is no work for seizure type classification on TUSZ dataset using raw EEG data. Consequently, a comparison with feature-based methods [Ahmedt-Aristizabal et al., 2019] [Asif et al., 2020] is handled, where our model greatly outperforms them.

### 4.3.2.2 Evaluation on CHB-MIT for seizure vs normal classification

Seizure detection problem consists in seizure vs normal classification task. This part is validated on data from the CHB-MIT dataset. The latter does not allow us to validate the model for seizure type classification due to the lack of seizure type labeled data. Only the start and the end of each onset is indicated for whole data in CHB-MIT, making it only usable for seizure vs normal classification or for seizure prediction as done in our previous paper [Baghdadi et al., 2020b].

When tuning hyper-parameters for this binary classification task, we do not fix a number of epochs. Although, we configured a callback for early stop function in order to control the learning process and avoid over-fitting. As previously mentioned, We opted for a 5-fold cross validation splitting strategy. Firstly, we evaluated the rate of dropout layer by plotting its trend over cross validation iterations. As shown in Figure 4.4a, the accuracy is still not improved

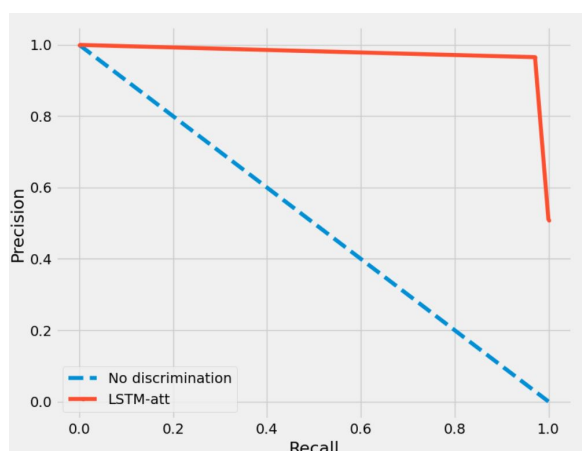
Table 4.4: Comparison with state-of-the-art methods validated on TUSZ dataset

Ref	Year	Input	Classifier	Results		
				F1-score	AUC	Accuracy
<b>Seizure detection</b>						
[Zhang et al., 2020b]	2020	Raw EEG	CNN	—	94.92	80.50
Ours	2021	Raw EEG	LSTM-att	96.60	<b>97.60</b>	<b>96.78</b>
<b>Seizure type classification</b>						
[Ahmedt-Aristizabal et al., 2019]	2019	EEG spectrograms	CNN	—	—	84.06
[Liu et al., 2020]	2019	Intensity values of STFT	Neural Memory Network	94.50	—	97.40
[Asif et al., 2020]	2020	EEG spectrograms	Extreme Gradient Boosting	70.70	—	—
[Baghdadi et al., 2021a]	2021	Raw EEG	LSTM-att	<b>96.87</b>	—	<b>98.41</b>

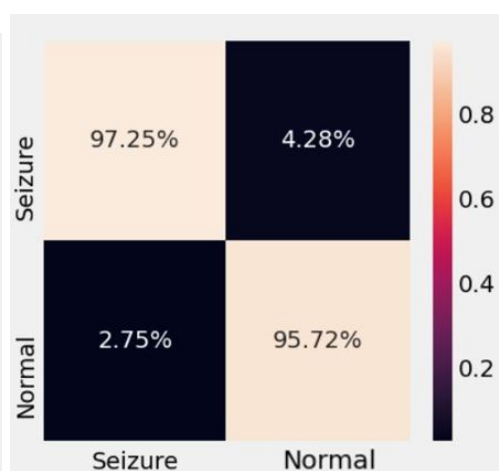
## Chapter 4. A novel region-aware attention with deep LSTM for EEG epileptic seizure classification

Table 4.5: Results on CHB-MIT dataset

Class	LSTM				LSTM-att			
	Accuracy	Precision	Recall	F1-score	Accuracy	Precision	Recall	F1-score
Seizure	87.47	88.00	84.15	86.03	97.25	97.25	95.88	96.56
Normal	89.33	85.24	89.66	87.39	95.72	95.72	97.65	96.67
Mean	88.40	86.50	87.35	86.44	<b>96.48</b>	<b>96.88</b>	<b>96.28</b>	<b>96.50</b>
Std	1.31	0.86	0.78	0.25	1.16	0.40	0.45	0.17
	AUC=0.916				<b>AUC=0.976</b>			



(a) Precision-Recall curve of seizure detection on TUSZ dataset



(b) Confusion matrix of seizure detection for the LSTM-att model with CHB-MIT dataset

Table 4.6: Comparison with state-of-the-art methods on seizure detection with CHB-MIT dataset

Ref	Year	Input	Classifier	Results		
				F1-score	AUC	ACC
[Yuan and Jia, 2019]	2019	Raw EEG	FusionAtt	89.53	96.22	<b>97.01</b>
[Yao et al., 2021]	2021	Raw EEG	BiLSTM-att	84.15	84.15	91.51
[Baghdadi et al., 2021a]	2021	Raw EEG	LSTM-att	<b>96.50</b>	<b>97.60</b>	96.48

from the CV=2 and it achieved the best value without a dropout layer (dropout rate=0.0).

According to Table 4.5, the LSTM model achieves an accuracy of  $88.40 \pm 1.31\%$ , while our LSTM-att model reaches  $96.48 \pm 1.16\%$ . In terms of AUC and F1-score, the LSTM-att model reached 97.60% and 96.50% with an improvement of approximately 6% and 10%, respectively. This can be explained by the fact that not all channels contribute equally to the decision of the presence or not of the seizure. The attention mechanism endows the LSTM model with a capability of weighting the channels such that they contribute differently and individually in

## Chapter 4. A novel region-aware attention with deep LSTM for EEG epileptic seizure classification

---

each EEG sample to make the final decision.

To further understand the LSTM-att behavior, the confusion matrix is plotted as shown in Figure 4.7b. Actually, the model missclassified 2.75% of the seizure samples as normal and 4.28% of the normal samples as seizure. In general, the proposed model is able to classify 97.25% correctly of seizure cases and 95.72% of normal cases. The achieved results are encouraging.

Table 4.6 illustrates the comparison with raw data-based works for seizure detection. While bidirectional parsing of EEG signals tends to collect richer information, our LSTM-att model outperforms the BiLSTM-att model [Yao et al., 2021] with an improvement of 12.35%, 12.45% and 4.97% for F1-score, AUC, and accuracy metrics, respectively. Another work known as FusionAtt achieves similar results on AUC and accuracy metrics compared to our LSTM-att model, but it degrades in term of F1-score with a percentage of 6.97%. We conceptualized our attention mechanism to recognize different brain region signals and to produce various weights across channels. A single patient may experience seizures in different types from various brain regions. Accordingly, it is more reasonable to adaptively calculate channel weights in our attention mechanism. In our method, a kernel matrix and a bias matrix are trainable parameters, which undergo transformations by combining them with data segments. The transformation outputs represent the segment attention weights. If a channel weight is close to 0, it indicates that the corresponding signal characteristics are comparably weak to characterize a seizure type. This does not entail a lack of contribution of the corresponding channel to this seizure type. EEG signal manifestations vary between the seizure-free segment and the onset segment according to the brain region contribution. In our seizure detection experiments, we observed that channels having great differences between seizure and normal signals were assigned rather large weights

An example of attention weights of 18 channels for a set of seizure segments is shown in Figure 4.8. The channels P7, C3, P3, FP2, F4, C4, O2, F8 and Cz have the large weights compared to other channels.

Since epileptic seizures have a patient-dependent characteristics, the plot of randomly selected ictal can't provide a relevant interpretation about the channels contribution on seizure detection for each patient. For this purpose, the model should be trained with patient-related

## Chapter 4. A novel region-aware attention with deep LSTM for EEG epileptic seizure classification

data separately in order to plot and interpret the attention weights learnt by the model. Based on the results shown in Figure 4.8, we can only deduce that for the randomly selected set of seizures, the aforementioned channels having the highest scores contribute the most to detecting seizure Vs normal segments.

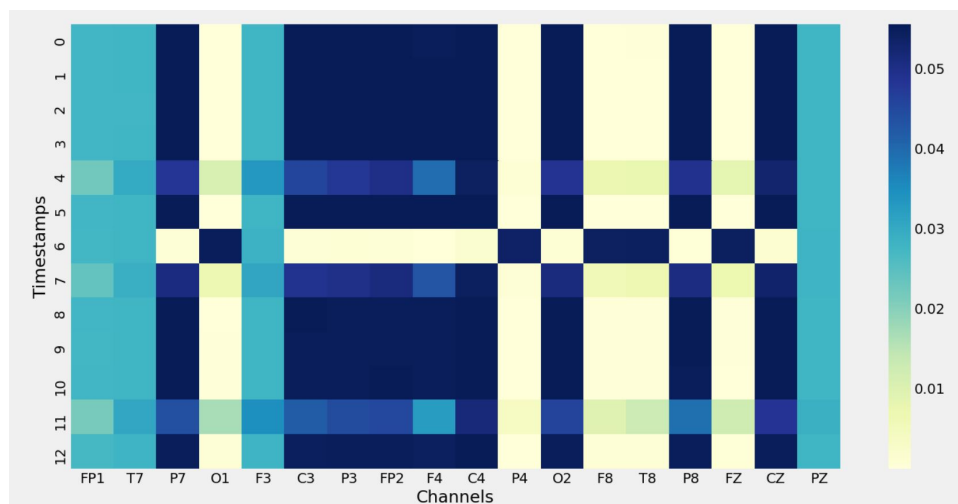


Figure 4.8: Mean attention weights on channels for a set of seizure samples from CHB-MIT

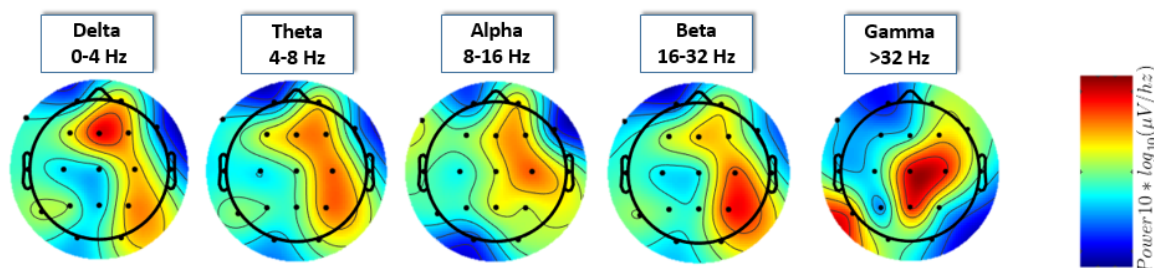


Figure 4.9: EEG bands topographical distribution of an ictal segments from the CHBMIT dataset

By analysing several Heatmaps related to seizure type classification, we observed that for different timestamps, the attention scores learnt by the attention mechanism are different. Specifically, when the seizure is generalized or begins as a focal and ends generalized, the distribution of attention scores are relatively uniform. This is because no such ictal pattern related to the seizure type is found within the whole channel views and hence the attention scores make even contribution to the seizure type classification. For some seizure types, we remarked that the attentional representations have the same view, then they depend on the seizure type.

## Chapter 4. A novel region-aware attention with deep LSTM for EEG epileptic seizure classification

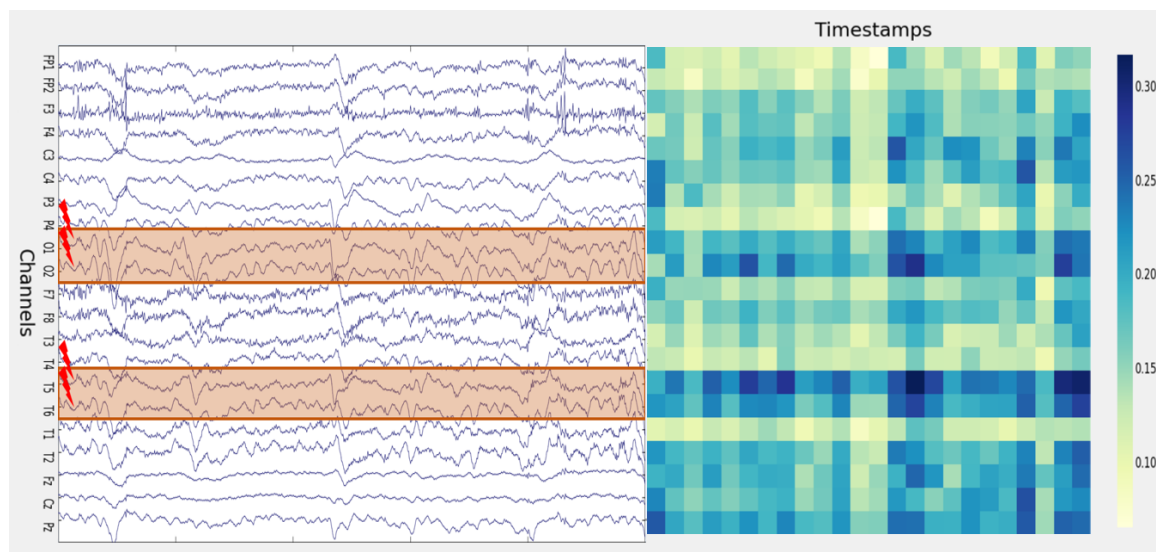


Figure 4.10: Left: Visualization of a multi-channel signal containing a Focal Non-specific seizure from TUSZ, Right: Correspondent Heatmap of calculated weights

According to the session-wise description attached to the data, there are a significant correlation between the neurological comments and our results. The larger attention score means the probability of seizure onset on this area is higher. In summary, the case study indicates that we can learn accurate attention scores with interpretable representations by our channel-wise Attention-based model, which not only improve the detection performance, but also identify the influential clinical concepts of seizure onset in healthcare. In our experiments, it was observed that relatively large weights were assigned to channels that contribute to characterize a specific seizure type. For this example of a Focal Non-Specific seizure, the neurologist reported a Nonconvulsive status epilepticus in a patient with a drug resistant epilepsy. The EEG plotted on the top of the Figure 4.13 demonstrates continuous 3 Hz bilateral temporo-occipital seizure activities, which coincided with the attention weights of 21 channels for correspondent seizure segments. The channels (O1,O2) and (T5,T6) have the large weights compared to other channels at the seizure start. The comments of the neurologist when reading the correspondent EEG signal correlate with our findings. Regarding a reported temporo-occipital origin, we demonstrated that the high weights are assigned to channels in this brain location as shown in the Figure 4.14.

Since there is no specific lobe that includes the median line channels (Fz,Cz and Pz), these ones are almost affected by the seizure, which explains the implication of these channels in the

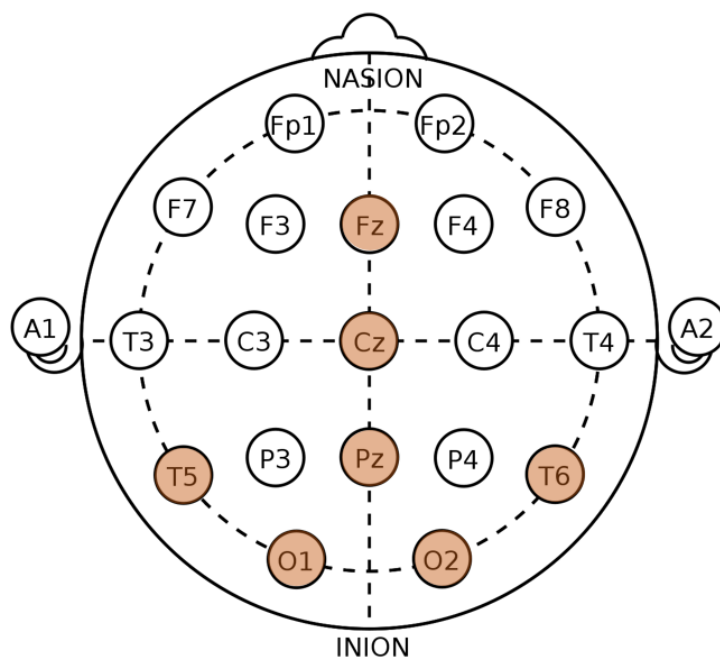


Figure 4.11: Position of high-weighted channels: Fz, Cz, Pz, (O1,O2) and (P5,P6) according to the 10-20 electrode system placement.

seizure type classification. As shown in the Heatmap of Figure 4.14, a medium level of scores is attributed to Fz,Cz and Pz.

## 4.4 Cases study

### 4.4.1 Myoclonic seizure

In this subsection, we discuss the learnt contribution scores in LSTM-Attention to justify the benefit of adopting the attention mechanism in clinical settings. Figure 4.13 presents a clinical case study of multi-channel EEG seizure type detection on the TUSZ dataset where a Myoclonic (MYSZ) epileptic seizure occurs. We display the scores of all fragments for the visualization.

In a Myoclonic seizure, jerking or twitching movements occur in the arms, legs, or upperbody. The figure 4.13 is a plot of a segment containing 5 myoclonic seizures manifested by a central spike waves.

Clinical history: 61 year old male status post code 06/14 for 10-15 minutes, now with my-

## Chapter 4. A novel region-aware attention with deep LSTM for EEG epileptic seizure classification

oclonic movements, DNR1, small cell lung cancer, DVT, VDRF, diabetes.

Description of the record: The background EEG is markedly abnormal. There is myoclonic activity with a high amplitude generalized poly spike activity. The activity is relatively symmetric and is posteriorly predominant. When it abates, there seems to be a focus of right delta. The epileptiform activity is associated with jerking of the chin and chest. Stimulation of the patient does not activate the record. The background is variable and consists of either a very suppressed pattern or a pattern with some 8 hertz alpha frequency activity which is probably part of the patient's ictal pattern.

Impression: Abnormal EEG due to a form of myoclonic status epilepticus with focal jerking, which demonstrates frequency evolution.

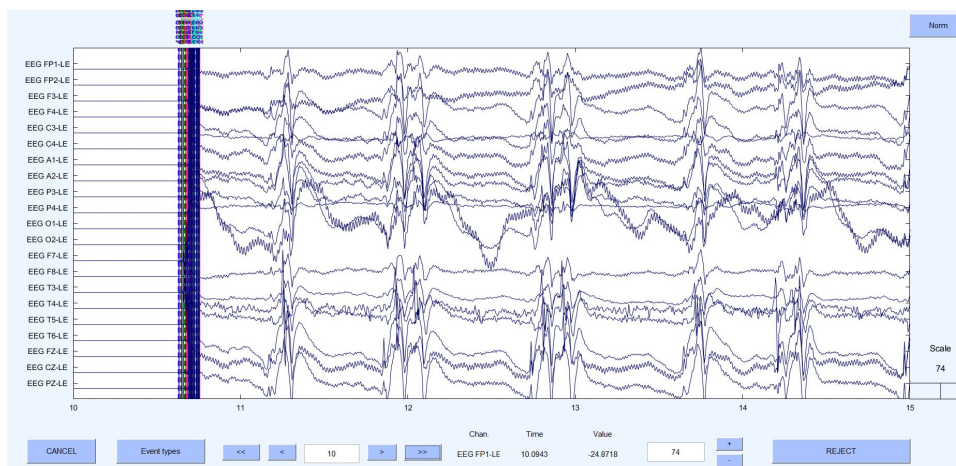


Figure 4.12: Visualization of a multi-channel signal containing a seizure from TUSZ: Myoclonic seizure

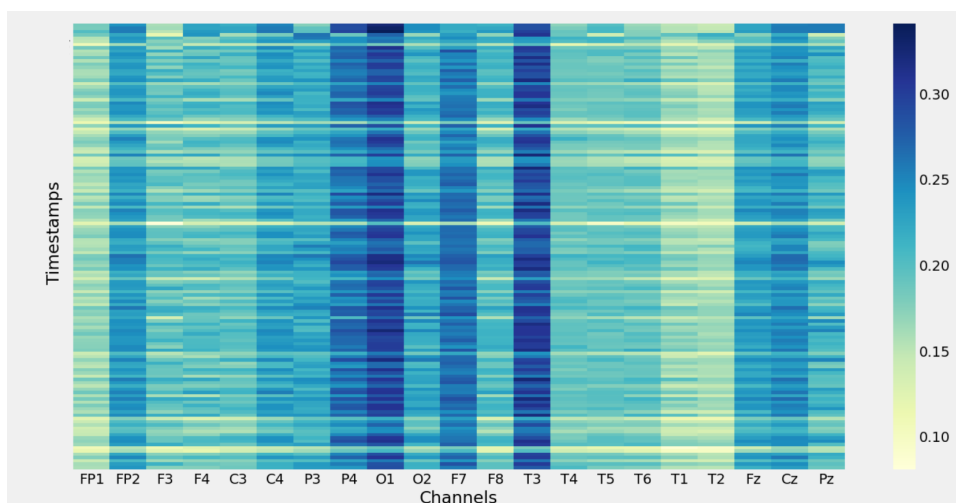


Figure 4.13: Heatmap of calculated weights of a Myoclonic seizure

## Chapter 4. A novel region-aware attention with deep LSTM for EEG epileptic seizure classification

The attention mechanism captures signal characteristics and assigns large weight values to the channels, which could distinguish between different seizure types. In our experiments, it was observed that relatively large weights were assigned to channels that contribute in characterizing a specific seizure type. For this example of a Myoclonic seizure, attention weights of 21 channels for a MYSZ seizure segments are shown in Figure 4.13; the channels of O1, T3, P4, F7, Fz, Cz, Pz and FP2 have the large weights compared to other channels. The comments of the neurologist when reading the EEG signals of this seizure correlate with our findings. Regarding a reported central posterior origin, we demonstrate that the high weights are assigned to channels in this location of the brain as shown in the Figure 4.14.

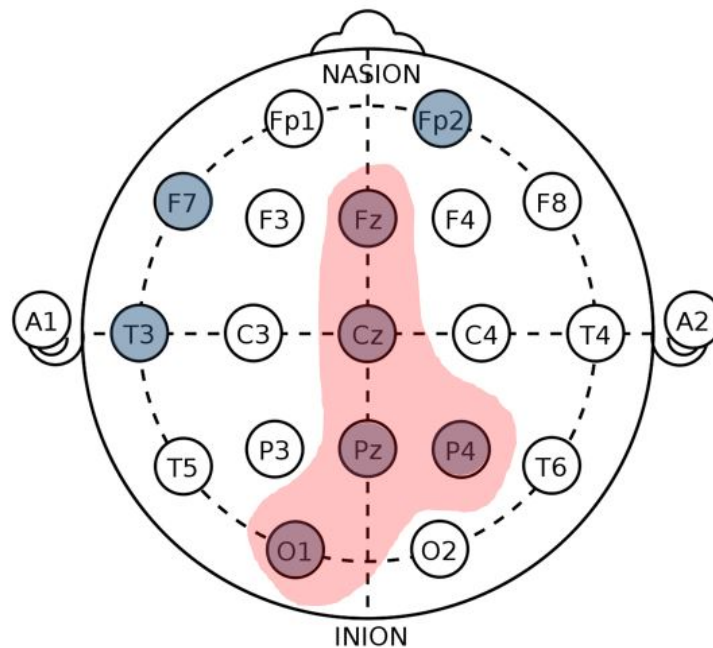


Figure 4.14: Position of high-weighted channels according to the 10-20 electrode system placement. Fz, Cz, Pz, O1 and P4 are central and posterior channels

### 4.4.2 Tonic-clonic seizure

Clinical infos: Continuous video EEG monitoring is performed in the unit. One seizure was recorded overnight.

Random wakefulness and sleep: In wakefulness and sleep, the background EEG remains poorly organized. There is rhythmic, sharply contoured delta activity, some of which demonstrates a

## Chapter 4. A novel region-aware attention with deep LSTM for EEG epileptic seizure classification

double phase reversal in the left frontocentral region.

Precise localization is challenging and the activity seems to emanate relatively symmetrically from the frontocentral regions with a generalized pattern at onset. The primary localizing feature is the behavior with elevation of the left arm and at the very, very onset of the seizure almost a fencer-like posture, but with more characteristic tonic-clonic activity on the right. However, it must be noted that the patient turns to the left at the onset of the seizure and then turns back to the right later on, again, raising concerns about actual localization of the seizure.

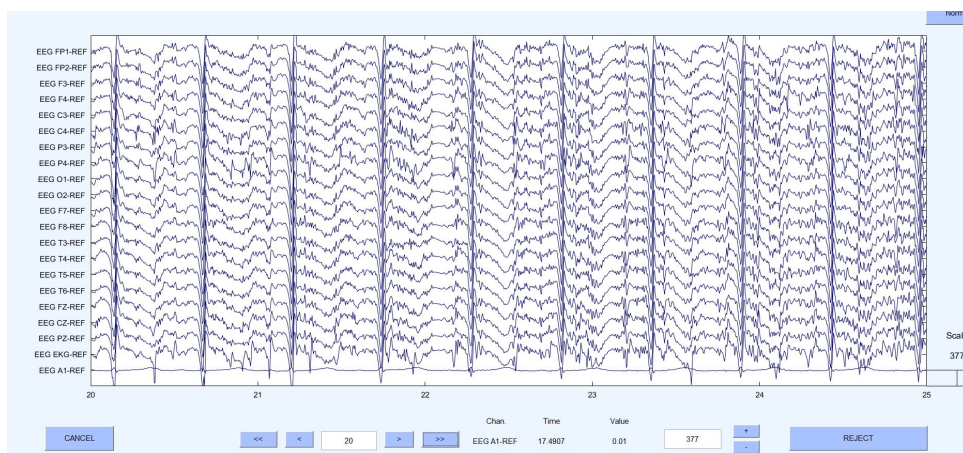


Figure 4.15: Tonic-Clonic seizure

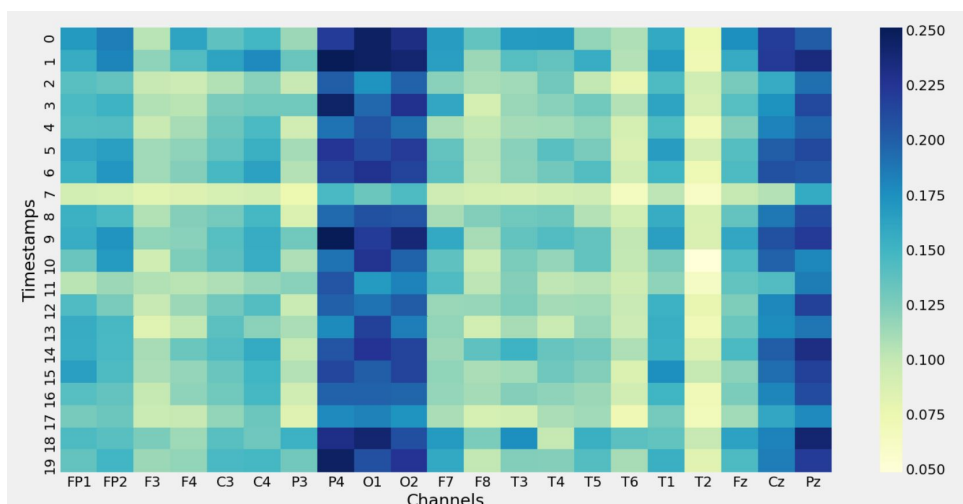


Figure 4.16: Heatmap of calculated weights of a tonic-clonic seizure

In this example, the patient experienced a Tonic-Clonic seizure that starts from the fronto-central region but patterns are generalized. The fast transition from focal to generalized seizure

## Chapter 4. A novel region-aware attention with deep LSTM for EEG epileptic seizure classification

---

is not captured by our model, and this can be justified in two ways: The transition is too fast and may be for a few short seconds, so it ignored when learning features and weights. The generalized pattern of poly-spikes is more dominant. For this example of a Tonic-Clonic seizure, attention weights of 21 channels for a seizure segments is shown in Figure 4.16, the channels of O1, O2, P4, Cz and Pz have the large weights compared to other channels, which do not correlate with the comments of the neurologist. Weights can be affected to the channels that contribute the most in identifying the type of the seizure and can not give a relevant information about the onset localisation, in particular in the case of a seizure with generalized pattern as in this example. Figure 4.17 shows us the position of the high weighted channels according to the 10-20 system.

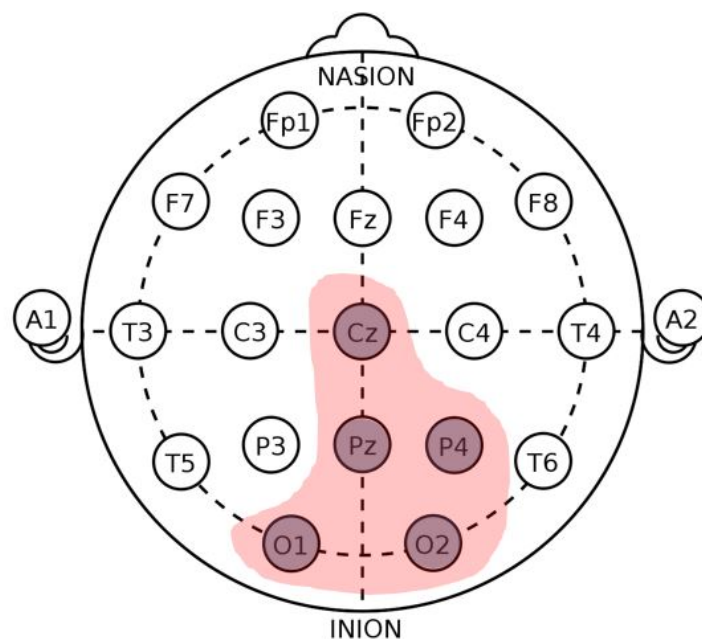


Figure 4.17: Position of high-weighted channels according to the 10-20 electrode system placement. P4, O1, O2, Pz and Cz are central and posterior channels

### 4.4.3 Complex partial seizure

Clinical history: 52 year old right handed male with head trauma, epilepsy, evaluate for 2-3 days. Change in mental statue.

Approximately 10 seconds into the arousal state with the bilateral alpha as the patient becomes agitated, more rhythmic 4-5 hertz activity emerges from the left central and parietal regions.

## Chapter 4. A novel region-aware attention with deep LSTM for EEG epileptic seizure classification

Impression: Abnormal EEG due to Complex partial status epilepticus characterized by recurrent seizures from the left hemisphere although they do begin with some bilateral fast activity.

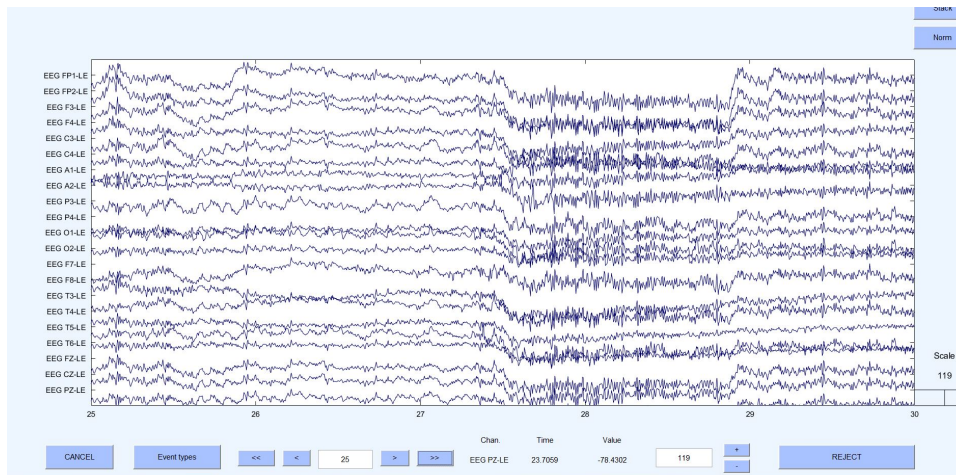


Figure 4.18: Complex partial seizure

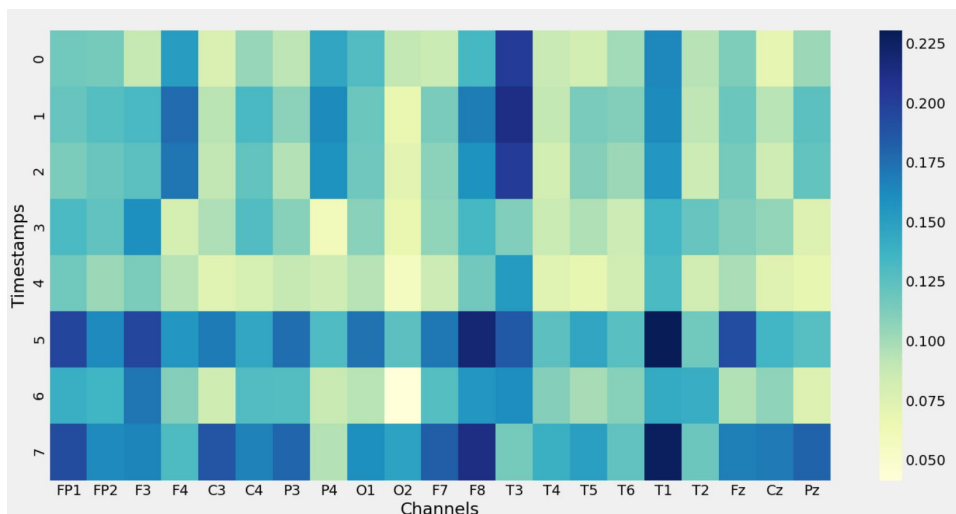


Figure 4.19: Heatmap of calculated weights of a complex partial seizure

By analyzing the Figure 4.19 we can observe that the highest attention is affected to the channel T3 for 15 seconds. After the 15 first seconds, the weights have a similar distribution over all channels. But we can observe a slightly dominance on the left hemisphere (impaired channel, like FP1 against FP2, F3 vs F4 ...). The interpretation of our results by the neurologist confirms that the biggest attention is allowed to the channels that mark the most changes on their signals and have more information about it.

## **4.5 Conclusion**

Classification of epileptic seizures has been a challenge for neurologists diagnosing epilepsy, prescribing treatment and arriving to a prognosis. The automated seizure classification method proposed in this chapter can assist clinical professionals in diagnosing the disease, reducing time and potentially improves accuracy and reliability

This chapter proposes a novel channel-wise attention-based deep LSTM model which demonstrates the capability of the attention layer in enhancing the classification performance. An explainability analysis of our model showed that a high correlation exists between neurological interpretation and the reading of the Heatmaps of the learnt features. The LSTM-attention model achieves a significant improvement in classification accuracy up to 98.41% on the TUSZ dataset for 8 types of epileptic seizures and 96.78% for a binary classification (seizure vs Normal). The model also generalizes well across different minority seizure types.

Future works can focus on improving the performance of this study for the minor classes, by using multi-modal data, primarily EEG videos.

# A spatio-temporel attention network for epileptic seizures prediction from EEG signals

---

## Contents

---

<b>5.1</b>	<b>Introduction</b>	<b>99</b>
<b>5.2</b>	<b>Epileptic states</b>	<b>100</b>
5.2.1	Interictal state	100
5.2.2	Preictal state	100
5.2.3	Ictal state	101
5.2.4	Postictal state	101
<b>5.3</b>	<b>Preictal biomarkers</b>	<b>102</b>
<b>5.4</b>	<b>Method</b>	<b>103</b>
5.4.1	Feature extraction	104
5.4.1.1	Extraction of statistical moments	104
5.4.1.2	Extraction of spectral power features	106
5.4.2	Spatio-temporal representation based on Convolutional Long Short-Term Memory model	107
5.4.2.1	Hyperparameters	110
5.4.3	Attention-based ConvLSTM model	111
<b>5.5</b>	<b>Experimental results and discussion</b>	<b>114</b>
5.5.1	EEG dataset and data preparation	115
5.5.2	Results on patient-dependent epileptic seizure prediction	116
5.5.2.1	Experimental set up	116
5.5.2.2	Results and discussion	119
5.5.3	Results on subject-independent epileptic seizure prediction	123
5.5.3.1	Hyperparameter settings	123
5.5.3.2	Results and discussion	124

## Chapter 5. A spatio-temporel attention network for epileptic seizures prediction from EEG signals

---

5.5.3.3 Model interpretability: a case study . . . . .	128
<b>5.6 Conclusion . . . . .</b>	<b>130</b>

---

### 5.1 Introduction

To conceptualize a robust EEG-based epileptic seizure prediction system, it is important to respect the common machine-learning approaches for epileptic states recognition. This process includes in general, an acquisition step in which EEG signals are recorded from epileptic patients. A preprocessing phase aiming to remove baseline and artifacts, a feature extraction and a classification steps. Recently and by the mean of deep learning approaches, the process was renewed by including a feature learning step instead of the handcrafted features.

Unlike the basic LSTM model, which is restricted to the temporal information learning, we propose the recent improvement of LSTM, ConvLstm replacing the matrix multiplication with convolution operation at each gate in the LSTM cell. Thus, it captures underlying spatial features by operations convolution on the EEG signal. In addition, we aim to investigate more about the importance of each preictal segment in the detection of an incoming onset, which is very important to recognize the triggers of seizures and relatives events. To allow this analysis, we add the segment-wise attention mechanism producing an interpretable output to automate feature learning or representation learning, i.e. a transformation of the contribution of each segment of raw data input into scores or weights to discover the most relevant segments that can be effectively exploited for the EEG-based Seizure prediction task. To evaluate the robustness of our model, we have also extracted the statistical moments features in the time domain and Power bands features in the time-frequency domain in order to compare basic features and the representations from the basic LSTM model with the proposed spatio-temporal representation and their impact on the classification performance. It is to note that our approach is based on raw EEG data with no further preprocessing step. The choice of this strategy is based on the amount of relevant information existing in a raw signal. In addition, preprocessing techniques have major issue when dealing with epileptic signals, thus, it can remove relevant information by miss-classifying artifacts and seizures. In this chapter, we introduce some preliminaries re-

## **Chapter 5. A spatio-temporel attention network for epileptic seizures prediction from EEG signals**

---

lated to the seizure prediction field. Then, we detail in the section 5.4 the proposed approach including feature extraction and convolutional Lstm feature learning parts. Section 5.5.1 illustrates the experiment results and the discussion.

### **5.2 Epileptic states**

The different stages of an epileptic seizure are referred to as ictal states. These states represent the different stages of an epileptic seizure in its most general sense [Pitkänen et al., 2017].

#### **5.2.1 Interictal state**

The interictal state designates the normal resting state with no seizure activity, but the EEG is still defined by the irregular neuronal activity. Considering the likeliness of seizures, the chronic interictal period is important due to the presence of natural homeostatic mechanisms preventing seizure generation. The mechanisms or factors helping maintain homeostasis in the brain are still unidentified, as well as whether these mechanisms differ for various epileptic syndromes and types of seizures. This period comprises more than 99% of patients' lives. As such, the interictal period can be exploited by neurologists in the purpose of diagnosing an epileptic condition. Some abnormalities and small spikes would normally appear in the EEG tracings, which are defined by neurologists as subclinical seizures. These are not real seizures, but rather little hints from the brain that something is abnormal [Pitkänen et al., 2017].

#### **5.2.2 Preictal state**

The preictal state does not refer to the normal state of the brain but rather to a period of time occurring before a seizure. The said state suggests that a seizure might occur within a certain time-frame [Pitkänen et al., 2017]. The notion that a preictal period exists is still a subject of debate by numerous researchers. Lehnertz and Litt specify that, in certain conditions, the transition between preictal and ictal states might be lengthy, enabling the seizure prediction using EEG techniques anywhere prior to the occurrence of the onset [Litt and Lehnertz, 2002]. It is defined by an abrupt change in the EEG's frequency characteristics. Alpha bands are likely

## **Chapter 5. A spatio-temporel attention network for epileptic seizures prediction from EEG signals**

---

to increase in amplitude and decrease in frequency. A gradual change from cluttered to regular waveforms is observed in the transition from the preictal to the ictal state. The transition may present major different characteristics and the transitional period can vary, depending on the type of epilepsy [Pitkänen et al., 2017].

### **5.2.3 Ictal state**

The ictal state refers to the time period during which the onset occurs. It is defined by higher amplitudes and frequencies. An alteration in rhythmicity and synchronization can be witnessed over multiple areas of the cerebral cortex [Sackellares, 2008]. Patterns, which are commonly seen all over the tracing for a resting state, abruptly become unpredictable and erratic. Involuntary muscle twitching and a loss of consciousness during this state is completely common, along with other symptoms like a lack of self-control. The patient generally loses control of his body at this stage and convulsions tend to be noticeable [Pitkänen et al., 2017].

### **5.2.4 Postictal state**

The end of an epileptic seizure represents a transition from the ictal state back to an individual's normal, or interictal state. This is referred to as the postictal state and signifies the recovery period of the brain. Focal or generalized neurological deficit, ranging from postictal depression to aphasia or paralysis is prevalent during this state. This period is associated with a difficulty in thinking clearly and a variety of other cognitive defects. The postictal state could last from seconds to hours depending on the severity of the seizure and the efficacy of the AEDs. Disturbances or aftershocks are seen in the EEG, which may just be the presence of natural mechanisms acting to terminate the seizure and restore homeostasis [Pitkänen et al., 2017]. Often postictal deficits are a consequence of the natural mechanisms that act to terminate a seizure suggesting that interventions designed to exploit these same homeostatic events could exacerbate postictal dysfunction [Pitkänen et al., 2017]. Attention and concentration is generally very difficult during this period. Poor short term memory and decreased verbal and interactive skills are noticeable. Postictal migraine headaches are very common due to the pressure resulting from cerebral edema. At this point, patients are unaware that they have had a seizure, but these

symptoms are evidence enough for an experienced epileptic [Pitkänen et al., 2017].

### 5.3 Preictal biomarkers

The preictal state is defined by a range of characteristics that occurs in the period immediately preceding a seizure and does not occur at another time. Expert neurologists may distinguish visually some of those characteristics that are apparent in the EEG signal. Otherwise, biomarkers may not be apparent and only an analysis of changes in the underlying EEG signal can lead to the identification of those biomarkers. Characteristics values range changes within the different phases of an epileptic signal and simplify the development of an alarm system for seizures prediction. Regarding the complex nature of EEG signal, the use of Raw data rather than characteristics for an alarm system is not recommended. Algorithms based on a predefined sets of features may work with some persons better than other regarding that biomarkers are patient-specific. The use of raw data allows for a large-range investigation of signal characteristics and open the space for the development of non sensitive systems face to patients variability, and even within the same patient.

The EEG signal is traditionally expressed in terms of particular frequency bands: Delta (less than 4 Hz), Theta [4-8 Hz), Alpha [8-13 Hz), Beta [13-30 Hz), and Gamma (equal or greater than 30 Hz). Mormann et al. [Mormann et al., 2005] indicated the relative decrease in the power of the Delta band in preictal period in comparison with the interictal period, which was accompanied by a relative increase of the power in other bands. The spectral power of raw EEG signal has been investigated by several studies, and proved the ability to track the transient changes from interictal to ictal states ([Cerf et al., 2000], [Mormann et al., 2005], [Park et al., 2011], [Bandarabadi et al., 2013], [Rasekhi et al., 2013]).

## Chapter 5. A spatio-temporel attention network for epileptic seizures prediction from EEG signals

---

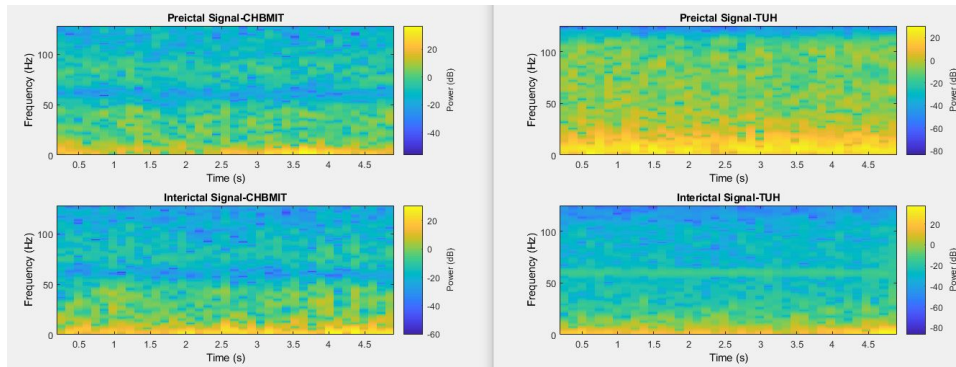


Figure 5.1: Spectrum of two random signals from CHB-MIT and TUH EEG Corpus, Segment of 5 seconds and channels are averaged

### 5.4 Method

The block diagram of the proposed seizure prediction method is depicted in Figure 5.2, where prediction relies on the classification model (ML or DL) with the aim to discriminate different states in the input EEG signal. The diagram also includes a step of feature extraction using 5-sec windows following the preprocessing unit, as well as a decision-making module for alarm generation. As seen in Figure 5.2, the first approach is based on a feature extractor applied to the windowed raw EEG signal, and the resulting combination of features is fed to the classifier to discriminate the resulting sequence into the two predefined brain states (preictal, interictal). The second approach is based on ConvLSTM for feature learning and classification. Thus, the input is a raw EEG signal passed with no further preprocessing to the attention-based ConvLSTM model to learn relevant features. These characteristics are classified by the final layer of the ConvLSTM model to detect the target class.

## Chapter 5. A spatio-temporel attention network for epileptic seizures prediction from EEG signals

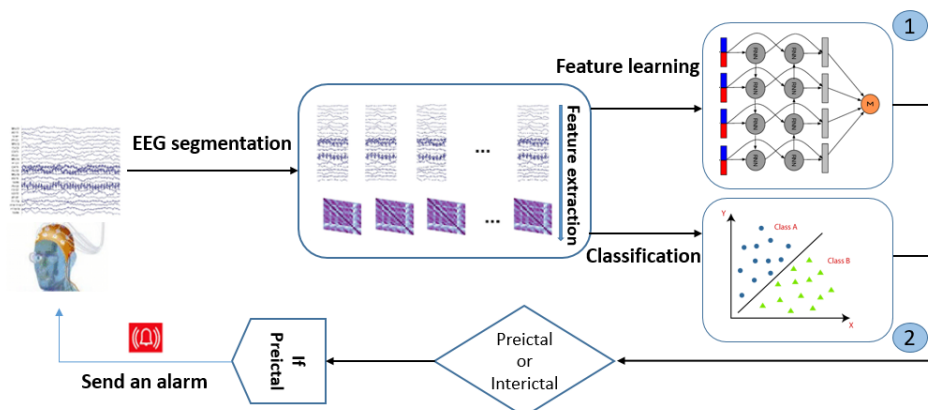


Figure 5.2: Overall diagram of the proposed method comprising the two approaches for seizure prediction

### 5.4.1 Feature extraction

#### 5.4.1.1 Extraction of statistical moments

The four statistical moments of mean, variance, skewness and kurtosis, also known as first, second, third and fourth moments respectively, provide information about the amplitude distribution of the time series. Skewness and kurtosis reveal information on the shape of the distribution, whereas mean and variance provide information on the location and variability (spread, dispersion).

Ideally, skewness is zero for symmetric amplitude distributions, and kurtosis measures the relative peakedness or flatness.

Studies have been made in [Mormann et al., 2005] employing these statistical measures to verify their ability to distinguish between the interictal and preictal periods using iEEG data. Also variance and kurtosis have shown significant changes in preictal period in comparison to the interictal period (a decrease for variance and an increase for kurtosis). As far as the time domain features are concerned, the four statistical moments are computed (i.e., mean value, variance, skewness and kurtosis), as well as the total signal area, peak-to-peak value (i.e. minimum to maximum), number of zero crossings and decorrelation time (i.e. time of first zero-crossing of the autocorrelation function).

Despite the simplicity of these measures, significant variations have been previously re-

## Chapter 5. A spatio-temporel attention network for epileptic seizures prediction from EEG signals

---

ported when entering the preictal state, with variance and decorrelation time decreasing compared to their respective interictal values, while kurtosis was found to increase towards seizure onset.

**Variance:** Variance is the measure of how the data is spread out from the mean. In EEG signals, variance signifies the change of amplitude, therefore conveying information of the general state of the brain, such as low difference from the mean describing low electrical activity and vice versa. The variance of each signal window has been calculated as shown in Equation 5.1

$$(\sigma^2)^{(n,m)} = \frac{\sum_i (x_i^{(n,m)} - \bar{x}^{(n,m)})^2}{L-1} \quad (5.1)$$

where  $x_i^{n,m}$  is the  $i^{th}$  point and  $\bar{x}^{n,m}$  is the mean of the  $n^{th}$  window and  $m^{th}$  EEG subcomponent.  $L$  is the length of the signal segment.

**Skewness:** Skewness is a dispersion measure which represents the asymmetry of a distribution [50]. In the case of EEG signals, negative or positive skewness reflects the dominance of larger or smaller amplitude values, respectively. Skewness of the  $m^{th}$  subcomponent in the  $n^{th}$  window is computed as shown in Equation 5.2

$$\alpha^{(n,m)} = \frac{1}{(\sigma^3)^{(n,m)}} \sum_{i=0}^{L-1} (x_i^{(n,m)} - \bar{x}^{(n,m)})^3 \quad (5.2)$$

**Kurtosis:** The flatness or the peakedness of the distribution of the EEG signals are measured by the kurtosis of each window [51]. In this sense, given the relation of EEG peaks to epileptic seizures, kurtosis relays information on the epileptic status of the EEG signal. Kurtosis of the  $n^{th}$  window's  $m^{th}$  subcomponent is calculated as in Equation 5.3

$$\beta^{(n,m)} = \frac{1}{(\sigma^4)^{(n,m)}} \sum_{i=0}^{L-1} (x_i^{(n,m)} - \bar{x}^{(n,m)})^4 \quad (5.3)$$

### Zero crossing:

Refers to the number of zero-crossing occurrences representing a change from negative to positive value or from positive to negative value [Elgohary et al., 2016]. The zero-crossing algorithm analyzes EEG dynamics based on the successive change of the waveform from negative to positive. It is known for its robustness against noise and artifacts where it removes some of

## Chapter 5. A spatio-temporel attention network for epileptic seizures prediction from EEG signals

the irrelevant components. It corresponds to the variation of the direction of the input signal between the interictal and the preictal states [Selim et al., 2019]

### 5.4.1.2 Extraction of spectral power features

In addition, the spectral information of the EEG signals is also taken into consideration, since various frequency domain features are also extracted including the total energy spectrum and the energy percentage across the fundamental rhythmic bands (i.e., Delta: 1–3 Hz, Theta: 4–7 Hz, Alpha: 8–13 Hz, Beta: 14–30 Hz, Gamma1: 31–55 Hz and Gamma2: 65–110 Hz).

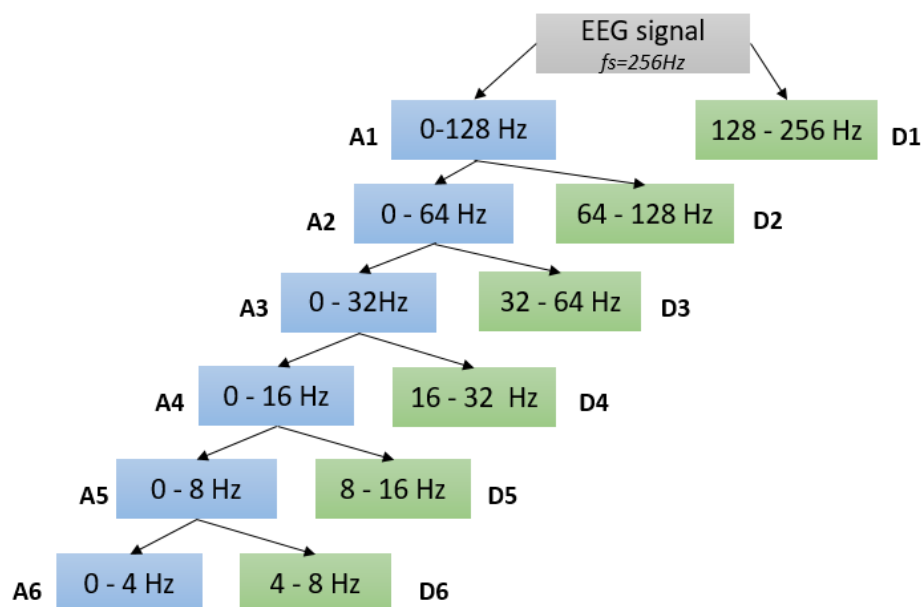


Figure 5.3: 6 levels decomposition of the original EEG signal, the decomposition level was chosen based on the frequency sampling.  $fs=256$  Hz

The EEG signal energy in each frequency band is extracted using the Discrete Fourier Transform (DFT). Along with DFT, the Discrete Wavelet Transform is also applied using a 6-level decomposition and the Daubechies 4 (db4) as the mother wavelet, to extract the detail (128-256 Hz, 64–128 Hz, 32–64 Hz, 16–32 Hz, 8–16 Hz, 4–8 Hz, 0–4 Hz) and approximation coefficients. Discrete wavelet transform (DWT) is a signal processing technique, which proceeds by the decomposition of the signal into different levels of approximation and detail corresponding to different frequency bands. It also keeps the temporal information of the signal. Compromise is done by downsampling the signal for each level. Correspondence of frequency bands and

## Chapter 5. A spatio-temporel attention network for epileptic seizures prediction from EEG signals

Table 5.1: EEG signal frequency bands and decomposition levels at  $f_s=256$  Hz

Bandwidth (Hz)	Frequency Band	Decomposition Level
0-4 Hz	Delta ( $\delta$ )	A6
4-8 Hz	Theta ( $\theta$ )	D6
8-16 Hz	Alpha ( $\alpha$ )	D5
16-32 Hz	Beta ( $\beta$ )	D4
32-64 Hz	Gamma1 ( $\Gamma_1$ )	D3
64-128 Hz	Gamma2 ( $\Gamma_2$ )	D2
128-256 Hz	HFO	D1

wavelet decomposition levels depends on the sampling frequency. In our case, the correspondent decomposition is given in the last column of Table 5.1 for  $f_s=256$  Hz.

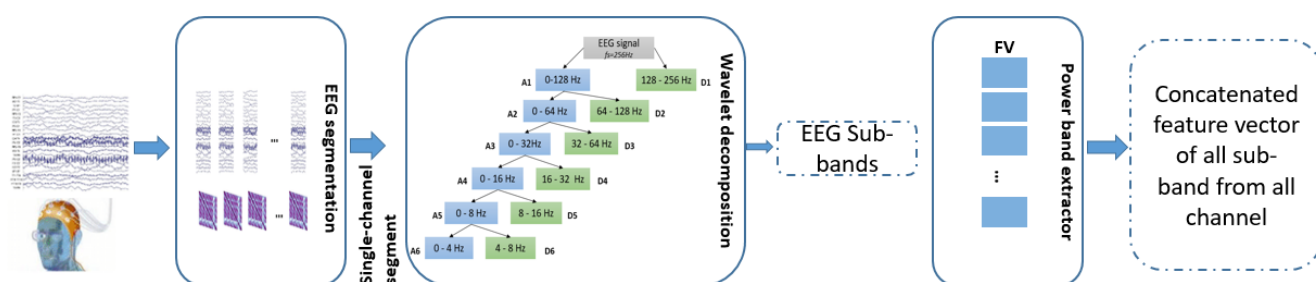


Figure 5.4: Power bands feature extraction

The 6-level decomposition is selected based on the 256 Hz sampling frequency used when assembling the CHB-MIT database, as it is the minimum depth required to cover the fundamental frequency bands and allow for the separation of below the 1 Hz that is most predominantly occupied by artifacts[Tsiouris et al., 2018].

### 5.4.2 Spatio-temporal representation based on Convolutional Long Short-Term Memory model

ConvLSTM is a variant of LSTM (Long Short-Term Memory) containing a convolution operation inside the LSTM cell. Both models are a special kind of RNN, capable of learning long-term dependencies. Shi et al. [Xingjian et al., 2015] treated precipitation nowcasting

## Chapter 5. A spatio-temporel attention network for epileptic seizures prediction from EEG signals

---

as a problem of predicting spatiotemporal sequences and modified the fully connected long short-term memory (FC-LSTM) by replacing the Hadamard product with a convolution operation in the input-to-state and state-to-state transitions. Therefore, the convolution operation in the input transformations and recurrent transformations of their proposed convolutional LSTM (ConvLSTM) helps to handle the spatial correlations.

ConvLSTM replaces matrix multiplication with convolution operation at each gate in the LSTM cell. By doing so, it captures underlying spatial features by convolution operations in multiple-dimensional data.

The main difference between ConvLSTM and LSTM is the number of input dimensions. As LSTM input data is one-dimensional, it is not suitable for spatial sequence data such as video, satellite, or radar image data set. ConvLSTM is designed for 3-D data as its input.

The LSTM layer adopted in the LSTM-att model for seizure detection and classification presented in the previous chapter does not take spatial correlation into consideration. Although the LSTM layer has proven powerful for handling temporal correlation, it contains too much redundancy for spatial data due to the lack of encoding spatial information between states. The reason for using ConvLSTM is that its convolutional structures includes input-to-state and state-to-state transitions, which can model spatiotemporal characteristic information quite well. The inputs, cell states, hidden states and gates of ConvLSTM are 4D tensors whose first dimension denotes the time step, the second and the third are spatial dimensions (height, width), and the last dimension is the feature map. The computation of the hidden value ( $h_t$ ) of a ConvLSTM cell is updated at every time  $t$ . ConvLstm layers can be stacked like the case with LSTM layers to address complex tasks. The input layer with the size (Timesteps, channels, Rows, Cols) in our model will be followed by one or more stacked ConvLSTM layers. After convolutions, the dimensionality of output is increased, so we use averagePooling layers to reduce the dimensions. For each convolution, the filter size  $F$  and the kernel  $K$  must be defined. The output layer like in LSTM, is a dense layer with an activation function and  $N$  number of neurons representing the number of target classes.

**Chapter 5. A spatio-temporal attention network for epileptic seizures prediction from EEG signals**

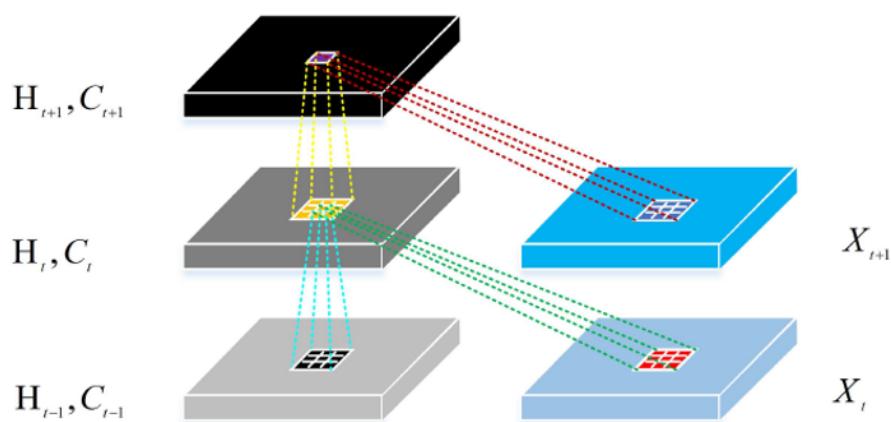


Figure 5.6: The inner architecture of a ConvLSTM model

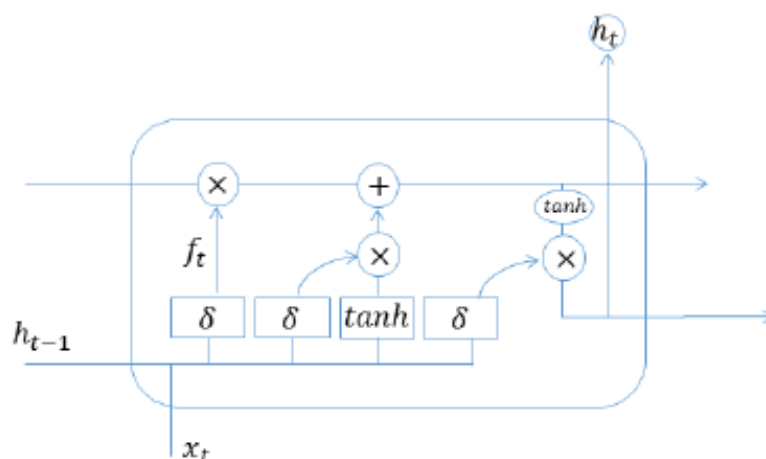


Figure 5.5: An instance of LSTM module

The key equations of ConvLSTM are shown in Eq. below, where \* denotes the convolution operator and ‘ $\circ$ ’, as before, denotes the Hadamard product:

$$i_t = \sigma(W_{xi} * X_t + W_{hi} * H_{t-1} + W_{ci} \circ C_{t-1} + b_i) \quad (5.4)$$

$$f_t = \sigma(W_{xf} * X_t + W_{hf} * H_{t-1} + W_{cf} \circ C_{t-1} + b_f) \quad (5.5)$$

$$C_t = f_t \circ C_{t-1} + i_t \circ \tanh(W_{xc} * X_t + W_{hc} * H_{t-1} + b_c) \quad (5.6)$$

$$o_t = \sigma(W_{xo} * X_t + W_{ho} * H_{t-1} + W_{co} \circ C_t + b_o) \quad (5.7)$$

## Chapter 5. A spatio-temporel attention network for epileptic seizures prediction from EEG signals

Layer	Parameter	Hyperparameter
ConvLSTM2D	Kernels	Kernel size, number of filters, stride, padding and activation function
Pooling layer	None	pooling method, Filter size, padding, stride
Fully connected layer	Weights	Number of weights, activation function
Others	None	BatchNormalization, optimizer, learning rate, loss function, Bach-size, epochs, regularization, weight initialization

Table 5.2: Parameters and hyperparameters of the a ConvLSTM model

$$H_t = o_t \circ \tanh(C_t) \quad (5.8)$$

$X_1, \dots, X_t$  are the inputs, cell outputs  $C_1, \dots, C_t$ , hidden states  $H_1, \dots, H_t$ , and gates  $i_t, f_t, o_t$  of the ConvLSTM are 3D tensors whose last two dimensions are spatial dimensions (rows and columns).

### 5.4.2.1 Hyperparameters

Note that a parameter in Table 5.2 is a variable that is automatically optimized during the training process and a hyperparameter is a variable that needs to be set beforehand.

The ConvLSTM determines the future state of a certain cell in the grid by the inputs and past states of its local neighbors. It uses the described convolution operation in the state-to-state and input-to-state transitions (see Figure 5.6).

The advantages of ConvLSTM are as follows:

- It can extract the spatial characteristics of echoes while capturing the time characteristics efficiently
- It allows the extraction of inter-channels characteristics using a 2D kernel size.
- It is the best for the prediction of long time and large-value EEG signal.

To summarize, the use of convolutions in the state-to-state and input-to-state transitions solves the issue of the lack of spatial information extraction, especially for a multi-channel EEG signal. The interpolation of multiple channels inside the convolution also can add new information about the signal and thus improve the prediction performances.

## Chapter 5. A spatio-temporal attention network for epileptic seizures prediction from EEG signals

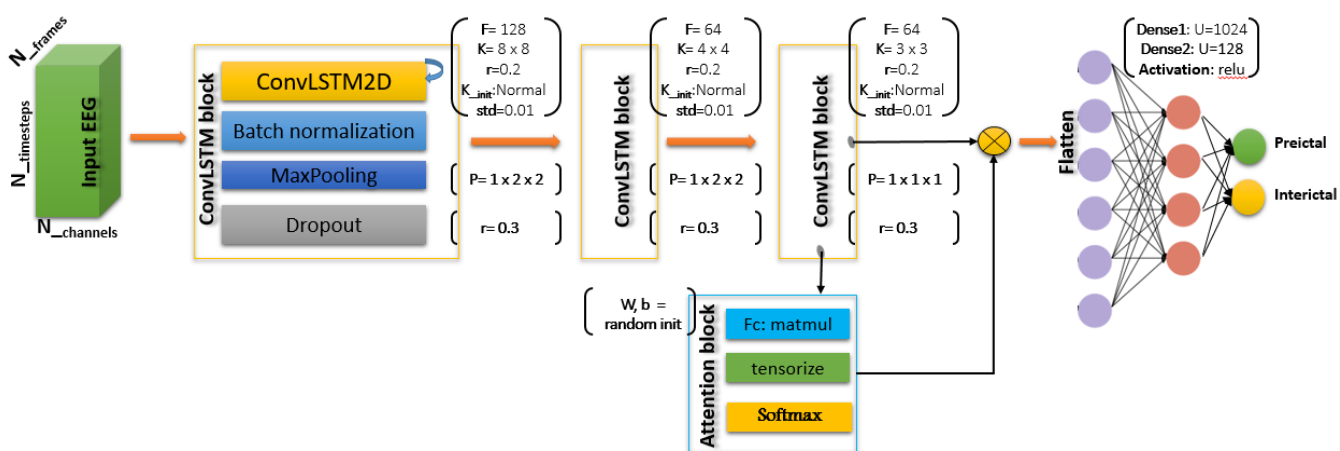


Figure 5.7: The proposed spatio-temporal ConvLSTM model is depicted by the three blocks of ConvLSTM. The attention block captures the relevance of each segment to the final decision.

### 5.4.3 Attention-based ConvLSTM model

Underlying the search for the prediction horizon is the assumption that changes in the brain occur prior to seizure onset making the seizure nearly inevitable. Despite this, seizure prediction based on EEG data has posed a challenge to the research community due to the absence of a clear and robust definition of preictal state biomarkers. The task of seizure prediction is defined as anticipating a seizure within some prediction horizon, or time window before seizure onset. Concretely defining the prediction horizon is difficult, since the optimal time window for prediction is not well understood. The goal behind the integration of an attention mechanism in the proposed spatio-temporal ConvLSTM2D model is to analyse in-depth the contribution of the constructed temporal Frames in the system's final decision. Thus, deriving a justifiable patient-independent prediction horizon containing the most effective frames. This analysis can provide a helping hand to neurologist in searching the reasons behind the onset release by identifying the triggers on most relevant frames. Defining the Optimal Preictal Period (OPP) can also be based on the attention weights of the frames included in the Selected Preictal Period (SPP), i.e. if the choice of the SPP is made to be within 1h for all patients, the attention scores calculated on all 1h frames can provide important information about the contribution of each fragment; thus the SPP can be reduced from 1h to 15min. Concluding that the first 45min of the preictal segment are not decisive. We assume that a preictal phase exists for all seizures and that there is an inflection point between interictal and preictal states. Figure 5.8 at

## Chapter 5. A spatio-temporel attention network for epileptic seizures prediction from EEG signals

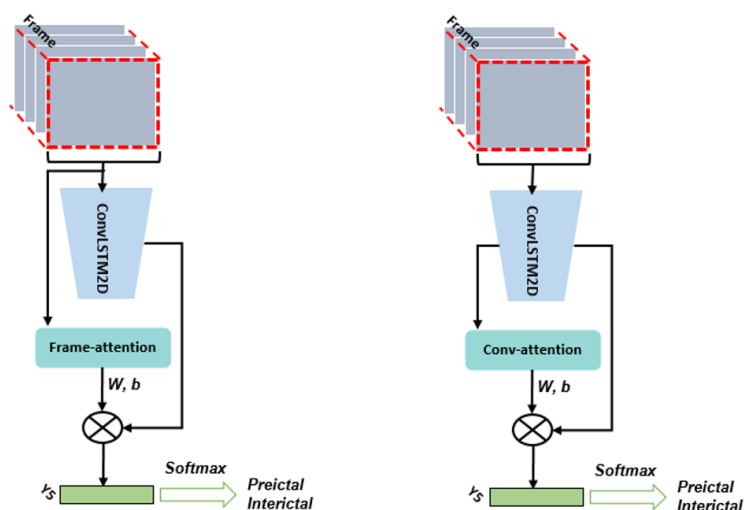


Figure 5.8: Frame-based vs Conv-based ConvLSTM attention model

the left. The introduced attention mechanism can learn the frame importance and pay different attention to various temporal segments as depicted in the Meanwhile, the model at the right is based on the last convolutional layer output to calculate attention related to the spatial feature map. The attention mechanism, as mentioned in the Fig 5.7, allows modeling of dependencies among 3D input sequences [Meng et al., 2019] and has shown success in some research topics [Hu et al., 2019]. Meanwhile, the excellent spatio-temporal feature learning ability of ConvLSTM Neural Networks has been widely used in research areas such as speech recognition, language modeling, diseases prediction and many other fields. Therefore, we propose an attention based ConvLSTM algorithm to automatically extract the distinctive information from the received multi-frames data.

First, to explore the importance among the different frames of reshaped signals into multi-frame signals, we employ the attention mechanism in a frame-wise manner into the EEG signals as shown in the bottom block of the structure diagram, Figure 5.7. In the case of seizure prediction, the optimal preictal period may differ from patient to another and only few segments can be able to contribute to the final decision result. The non informative frames can cause the demeaning of the system capabilities.

We adopt the adaptive frame-wise mechanism, which takes into consideration the information of all 3D fragments and assigns weights to the temporal segments based on importance. This mechanism will allow us to interpret our deep model and make results more explainable.

## Chapter 5. A spatio-temporel attention network for epileptic seizures prediction from EEG signals

---

Consider that,  $X = [X_1, X_2, \dots, X_n]$  represents EEG samples from the CHBMIT 256 Hz re-sampled dataset, and  $X_i = [x_1, x_2, \dots, x_k]$  where  $x_k$  represents the  $k^{th}$  channel of EEG sample  $X_i$ , and  $k$  is the total number of channels of each sample.

The original input with the shape  $[N_{samples}, N_{timesteps}, N_{channels}]$  was reshaped into a 5D tensor to adaptively be fed into an ConvLSTM2D layer. The new shape of the input data is:  $[N_{samples}, N_{frames}, N_{cols}, N_{rows}, N_{channels}]$ . In the frame-based model, the attention scores are directly learnt from the EEG frame which have the size of  $[N_{frames}, N_{cols}, N_{rows}]$

The attention layer, shown in Figure 5.8, is to generate attention weights for each Frame composed from a set of images  $N_{cols}, N_{rows}$  and then executes an element-wise multiplication with the output of the last convolutional Layer of the ConvLSTM block. The set of frames are input into a fully connected module where the parameters  $W$  and  $b$  are initialised for all frames. The attention matrix is element-wisely multiplied by the reshaped inputs. The outputs of the fully connected module are multiplied by the reshaped output of the dense layer of the ConvLSTM model. Then, the obtained values are fed into a new FC layer with Softmax activation to extract further features and to reduce the last dimension of input matrix into a number of classes.

The attention layer is computed using the following equations:

$$Y_1 = f_{nor}(X_0) \quad (5.9)$$

$$Y_2 = w_{al} * Y_1 + b_{al} \quad (5.10)$$

$$Y_3 = f_{tens}(X_2) \quad (5.11)$$

$$Y_4 = \sigma(Y_3) \quad (5.12)$$

Here,  $X_0$  denotes an input tensor of size  $[N_{samples}, N_{frames}, N_{cols}, N_{rows}, N_{channels}]$ . Symbols  $N_{samples}$ ,  $N_{frames}$ ,  $N_{cols}$ ,  $N_{rows}$  and  $N_{channels}$  represent the number of samples, the number of images per frame, the width and high of an image and the number of dimension of an image, respectively.  $Y_1$  is a normalized matrix of  $X_0$  size.  $W_{al}$  is a weight matrix of size  $(N_{rows}, N_{dimension})$ , a bias matrix  $B_{al}$  of  $N_{frames}$ , and  $Y_2$  have the same size as  $Y_1$ . A symbol  $\sigma(\cdot)$  represents a nonlinear, which transform the importance of frames to probability distribution function, like softmax(.) and sigmoid(.).  $Y_2$  is a tensorized matrix of  $Y_2$ .

## Chapter 5. A spatio-temporal attention network for epileptic seizures prediction from EEG signals

---

Functions  $f_{nor}(\cdot)$  and  $f_{tens}(\cdot)$  are to normalize and tensorize a matrix.

$$att_{scores} = Y_3 = [att_1; att_2; \dots; att(N_{frames})] \quad (5.13)$$

The Top block of the Figure 4.2 shows the spatio-temporal feature learning module, which comprises three convLSTM layers. The predicted class  $Y_5$  is the multiplication of the ConvLSTM block output and the learnt attention scores:

$$Y_5 = Dense_{out} \odot att_{scores} \quad (5.14)$$

The symbol  $\odot$  means an element-wise multiplication between matrices.

For this task, Attention-based ConvLSTM comes to improve the task of seizure prediction compared to the LSTM and ML classifier used on handcrafted features.

In the previous chapter, we have elaborated a study on the most relevant channels for seizure detection task (Seizure Vs Normal) and the seizure type classification (8 types of seizures). And we have demonstrated for many cases that the main brain region that contribute in a specific seizure type contains the most rated channels (based on our LSTM-attention model). In this chapter, we aim to investigate the most important segment of the preictal period containing the relevant information about an incoming seizure. For this aim, we designed an attention Layer that will be applied on the frames of the input signal. i.e., we have 10 frames of size 128x18, we applied a calculation of weights of every frame and the scores will be concatenated with the output of the ConvLSTM block.

## 5.5 Experimental results and discussion

In this section, we present and discuss our results using different configurations. To validate our method, we tested it on CHBMIT benchmarks enabling a comparison with the current state-of-the-art methods. Details of experimental settings are provided. An interpretation of seizure prediction results is done. Finally, an investigation for the most decisive frames from the preictal segments is elaborated.

- Patient-dependent method: with random augmentation of the preictal data in order to

## Chapter 5. A spatio-temporel attention network for epileptic seizures prediction from EEG signals

---

balance the dataset per patient.

- Patient-independent method: for each patient we extract from the interictal data a set to be equal to the preictal data of the same patient. After all, data are concatenated and fed to the trainer.
- Patient-independent method: a randomly selected signals from the global preictal and interictal segments. In these approaches, some patients may not appear in the selected set.

In order to enable an exhaustive comparison of different approaches, we have accomplished a feature based SP, an LSTM-based SP from raw EEG signals and we contributed with the novel Spatio-Temporal ConvLSTM model.

### 5.5.1 EEG dataset and data preparation

We evaluated performances of our proposed method using data from the CHB-MIT scalp long-term EEG dataset [Shoeb, 2009] described in chapter 2 (refer to Table 2.3). Analysing files of all cases summary, we note that the montage of channels changes within the case, so we opt for a manual channel selection process to discern the common montage over all epochs. Finally, we discern the 18 channels to be used in this work: FP1, T7, P7, O1, F3, C3, P3, FP2, F4, C4, P4, O2, F8, T8, P8, FZ, CZ and PZ. We used the complete data amount from the CHB-MIT dataset (except three segments from the case 12: chb12-27/28/29 since we cannot find the common montage of selected channels in these epochs like in the work of Tsiouris et al. [Tsiouris et al., 2018]). For the aim of seizure prediction, our deep network is deployed to accomplish the high-level characteristics learning of preictal and interictal states. Based on the findings of the work done by Tsiouris et al. [Tsiouris et al., 2018] in which they tested four windows to extract preictal states: 15-30-60-120 minutes and compared the obtained results, we decided to choose one window for the rest of the analysis. Since there are not a lot of differences between the average rate of sensitivity of all tested windows and leafing through all annotation files, we discover that some seizures occur in the beginning of the epochs, thus, there is not a sufficient duration to extract preictal segments with a 60-120 windows. Furthermore,

## Chapter 5. A spatio-temporel attention network for epileptic seizures prediction from EEG signals

---

some seizures occur consecutively with an interval of less than 60-120 minutes. For these reasons, we opt to test our method using a preictal window of 15 minutes.

For the purpose of this study, ictal segments (when the seizure occurs, annotated on the file 'seizures-info') are not included. For each case, we extract preictal and interictal epochs, then we apply a segmentation script in order to obtain 5sec epochs. This segmentation window has been proven by [Tsiouris et al., 2018] [Barata et al., 2018] to be the best for epileptic seizures analysis. All obtained epochs were labeled based on the annotation files accompanied with the database.

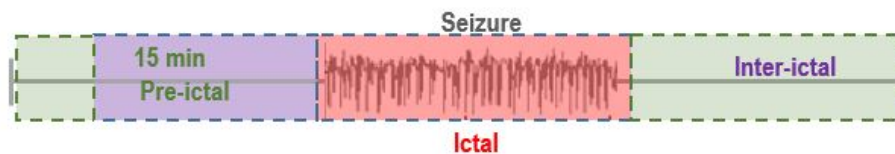


Figure 5.9: Different states representation of an epileptic patient's EEG segment

We test different methods when preparing the data to be fed into the model.

The Figure 5.9 shows how to differentiate between preictal, ictal and interictal periods. The borders are generally identified by epileptologists. In the case where two onsets occur consecutively, the set of segments between the first and second onsets can be miss-labeled as interictal and preictal states. To resolve this problem, all consecutive seizures should be processed separately to ensure a correct labeling of the overlapped segments.

### 5.5.2 Results on patient-dependent epileptic seizure prediction

#### 5.5.2.1 Experimental set up

To overcome the imbalanced aspect of data, we carried out an over-sampling augmentation technique to expand the amount of samples in the preictal class (patient-independent approach). The ratio of preictal:interictal class differs between cases. Thus, for each case, we tried to reach the ratio 1:1 or 1:2 to guarantee a significant classification rate. Duplicated trials were selected randomly, then the resulted set was shuffled.

We contribute by proving that the seizures prediction can be carried out with a raw EEG

## Chapter 5. A spatio-temporel attention network for epileptic seizures prediction from EEG signals

---

signal. Thus, reducing extra-time of feature extraction and making it suitable for a real time application.

We conceptualize an LSTM model adapted to the nature of the EEG signals with two LSTM Layers. Since the input signal is a complex time series of 18x1280 time points, we fixed the number of memory units at 500 for both LSTM layers. We included a dropout layer with a probability of training equal to 0.2. Two layers follow the LSTM layers: a fully connected layer activated with ReLu function, and a dense layer to discriminate between the preictal and interictal states. The “softmax” activation was used as function in the dense layer. We personalized the model parameters using the popular Adaptive Moment Estimation (Adam) optimizer. The LSTM network was built in a Matlab environment using the deep learning toolbox.

The training and testing phases are performed separately for every subject, therefore making a subject-dependent approach. This selection was predicated in-line with our review of recent studies on onsets prediction and the insufficient subject-independent studies. Furthermore, carrying out a subject-dependent experiments allows to handle the variability and specificity of each subject and to compare the obtained results with existing ones.

The evaluation of our model was elaborated through a 10-folds cross-validation. For each case, trials were shuffled and divided into 10 groups. One group was designed to hold-out set and the remaining groups were used as training sets.

Since LSTM models have not been used for seizure prediction with Raw EEG data, there are no references in the literature regarding an optimal internal architecture. Thus, a pre-analysis is performed in this section testing the three different internal architectures, moving from simple to more complex networks. In the LSTM\_1 architecture, which consists of the simplest approach, the network is composed of a single layer with 50 memory units. The number of memory units is increased to 100 using a BiLSTM in the second architecture design, LSTM\_2, maintaining the single layer approach. Finally, in LSTM\_3 the number of memory units is retained at 100 but another layer of equal dimension is included as well and LSTM is used instead BiLSTM since the BiLSTM with a double layer requires a lot of resources, thus rendering it a time consuming approach, which should be avoided. All networks are followed by a fully connected layer with an output of 30 units using the “relu” activation function and a final dense

## Chapter 5. A spatio-temporel attention network for epileptic seizures prediction from EEG signals

---

layer that outputs the binary classification as a one hot encoded result (i.e. preictal or interictal), using the “softmax” activation. The batch size is set to 128 and the cross-entropy loss function is selected as the cost function, using the Adaptive Moment Estimation (Adam) optimizer.

The activation function to use is depending on the application. For our problem at hand, we have multiple classes (interictal and preictal) but only one of the classes can be present at a time. For these types of problems, generally, the softmax activation function works best, because it allows us to interpret the outputs as probabilities.

The loss and activation functions are often chosen together. Using the softmax activation function points us to cross-entropy as our preferred loss function or more precisely, the binary cross-entropy, since we are faced with a binary classification problem. Those two functions work well with each other because the cross-entropy function cancels out the plateaus at each end of the soft-max function, and therefore, speeds up the learning process.

For choosing the optimizer, adaptive moment estimation, short Adam, has been shown to work well in most practical applications and works well with only little changes in the hyperparameters. Last but not least we have to decide, after which metric we want to judge our model. The architecture previously described in Section 5.5.2.1 is used to perform the classification. In this approach, we do not elaborate a feature extraction step. We consider the raw data as input to the LSTM model. In general, a minimum of feature extraction is always needed. The unique case where we would not need any feature extraction is when our algorithm can perform feature extraction by itself as in the deep learning neural networks, which can get a low dimensional representation of high dimensional data, which is the case of this work.

Deep Learning methods offer an automatic learning of temporal dependency. In this work, we implemented a deep architecture of an LSTM model for features learning applicable for epileptic seizures prediction. The model was tested on the CHB-MIT database using only Raw data. As it is known, neural networks are invulnerable to the noise in the input data and in the mapping function, and can carry out the tasks of learning and prediction even if some values are missing. Neural networks have a high capacity to readily learn linear and nonlinear relationships. For these reasons, we have chosen to feed our LSTM raw EEG segments with no pre-processing against noise and artifact and to demonstrate that even with raw data, we can perform the task of seizure prediction with satisfying performances.

## Chapter 5. A spatio-temporel attention network for epileptic seizures prediction from EEG signals

---

On the other hand, we are facing the problem of imbalanced data since the number of preictal segments for each case are minimum compared to the amount of interictal segments (for example: For the chb024, the ratio of interictal-class to preictal-class instances is 5:1; for some other cases it is even more imbalanced). This problem can affect notably the classification rate, in the case where the accuracy measures indicate excellent rates (such as 90%). However, the accuracy is really only reflecting the underlying class distribution.

To resolve this problem, we chose to deal with it by an random over-sampling technique that consists of adding copies of instances from the under-represented preictal-class.

The new datasets are fed to the LSTM model with a sequence of 18 channels x 1280 time points.

### 5.5.2.2 Results and discussion

For the 24 cases in CHB-MIT, the average SENS, SPEC and ACC are 84.60%, 90.16% and 88.89%, respectively as reported in the table 5.3. The model provides a low FPR of 0.27 false alarms per hour. The minimum FPR is obtained for the cases chb04, chb07 and chb11. The standard deviations of sensitivity, specificity and accuracy are 0.11, 0.08, and 0.09, respectively. As it can be seen in Table 5.3, using raw EEG samples of every 5-s segments, we can achieve high performances varying across cases. The best sensitivity attained for cases chb07 and chb11 is 0.98. On the other hand, we have obtained as worst result a 0.67 sensitivity rate for the case chb24. We deduce that when seizures number exceeds 10, the LSTM network underperforms in prediction seizures, which can be justified by a high number of non-spaced seizures causing a miss-classification of adjacent states as explained in Section 5.5.2.1 .

Cross-patient sensitivity, specificity and accuracy results over all cases were illustrated on the Bar Chart 5.14. We can notice a degradation of rates that affects some specific cases, mainly ch012 and chb24. Many reasons can justify the under-performances such as: signals with high signal to noise ratio, number of consecutive seizures and the patients' medical history (we cannot confirm this fact since patients' personal information are private and cannot be accessed by the database users). In order to defend their methodology choice, Tsiouris *et al.* [Tsiouris et al., 2018] applied the proposed architecture on raw EEG data for only 3 cases (chb01, chb02 and chb14) and showed that the results accuracy are better with feature extraction

## Chapter 5. A spatio-temporel attention network for epileptic seizures prediction from EEG signals

Table 5.3: EEG-based seizure prediction results

Case	#seizures	preictal window: 15min			
		RAW EEG			
		SENS	SPEC	ACC	FPR ( $h^{-1}$ )
case01	7	0.92	0.94	93.42	0.12
case02	3	0.95	0.97	96.91	0.14
case03	7	0.93	0.93	93.53	0.11
case04	4	0.95	0.97	96.78	0.02
case05	5	0.88	0.90	89.48	0.25
case06	10	0.70	0.79	76.51	0.4
case07	3	0.98	0.98	98.74	0.02
case08	5	0.90	0.94	92.47	0.12
case09	4	0.92	0.97	95.53	0.03
case10	7	0.83	0.82	82.62	0.36
case11	3	0.96	0.99	98.24	0.02
case12	27	0.53	0.74	65.84	1.21
case13	12	0.82	0.87	84.96	0.37
case14	8	0.71	0.82	76.54	0.69
case15	20	0.73	0.81	78.09	0.47
case16	10	0.78	0.89	84.16	0.53
case17	3	0.96	0.99	97.99	0.03
case18	6	0.92	0.95	95.49	0.11
case19	3	0.95	0.96	96.04	0.12
case20	8	0.88	0.91	90.49	0.3
case21	4	0.95	0.95	95.49	0.13
case22	3	0.95	0.96	96.10	0.1
case23	7	0.88	0.88	88.21	0.45
case24	16	0.67	0.71	69.92	0.46
<b>MEAN</b>	–	0.84	0.90	88.89	0.27
<b>STD</b>	–	0.11	0.08	0.09	0.27

against feature learning. They obtained an average accuracy of 74.00% since their architecture failed to deal with the character of a Raw EEG signal because it does not include a sufficient number of hidden memory units.

Along with their hypothesis, we decided to investigate more in this direction and conceptualize a model adequate to receive a raw EEG signal as input.

Since we did not find an other research that deploys LSTM with a raw EEG segments for the aim of seizures prediction, we compared our method with three different approaches proposed recently by [Yao et al., 2018] in order to detect seizures and no-seizures segments. The comparison focuses on this study, which was evaluated with the complete volume of CHB-MIT database, being the premier public database consisting of long-term EEG signals. As shown

## Chapter 5. A spatio-temporel attention network for epileptic seizures prediction from EEG signals

---

in Table 5.4, our system outperforms the three aforementioned models, in terms of specificity and accuracy. Thus, the projected LSTM model is ready to produce higher seizure prediction performance as compared with the work of Yao *et al.* [Yao et al., 2018].

Assuming once again that the proposed deep LSTM model is conceptualized to handle the complex nature of the EEG signal, using two LSTM layers and more hidden memory units allowing for better feature learning. Our model is more appropriate for real time applications than other based on feature extraction techniques requiring high level of expertise and familiarity with epileptic seizures characteristics.

Typical feature representation is learned by our model leading to very satisfying results for seizures prediction. Furthermore, we can apply the same architecture for seizures detection by including ictal segments to the overall process.

To further analyze the variation between patients, t-Distributed Stochastic Neighbor Embedding (t-SNE) was applied on two selected patients (chb01, having a high sensitivity rate, and chb12, having the poorest sensitivity rate). t-SNE allows the visualization of high-dimensional data. Interictal segments (red dots) are more overlapped with Preictal segments (Blue dots) in the Figure 5.11. This overlapping is responsible of the obtained dependent results for the chb12. It means that segments of the chb12 are less discriminative than those of the chb12 and the LSTM model was not able to learn a discriminative features to predict the fragment class with high sensitivity.

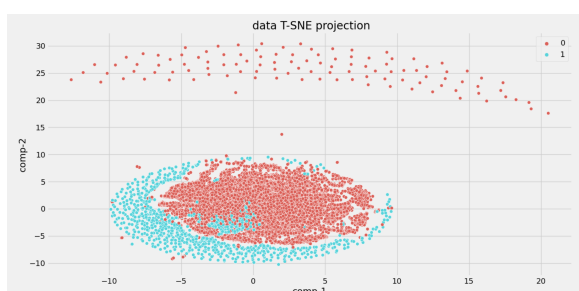


Figure 5.10: T-sne projection of data from chb01

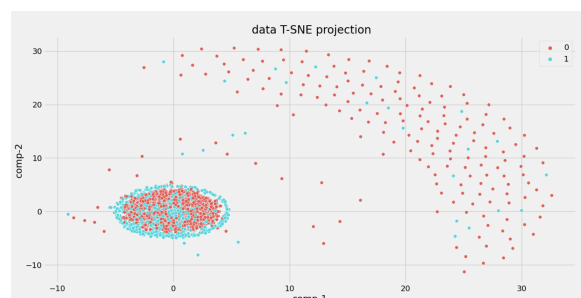


Figure 5.11: T-sne projection of data from chb12

## Chapter 5. A spatio-temporal attention network for epileptic seizures prediction from EEG signals

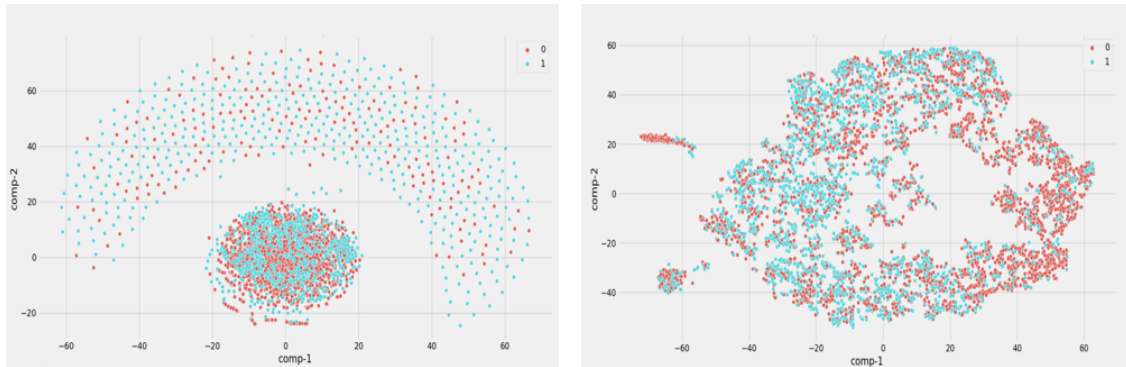


Figure 5.12: T-sne projection of raw data from the test set (left) and of learnt features (right)

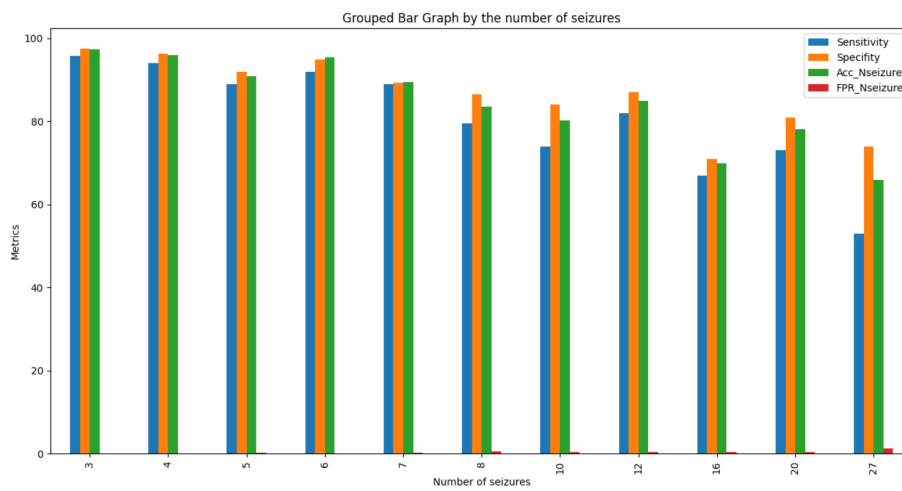


Figure 5.13: Results of all cases grouped by the number of seizures, for patients who have the same number of seizure we plotted the mean values

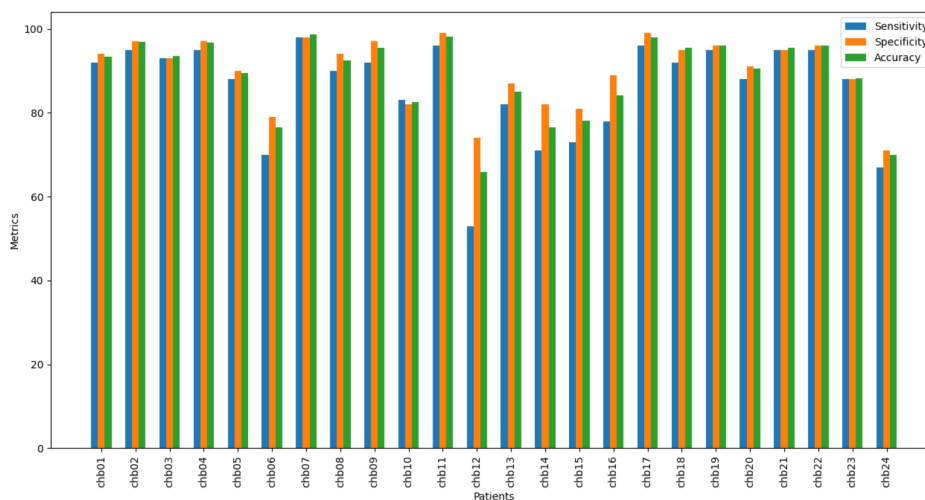


Figure 5.14: Results of all cases grouped by SENS, SPEC and ACC

## Chapter 5. A spatio-temporel attention network for epileptic seizures prediction from EEG signals

Table 5.4: Performance comparison of the proposed work with a raw EEG-based approach

Ref	#Cases	#Channels	Method	Results		
				SENS	SPEC	ACC
[Yao et al., 2018]	24	17	BILSTM	0.86	0.82	84.00
			Attention mechanism + LSTM	0.83	0.88	86.00
			Attention mechanism + BILSTM	0.87	0.88	87.80
[Tsiouris et al., 2018]	24	18	LSTM	–	–	74.00
[Baghdadi et al., 2021b]	24	18	Deep LSTM	0.84	<b>0.9</b>	<b>88.89</b>

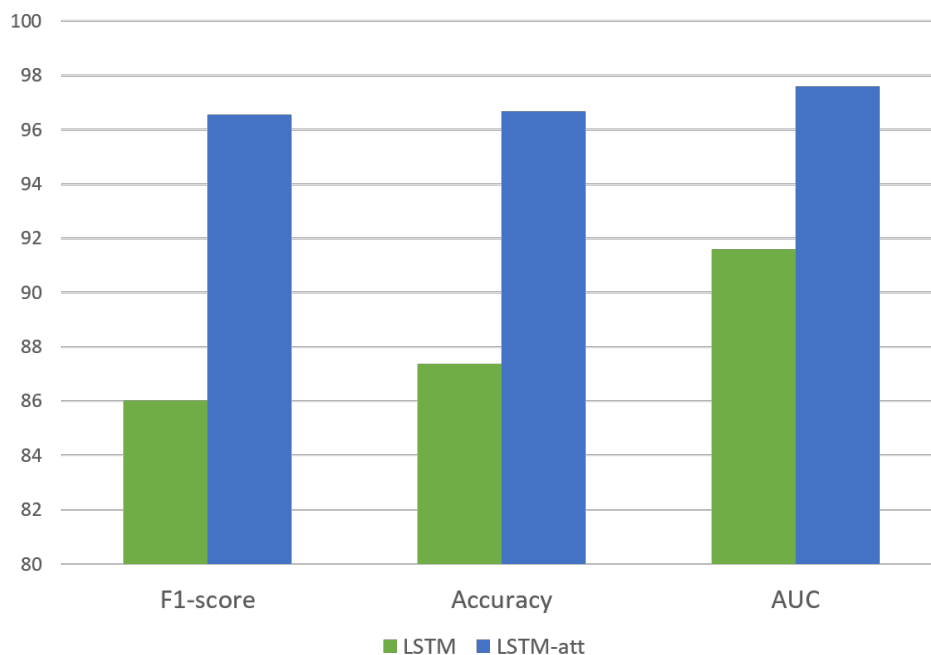


Figure 5.15: Improved results by the proposed LSTM-att method

### 5.5.3 Results on subject-independent epileptic seizure prediction

#### 5.5.3.1 Hyperparameter settings

Patient-independent studies aim to design a model that can recognize seizures across multiple subjects. When designing such models, the entire dataset is utilized, and the objective is to learn a global predictive function that has the ability to perform prediction across multiple subjects in the dataset. To get a balanced dataset for the model training, we selected an equal

## Chapter 5. A spatio-temporel attention network for epileptic seizures prediction from EEG signals

Table 5.5: The parameter settings of the proposed Convolution based ConvLSTM attention

Layer Name	Output Shape	Filter Size	Padding	Layer Name	Output Shape
Input Layer	10x128x18x1	—	—	Dropout	10x8x1x64
ConvLSTM2D Layer	10x128x18x16	3x3	same	Reshape	10x512
batch Normalization	10x128x18x16	—	—	Attention Layer	1x10
Max pooling3D	10x64x9x16	1x2x2	—	Multiplication Layer	512x10
Dropout	10x64x9x16	—	—	Flatten	5120
ConvLSTM2D Layer	10x64x9x32	3x3	same	Dense	1024
batch Normalization	10x64x9x32	—	—	Dense	128
max pooling3D	10x32x4x32	1x2x2	—	Dense	2
Dropout	10x32x4x32	—	—		
ConvLSTM2D Layer	10x32x4x64	3x3	same		
batch Normalization	10x32x4x64	—	—		
max pooling3D	10x8x1x64	1x4x4	—		

sets of preictal and interictal segments across patients. After selecting preictal and interictal samples from each patient, we obtained a 63,905 sample balanced dataset where each sample has a duration of 5s and 18 channels. When constructing this balanced dataset, we do not use an overlapping window for the segmentation.

For convolution based ConvLSTM attention, the parameter settings are summarized in Table 5.5. The number of filters in the two models is set to 16,32 and 64, respectively. In addition, the kernel size of each convolution is fixed to 3 x 3. In order to make the categorical loss function of the proposed deep models converge to the greatest extent, the number of training epochs is fixed to 50. The learning rate is fixed to 0.001 on the Adam optimizer.

For hardware system configuration, all the following experiments are completed on a desktop with an Intel Core i7-6700HQ CPU 2.60GHz 2.59 GHz, 16 GB of DDR4 RAM, an Nvidia GeForce GTX 960M GPU with 4 GB memory. For software system configuration, we adopt Windows 10 x64 as our operating system for all experiments. CUDA 10.1 and cuDNN 10.1, Tensorflow-gpu with 2.1 and python 3.8.7 are the main programming environment. Specially, all methods involved in our experiments are completed in Pycharm 2.1

### 5.5.3.2 Results and discussion

We are talking about subject-independent classification when the entire volume of the data is mixed and used for training and testing phases. Data from the 24 cases are used for the processing including the labeling, segmentation, feature extraction and channel selection. All

## Chapter 5. A spatio-temporel attention network for epileptic seizures prediction from EEG signals

---

results are presented on the end of this section.

As previously mentioned, we set the prediction horizon as 15 minutes, and our dataset contains 5s 18-Channel EEG samples from all 24 subjects. We trained our models for 50 epochs with a batch size of 64. We used the Adam optimizer with a 0.001 learning rate. The following list demonstrates the 5 Fold Cross Validation results for our two models:

- Model I: ConvLSTM on raw EEG data, Accuracy: preictal-interictal state detection 90.62%, Precision:, Recall: 90.71% and F1-score:90.62%
- Model II: ConvLSTMatt on raw EEG data, preictal-interictal state detection; Accuracy:94.45%, Precision: 94.53%, Recall: 94.38% and F1-score: 94.43%

Examining the proposed models, both architectures consist of a ConvLSTM network followed by an additional linear layers. Looking at the number of trainable parameters in each classifier: the deep ConvLSTM model contains 2,5M parameters and the attention-based ConvLSTM holds 5.6M parameters. Even though the proposed models have similar architectural arrangements, they employ two different strategies to valorize the contribution of EEG frames, and output produced by both models differ.

Table 5.6: Results of the proposed ConvLSTM and ConvLSTM attention

Class	Accuracy	Precision	Recall	F1-score
ConvLSTM model				
Interictal	93.22	93.22	88.34	90.72
Preictal	88.10	88.10	93.07	90.52
ConvLSTM model attention				
Interictal	93.35	93.35	96.16	94.73
Preictal	95.72	95.72	93.61	94.14

Table 5.7 resumes all obtained results in term of accuracy for the five different methods deployed for seizure prediction and evaluated on the CHBMIT dataset. As mentioned, we have extracted 3 sets of features from the time domain and time-frequency domain in order to allow a comparison with the proposed deep models. The best accuracy rate obtained for the hand-crafted features is 67.7.% using the coefficient of the DWT at 6 levels. Furthermore, accuracy

## Chapter 5. A spatio-temporel attention network for epileptic seizures prediction from EEG signals

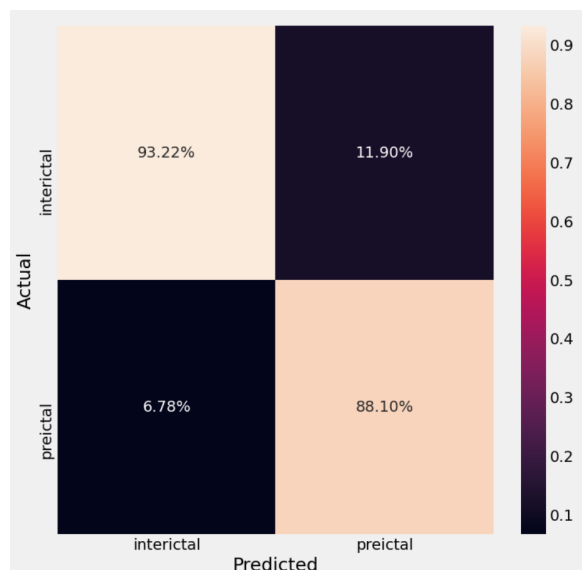


Figure 5.16: Confusion matrix of the ConvLSTM model

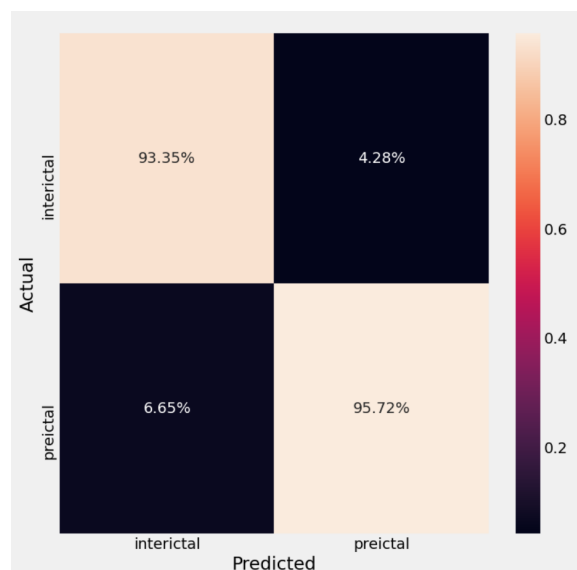


Figure 5.17: Confusion matrix of the frame-based attention ConvLSTM model

is poor (57.00%) when using statistical features to characterize the preictal and interictal segments. Even the extracted energy of EEG bands do not improve the accuracy above 61.10%. Channels selection slightly improves the results and reduces the dimension of input data. The best obtained accuracy is 84.45% using 5 channels with feature learning. The channel selection was achieved based on the one-channel signal accuracy for SP. Five top rated channels were chosen and concatenated to relearn a new LSTM model. The improvement is very light but the dimensionality reduction is very important since we pass from a 18x1280 input shape to a 5x1280 shape. A dimensionality reduction induce a lower computational time and complexity.

The proposed attention-based ConvLSTM model on Raw EEG data for SP shows best results compared to the previously evaluated methods. The attention mechanism implemented improve the accuracy of the model with 4% and allow as to interpret and explain the hidden mechanism of the ConvLSTM model. A confusion matrix is used to evaluate the performance of the two models. Figures 5.16 and 5.17 depict the confusion matrix for traditional ConvLSTM model and the proposed ConvLSTMatt model. The latter detects true positives of the preictal state with an accuracy of 95.72% and only 4.29% of false positives. The ConvLSTM model misclassify 11.90% of the preictal data compared to only 4.29% misclassified by the convLSTMatt model. The proposed ConvLSTMatt achieved 94.45% of test accuracy, 94.53% of precision, 94.38% of recall and an F1-score equal to 94.43%. According to these results, it outperform

## Chapter 5. A spatio-temporel attention network for epileptic seizures prediction from EEG signals

other methods with an improvement of 37.45%, 26.75%, 33.35%, 10.97%, 10.00%, 3.83% for feature based, LSTM full channel, LSTM 5 channels and ConvLSTM only respectively.

Table 5.7: Results of patient-independent seizure prediction approaches

Method	Input type	Input dimension	Accuracy (%)
Feature extraction	Statistical features	126	57.00
	Energy of 7 eeg bands	126	61.10
LSTM deep model	Raw EEG	18x 1280	83.48
LSTM deep model with channel selection	Raw EEG	5x1280	84.45
ConvLSTM model	Raw EEG	10x128x18x1	90.62
Attention-based model	ConvLSTM	Raw EEG	<b>94.45</b>

For each one of the three test seizures, we considered the advance prediction time  $P_{delay}$  defined as the difference between the beginning time marked in the database and the one determined by the system. The latter is the time in which the system starts to classify the raw segments as preictal samples without interruption. By definition, a seizure is correctly predicted if and only if the corresponding advance prediction time  $P_{delay}$  is strictly positive. The positive value of  $P_{delay}$  clearly indicates how early an ictal phase is predicted. In order to evaluate the system's behavior in terms of false alarms, the FPR (defined as the number of false positives per hour) is adopted. More precisely, the classification of a raw segment, belonging either to a preictal or to an interictal phase, produces a false positive whenever the output  $y_p$  of the system vary before the onset of the next seizure as illustrated by the Figure 5.18. In table 5.8, we reported the performances of the system evaluated with three test seizures. For these seizures our model detect preictal against interictal segment with a recall rate of 88.33%, 92.22% and 78.33% respectively. A mean False Positive Rate of  $0.11 h^{-1}$  is reported. We calculated the delay of prediction within the 15 minutes of pre-ictal period, as shown in the last column of the table 5.8, the  $P_{delay}$  is variable. The seizure number 3 from the case01 was predicted before 12min91sec from the onset time, while the seizure number 4 from the same case was predicted before 07min83sec before the onset time.

## Chapter 5. A spatio-temporel attention network for epileptic seizures prediction from EEG signals

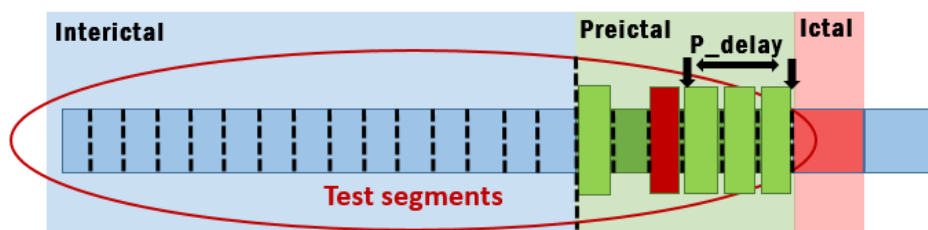


Figure 5.18: Illustration of the prediction process

Table 5.8: Evaluation of the system's behavior for three different seizures

Case N°	Seizure file N°	Total duration (hh:mm)	Total segments	Recall (%)	FPR ( $h^{-1}$ )	$P_{delay}$ (mm:ss)
1	3	02:50	2040	88.33	0.11	12:91
1	4	00:24	288	92.22	0.10	07:83
10	12	09:45	7020	78.33	0.13	09:41

### 5.5.3.3 Model interpretability: a case study

In the healthcare domain, it is important to provide credible results to the neurologist. A scientist is required to know exactly how the model acquired its knowledge and how it concludes for the prediction. The explainability of deep Neural network aims to provide the correspondent answers and enhance the understanding of the seizure prediction domain. For the seizure prediction task, it is important to know how the model classifies interictal and preictal state and if there are any indication about the most important EEG segments contributing to the decisive stage. For this end, we proposed in the section, an attention module that attributes importance to spatio-temporal EEG patterns over time, during the chosen preictal period. Some indicative biomarkers, like spike wave, can be present in both preictal and interictal signals, hence a standard model can't correctly classify the two states. But, when analyzing the temporal pattern of a larger time, we can see the difference between preictal and interictal EEG. The use of the RNN LSTM have the advantage of memorizing the time dependencies, thus capturing the changes of an EEG signal. DNN have shown its effectiveness in identifying relevant discriminative information that can be spatial or temporal. CNNs were conceptualized for spatial information extraction, although temporal information was addressed by RNN, especially neural networks with memory like LSTM. Researchers who proposed a stacked CNN and LSTM for spatio-

## Chapter 5. A spatio-temporal attention network for epileptic seizures prediction from EEG signals

---

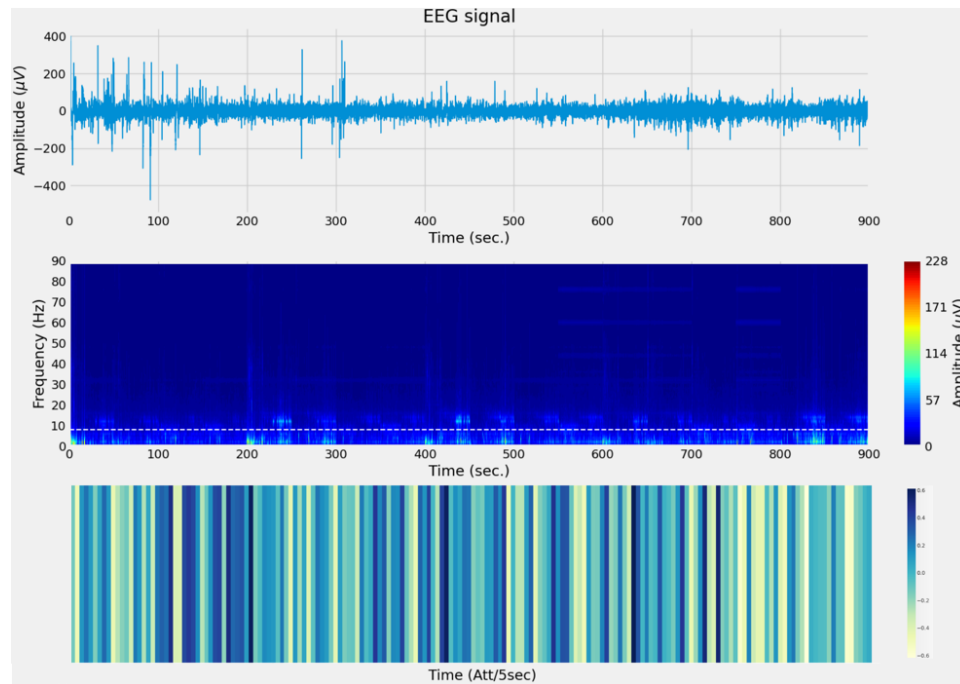


Figure 5.19: EEG Signal plot vs Spectrogram vs attention Heatmap of 15 minutes from a preictal state

temporal representation omit that sequential layers will forget the relation between the spatial and temporal slices and thus neglect a discriminative part of the information. ConvLSTM provides a parallel extraction of the spatio-temporal characteristics using spatial convolutions as input to the LSTM gates. Hence, we hypothesize that the model can simultaneously identify not only important locations, but also the time intervals during which the spatial importance. This facilitates effective discrimination between different classes to improve the accuracy of the models, and also enhance their explainability. In the context of seizure prediction, earning scientific insights about the most discriminative time intervals during a preictal period is of high importance for neuroscientists and neurologists. This is a method to highlight underlined triggers of an epileptic onset and to open future investigations. In the Figure 5.19, 15 minutes of a random CHBMIT case are analysed. Spectrogram is used as a way of visualizing the change of a nonstationary EEG signal frequency over time. The range of frequency that present variation is between [0-15] which correspond to theta (4–7 Hz) and alpha (8–12 Hz) bands. The presented attention weights (bottom of the Figure 5.19) are calculation for every 5s to analyse the data, slices with high weight indicate a high contribution to the decision of seizure prediction. The neurologist confirm after reading the EEG and the correspondent attention heatmap that

## Chapter 5. A spatio-temporel attention network for epileptic seizures prediction from EEG signals

---

segments at  $t=150s$  to  $t=205s$  contains more spikes than the rest of the EEG signal, also for segments at  $t=550s$  to  $t=570s$ . Changes on frequency and amplitudes in the raw EEG segments was highlighted by our system by affecting high attention score to the correspondent segments.

### 5.6 Conclusion

Assuming once again that the proposed deep models are conceptualized to handle the complex nature of the EEG signal, starting from adding layers to the LSTM model and increasing the number of hidden memory units to the implementation of more sophisticated networks and exploiting the strength of the attention mechanism to give our models more explainability analysis. This process aims to allow better feature learning. Our models are more appropriate for real time applications than others based on feature extraction techniques, which are implemented for a comparison aim, requiring high level of expertise and familiarity with epileptic seizures characteristics.

Typical feature representation is learned by our models leading to very satisfying results for seizures prediction. Furthermore, we can apply the same architecture for seizures detection by including ictal segments to the overall process.

In the beginning of this chapter, we have seen that many different approaches to extract EEG seizure-related features have been investigated. Seizure prediction in the first approach has been addressed as a machine-learning problem. The main steps of this classification problem are: extracting relevant features and designing an adequate classifier. Once features are extracted, it remains essential to define the decision making method. The classifier should be able to generalize well and show good performance. Annotations made by a neurologist are often considered as the reference point in the problem setting. Machine-learning methods that have been applied in this field include expert systems, decision trees, clustering algorithms, self-organizing maps, and a variety of artificial neural network configurations.

After which, we moved through deep learning models, to demonstrate the capabilities of deep model in learning spatio-temporal information. We have also implemented an LSTM model for the learning of temporal dependencies in order to show the improvement achieved by the novel Spatio-temporal ConvLSTM model.

## **Chapter 5. A spatio-temporel attention network for epileptic seizures prediction from EEG signals**

---

The main objective of this study was to design deep learning models for patient-independent epileptic seizure prediction. Such models, can be used in situations where subjects in the dataset have fewer labeled examples (EEG recordings). We recognize this is a typical case in Intensive Care Unit (ICU) monitoring scenarios where an adequate number of samples cannot be obtained to train a prediction model.

# Conclusion and Future Works

---

## Contents

---

<b>6.1</b>	<b>Summary of contributions . . . . .</b>	<b>133</b>
<b>6.2</b>	<b>Future works . . . . .</b>	<b>134</b>
6.2.1	Investigation of the relation between anxiety and epileptic seizures . . . . .	135
6.2.2	Data augmentation using adversarial neural network for the TUHSZ dataset addressing the issue of imbalanced classification task . . . . .	136
6.2.3	Automated hyper-parameters optimization . . . . .	136

---

AI-related applications based on EEG analysis have addressed the technological gap in the clinical field. Also for personal use, the benefit of this intelligence have been used to save lives and improve the well being of affected people. The use of physiological signals for smart health applications has experienced a relative uprising. Meanwhile, people do not have the practice to wear a neuro-headset and may feel uncomfortable. This habit becomes more and more established. Since the use of one-channel neuro-headset was enabled by the smart health monitoring for exercises and meditation, people try to follow this trend and are able to further assimilate technologies based on EEG monitoring. Recent years have witnessed growing interests in AI-related applications, mainly in the research and industry fields. In this thesis, we have explored several research problems related to this topic. Can we decode human anxiety using physiological signals? Specifically, the stimulation of anxiety following a psychological strategy. EEG signals were recorded during the session for a further analysis and used in the proposed anxiety levels detection approach. DASPS, as a new dataset for anxiety levels recognition, has been developed to promote scientific co-operations in the field. The proposed computational models and prototype demonstration are systematically evaluated and compared to the state-of-the art

methods.

### 6.1 Summary of contributions

In this thesis we grant attention to one of the most useful modality for the purpose of neurological disorders analysis, which is the Electroencephalogram (EEG). EEG recordings have shown efficiency in many field thanks to its wealth of temporal and spectral information.

Up until the past few years, traditional machine learning techniques (i.e. non-deep learning algorithms) have been the only viable option in EEG analysis, and in fact, continue to be extensively used combined with various feature extraction and feature selection algorithms.

In a relative newer trend, deep learning algorithms have found applications in medical image and signal processing, due to the advancements and availability of computational power and big data, showing high potential and significant impact as, in most cases, their performance exceeds the rates that have been previously achieved with traditional machine learning techniques.

In chapter three, we started with an oriented handcrafted feature methodology for anxiety levels detection. This contribution was elaborated in collaboration with a psychotherapist in order to propose a novel psychological stimulation method for anxiety elicitation. The produced dataset have an academic broader impact by improving the researches on anxiety detection since it is the first public dataset for the mentioned purpose. To this day, we are allowing many researchers to use the dataset in their studies. In the same chapter, we have detailed our approach for binary and multi-class recognition tasks. In addition, we concluded the chapter by a presentation of an application for anxiety level detection based on a deep learning method. The challenge was revealed during a national workshop.

Chapter four was mainly structured into two main Sections, reporting the work addressing the seizure detection and seizure classification problems. The motivation behind this contribution is the crucial need of an interpretable model for epileptic seizure classification for the neurology service. The question triggering the work was: Can we find an effective correlation between the expertise-based reading and diagnosis of a clinician, and the decisive information generated by a deep model? For this aim, we have proposed an attention-based LSTM model to investigate the contribution of EEG channels and brain regions in the final decision

## Chapter 6. Conclusion and Future Works

---

of the model. Consistency with the neurological findings was proved by the team of neurology collaborating with us to produce this study.

Since LSTM is a more intelligent version of RNNs, offering the ability to better control the storage of information in the memory units, we proposed the exploitation of this technique for seizure prediction purposes and results was promising. Considering that EEG signals are essentially highly dynamic, non-linear time series data, LSTM networks have by design an advantage over CNN in isolating temporal characteristics of brain activity during different states as reported in various applications, such as emotion recognition [Du et al., 2020], anxiety recognition [Baghdadi et al., 2020a] and speech recognition. Despite their inherent advantage in EEG analysis, the basis of LSTM model neglect the spatial information of the input data. Meanwhile, the ConvLSTM proposed by [Xingjian et al., 2015] have exploited the advantages of the spatial convolutions and the power of the gates architecture of LSTM. To the best of our knowledge, ConvLSTM was not studied in the field of seizure prediction based on EEG signals. Further more, we proposed our attention-based ConvLSTM to analyze the contribution of different temporal slices of EEG input as a set of frames. The studied models have not gained the appropriate attention in seizure prediction. These contributions were detailed in chapter five.

### 6.2 Future works

Researches can never end even by the implementation and the realisation of end-to-end products. AI was the most serving technology for the medical field, aiming to make the diagnosis and the prognostics of disease easier. Even for suffering patients, AI helped to improve their quality of life and keep their states under control.

Neurologists and psychotherapists are still searching for an explanation about many body manifestations face to diseases, recognition problems and emotional alteration. It is very important for them to know what events are considered as triggers for the manifestation of anxiety attacks or for seizure onset. Around this table of discovery, many questions are still unanswered and many researches are not practically achieved and remain theoretical.

In the previous section, we have summarized the main contributions of this thesis, and as

## Chapter 6. Conclusion and Future Works

---

explained there, is a need to extend the researches done for anxiety detection to serve the diagnosis of anxiety disorders, which is a larger field than anxiety states detection. Furthermore, we propose to start an investigation about the relation between anxiety and epilepsy in order to answer the question: Can anxiety be considered as an epileptic onset trigger?

The problem of imbalanced datasets keep demanding a solution for many tasks. For seizure type classification, the only public dataset is TUHSZ, which suffers from a huge problem of imbalanced data. We talk here about a ratio of 1:1000 or more between major and minor classes. Regular papers have addressed this problem by the traditional ways of oversampling. But results were not satisfying and many papers don't give this problem a lot of interest and use the existing amount of data.

### 6.2.1 Investigation of the relation between anxiety and epileptic seizures

Electroencephalography (EEG) biomarkers are a set of neurological manifestation detected in the EEG signal, which are exploited to give a print to a brain reaction face to traumatic emotion, anxiety or stress. Many people struggle to manage their emotions, which is why, they have a high probability that their defense system shuts down. Epileptic patients can be faced to a Pseudoseizures (PNES). The latter are not the same type of neurological seizures that are caused by uncontrolled activity in the brain. Instead, PNES are an extreme response to stress and anxiety and are therefore considered psychiatric in nature. If an extreme response of an epileptic patient's brain to stress and anxiety may cause PNES, how much anxiety biomarkers can be present in the preictal state of a seizure. As we know that some EEG biomarkers have a great correlation with an anxious state, like discussed in the Chapter Three, we propose to search the presence of these prints in the preictal segments. The study should provide a comparison between preictal - ictal and interictal values of the chosen biomarker. If a correlation is found, a model can be proposed to discriminate between the three states based on the extracted feature. This work can be applied for seizure prediction or seizure detection.

### 6.2.2 Data augmentation using adversarial neural network for the TUHSZ dataset addressing the issue of imbalanced classification task

Data augmentation helps increase the available training data, and facilitate the use of more complex DL models. It can also reduce overfitting and improve the accuracy and stability of the classifiers. In the EE-based domains, we found that DA has been more or less successfully applied to many EEG tasks such as: Sleep stages, Motor imagery Mental workload and Emotion recognition tasks. The contribution presented in Chapter Four was evaluated on two datasets, one of them is the TUSZ. This dataset is the only free publicly available dataset for seizure type classification. The major drawback of this dataset is the unavailability of a similar amount of data in each class, which makes it a very imbalanced dataset. With the emergence of Generative Adversarial Networks (GANs) [Goodfellow et al., 2014], it is possible nowadays to proceed to data augmentation using GAN. With sufficient and enough data, training a deep neural network will be efficient. For epileptic patients, it is hard to record a seizure during a consultation. Also, some types of seizures are rare, which makes the amount of recorded signals very small. By nature, the raw EEG data is usually mixed with noise and various artifacts, because of which researchers have to discard some bad channels and data.

Designing a data augmentation strategy [Luo et al., 2018] [Luo et al., 2019] [Aznan et al., 2019] is thereby a necessity to make the dataset balanced and thus the classification unbiased. This perspective has two major contributions. First, the proposition of a GAN architecture for data generation from raw EEG data and not from EEG feature vectors with an extensive validation on two benchmarks, notably TUSZ [Obeid and Picone, 2016] (8 seizure types) and CHBMIT [Shoeb, 2009] (3 seizure states). Second, the generated data are used in the training set and thus it can be used for the classification of EEG signals by deep models.

### 6.2.3 Automated hyper-parameters optimization

Since deep neural networks were developed, they have made huge contributions to peoples everyday lives. However, despite this achievement, the design and training of neural net-

## Chapter 6. Conclusion and Future Works

---

works are still challenging and unpredictable procedures that have been alleged to be alchemy. To lower the technical thresholds for common users, automated hyper-parameter optimization (HPO) has become a popular topic in both academic and industrial areas.

LR is a positive scalar that determines the length of step during SGD [Goodfellow et al., 2016]. In most cases, the LR must be manually adjusted during model training, and this adjustment is often necessary for enhanced accuracy [Bengio, 2012].

Dropout is a technique used to select neurons randomly with a given probability that are not used during training, which makes the network less sensitive to the specific weights of neurons [Hinton et al., 2012]. An overlarge dropout rate will over-simplify the model, whereas a small value will have little effect. In addition, a larger LR with decay and a larger momentum are suggested because fewer neurons updated with dropout requires more update for each batch [Brownlee, 2016].

The number of hidden layers is a critical parameter for determining the overall structure of neural networks, which has a direct influence on the final output [Hinton et al., 2006]. Deep learning networks with more layers are likely to obtain more complex features and relatively higher accuracy.

The number of neurons in each layer must also be carefully considered. Too few neurons in the hidden layers may cause underfitting because the model lacks complexity. By contrast, too many neurons may result in overfitting and increase the training time.

Activation functions are crucial in deep learning for introducing nonlinear properties to the output of neurons. Without an activation function, a neural network will simply be a linear regression model that is unable to represent complicated features of data. The most popular and widely used activation functions include sigmoid, hyperbolic tangent (tanh), rectified linear units (ReLU) [Nair and Hinton, 2010]. Automatic search techniques have been applied in search of proper activation functions, including the structure of functions and related hyper-parameters.

It is of high importance to study the optimization algorithms like the Random search, Grid search, Bayesian Optimization, Multi-banded methods and the Population-based trainig (BPT) methods to select the best hyper-parameters of our deep models conceptualized for the tasks of seizure detection, classification and prediction.

# Bibliography

- [Abbasi et al., 2019] Abbasi, M. U., Rashad, A., Basalamah, A., and Tariq, M. (2019). Detection of epilepsy seizures in neo-natal eeg using lstm architecture. *IEEE Access*, 7:179074–179085. (Cited on page 79.)
- [Acharya et al., 2018] Acharya, U. R., Oh, S. L., Hagiwara, Y., Tan, J. H., and Adeli, H. (2018). Deep convolutional neural network for the automated detection and diagnosis of seizure using eeg signals. *Computers in biology and medicine*, 100:270–278. (Cited on pages 29 and 34.)
- [ADAA, 2018] ADAA (2018). Anxiety and depression association of america. (Cited on page 40.)
- [Ahmedt-Aristizabal et al., 2019] Ahmedt-Aristizabal, D., Fernando, T., Denman, S., Peterson, L., Aburn, M. J., and Fookes, C. (2019). Neural memory networks for robust classification of seizure type. *arXiv preprint arXiv:1912.04968*. (Cited on pages 36, 37, 85 and 86.)
- [Alexander et al., 2017] Alexander, L. M., Escalera, J., Ai, L., Andreotti, C., Febre, K., Mangone, A., Vega-Potler, N., Langer, N., Alexander, A., Kovacs, M., et al. (2017). An open resource for transdiagnostic research in pediatric mental health and learning disorders. *Scientific data*, 4:170181. (Cited on page 21.)
- [Anh et al., 2012] Anh, V. H., Van, M. N., Ha, B. B., and Quyet, T. H. (2012). A real-time model based support vector machine for emotion recognition through eeg. In *Control, Automation and Information Sciences (ICCAIS), 2012 International Conference on*, pages 191–196. IEEE. (Cited on page 46.)
- [Antoniades et al., 2017] Antoniades, A., Spyrou, L., Martin-Lopez, D., Valentin, A., Alarcon, G., Sanei, S., and Took, C. C. (2017). Detection of interictal discharges with convolutional neural networks using discrete ordered multichannel intracranial eeg. *IEEE Transactions on Neural Systems and Rehabilitation Engineering*, 25(12):2285–2294. (Cited on page 29.)
- [Arsalan et al., 2019] Arsalan, A., Majid, M., Butt, A. R., and Anwar, S. M. (2019). Classification of perceived mental stress using a commercially available eeg headband. *IEEE journal of biomedical and health informatics*, 23(6):2257–2264. (Cited on pages 20, 22, 63 and 64.)
- [Asif et al., 2020] Asif, U., Roy, S., Tang, J., and Harrer, S. (2020). SeizureNet: Multi-spectral deep feature learning for seizure type classification. In *Machine Learning in Clinical Neuroimaging and Radiogenomics in Neuro-oncology*, pages 77–87. Springer. (Cited on pages 36, 37, 85 and 86.)
- [Aznan et al., 2019] Aznan, N. K. N., Atapour-Abarghouei, A., Bonner, S., Connolly, J. D., Al Moubayed, N., and Breckon, T. P. (2019). Simulating brain signals: Creating synthetic eeg data via neural-based generative models for improved ssvep classification. In *2019 IEEE International Joint Conference on Neural Networks (IJCNN)*, pages 1–8. (Cited on page 136.)

## Bibliography

---

- [Baghdadi and Aribi, 2019] Baghdadi, A. and Aribi, Y. (2019). Effectiveness of dominance for anxiety vs anger detection. In *2019 Fifth IEEE International Conference on Advances in Biomedical Engineering (ICABME)*, pages 1–4. (Cited on page 8.)
- [Baghdadi et al., 2016] Baghdadi, A., Aribi, Y., and Alimi, A. M. (2016). A survey of methods and performances for eeg-based emotion recognition. In *International Conference on Hybrid Intelligent Systems*, pages 164–174. Springer. (Cited on pages 8 and 21.)
- [Baghdadi et al., 2017] Baghdadi, A., Aribi, Y., and Alimi, A. M. (2017). Efficient human stress detection system based on frontal alpha asymmetry. In *International Conference on Neural Information Processing*, pages 858–867. Springer. (Cited on page 8.)
- [Baghdadi et al., 2020a] Baghdadi, A., Aribi, Y., Fourati, R., Halouani, N., Siarry, P., and Alimi, A. (2020a). Psychological stimulation for anxious states detection based on eeg-related features. *Journal of Ambient Intelligence and Humanized Computing*, pages 1–15. (Cited on pages 7, 20, 63, 78 and 134.)
- [Baghdadi et al., 2021a] Baghdadi, A., Fourati, R., Aribi, Y., , Daoud, S., Dammak, M., Mhiri, C., Siarry, P., and Alimi, A. (2021a). A channel-wise attention-based representation learning method for epileptic seizure detection. *IEEE Journal of Biomedical and Health Informatics*, page submitted. (Cited on pages 86 and 87.)
- [Baghdadi et al., 2021b] Baghdadi, A., Fourati, R., Aribi, Y., , Daoud, S., Dammak, M., Mhiri, C., Siarry, P., and Alimi, A. (2021b). A spatio-temporal attention network for eeg-based epileptic seizure prediction. *IEEE Transactions on Neural Networks and Learning Systems*, page submitted. (Cited on page 123.)
- [Baghdadi et al., 2020b] Baghdadi, A., Fourati, R., Aribi, Y., Siarry, P., and Alimi, A. M. (2020b). Robust feature learning method for epileptic seizures prediction based on long-term eeg signals. In *2020 International Joint Conference on Neural Networks (IJCNN)*, pages 1–7. IEEE. (Cited on pages 8 and 85.)
- [Bahdanau et al., 2015] Bahdanau, D., Cho, K., and Bengio, Y. (2015). Neural machine translation by jointly learning to align and translate. In Bengio, Y. and LeCun, Y., editors, *3rd International Conference on Learning Representations, ICLR 2015, San Diego, CA, USA, May 7-9, 2015, Conference Track Proceedings*. (Cited on page 75.)
- [Bandarabadi et al., 2013] Bandarabadi, M., Dourado, A., Teixeira, C. A., Netoff, T. I., and Parhi, K. K. (2013). Seizure prediction with bipolar spectral power features using adaboost and svm classifiers. In *2013 35th Annual International Conference of the IEEE Engineering in Medicine and Biology Society (EMBC)*, pages 6305–6308. IEEE. (Cited on page 102.)
- [Barata et al., 2018] Barata, R., Ribeiro, B., Dourado, A., and Teixeira, C. (2018). Epileptic seizure prediction with stacked auto-encoders: Lessons from the evaluation on a large and collaborative database. In *Precision Medicine Powered by pHealth and Connected Health*, pages 9–13. Springer. (Cited on page 116.)
- [Bengio, 2012] Bengio, Y. (2012). Deep learning of representations for unsupervised and transfer learning. In *Proceedings of ICML workshop on unsupervised and transfer learning*, pages 17–36. JMLR Workshop and Conference Proceedings. (Cited on page 137.)

## Bibliography

---

- [Benitez et al., 2016] Benitez, D. S., Toscano, S., and Silva, A. (2016). On the use of the emotiv epoc neuroheadset as a low cost alternative for eeg signal acquisition. In *2016 IEEE Colombian Conference on Communications and Computing (COLCOM)*, pages 1–6. (Cited on page 46.)
- [Bhattacharyya and Pachori, 2017] Bhattacharyya, A. and Pachori, R. B. (2017). A multivariate approach for patient-specific eeg seizure detection using empirical wavelet transform. *IEEE Transactions on Biomedical Engineering*, 64(9):2003–2015. (Cited on page 27.)
- [Bhattacharyya et al., 2017] Bhattacharyya, A., Pachori, R. B., Upadhyay, A., and Acharya, U. R. (2017). Tunable-q wavelet transform based multiscale entropy measure for automated classification of epileptic eeg signals. *Applied Sciences*, 7(4):385. (Cited on pages 28 and 34.)
- [Bradley and Lang, 1994] Bradley, M. M. and Lang, P. J. (1994). Measuring emotion: the self-assessment manikin and the semantic differential. *Journal of behavior therapy and experimental psychiatry*, 25(1):49–59. (Cited on page 43.)
- [Brinkmann et al., 2016] Brinkmann, B. H., Wagenaar, J., Abbot, D., Adkins, P., Bosshard, S. C., Chen, M., Tieng, Q. M., He, J., Muñoz-Almaraz, F., Botella-Rocamora, P., et al. (2016). Crowdsourcing reproducible seizure forecasting in human and canine epilepsy. *Brain*, 139(6):1713–1722. (Cited on pages 32 and 33.)
- [Brownlee, 2016] Brownlee, J. (2016). *Master Machine Learning Algorithms: discover how they work and implement them from scratch*. Machine Learning Mastery. (Cited on page 137.)
- [Cerf et al., 2000] Cerf, R. et al. (2000). Spectral analysis of stereo-electroencephalograms: preictal slowing in partial epilepsies. *Biological cybernetics*, 83(5):399–405. (Cited on page 102.)
- [Chen et al., 2017] Chen, L., Zhang, H., Xiao, J., Nie, L., Shao, J., Liu, W., and Chua, T. (2017). Sca-cnn: Spatial and channel-wise attention in convolutional networks for image captioning. pages 6298–6306. (Cited on page 75.)
- [Cisotto et al., 2020] Cisotto, G., Zanga, A., Chlebus, J., Zoppis, I., Manzoni, S., and Markowska-Kaczmar, U. (2020). Comparison of attention-based deep learning models for eeg classification. *arXiv preprint arXiv:2012.01074*. (Cited on pages 37 and 76.)
- [Coan and Allen, 2003] Coan, J. A. and Allen, J. J. (2003). Frontal eeg asymmetry and the behavioral activation and inhibition systems. *Psychophysiology*, 40(1):106–114. (Cited on page 46.)
- [Cook et al., 2013] Cook, M. J., O’Brien, T. J., Berkovic, S. F., Murphy, M., Morokoff, A., Fabinyi, G., D’Souza, W., Yerra, R., Archer, J., Litewka, L., et al. (2013). Prediction of seizure likelihood with a long-term, implanted seizure advisory system in patients with drug-resistant epilepsy: a first-in-man study. *The Lancet Neurology*, 12(6):563–571. (Cited on page 31.)

## Bibliography

---

- [Craik et al., 2019] Craik, A., He, Y., and Contreras-Vidal, J. L. (2019). Deep learning for electroencephalogram (eeg) classification tasks: a review. *Journal of Neural Engineering*, 16(3):031001. (Cited on page 79.)
- [De Clercq et al., 2006] De Clercq, W., Vergult, A., Vanrumste, B., Van Paesschen, W., and Van Huffel, S. (2006). Canonical correlation analysis applied to remove muscle artifacts from the electroencephalogram. *IEEE transactions on Biomedical Engineering*, 53(12):2583–2587. (Cited on page 52.)
- [Delorme and Makeig, 2004] Delorme, A. and Makeig, S. (2004). Eeglab: an open source toolbox for analysis of single-trial eeg dynamics including independent component analysis. *Journal of neuroscience methods*, 134(1):9–21. (Cited on page 52.)
- [Demerdzieva and Pop-Jordanova, 2015] Demerdzieva, A. and Pop-Jordanova, N. (2015). Relation between frontal alpha asymmetry and anxiety in young patients with generalized anxiety disorder. *Prilozi*, 36(2):157–177. (Cited on page 57.)
- [Dr. Aaron T, 1991] Dr. Aaron T, R. A. S. (1991). Relationship between the beck anxiety inventory and the hamilton anxiety rating scale with anxious outpatients. *Journal of Anxiety Disorders*, 5:213–223. (Cited on page 47.)
- [Du et al., 2020] Du, X., Ma, C., Zhang, G., Li, J., Lai, Y.-K., Zhao, G., Deng, X., Liu, Y.-J., and Wang, H. (2020). An efficient lstm network for emotion recognition from multichannel eeg signals. *IEEE Transactions on Affective Computing*. (Cited on page 134.)
- [Eftekhari et al., 2006] Eftekhari, A., Stines, L. R., and Zoellner, L. A. (2006). Do you need to talk about it? prolonged exposure for the treatment of chronic ptsd. *The Behavior Analyst Today*, 7(1):70. (Cited on page 47.)
- [Ekanayake, 2010] Ekanayake, H. (2010). P300 and emotiv epoc: Does emotiv epoc capture real eeg? *Web publication <http://neurofeedback.visaduma.info/emotivresearch.htm>*. (Cited on page 45.)
- [Elgohary et al., 2016] Elgohary, S., Eldawlatly, S., and Khalil, M. I. (2016). Epileptic seizure prediction using zero-crossings analysis of eeg wavelet detail coefficients. In *2016 IEEE conference on computational intelligence in bioinformatics and computational biology (CIBCB)*, pages 1–6. (Cited on page 105.)
- [Eom et al., 2020] Eom, H., Lee, D., Han, S., Hariyani, Y. S., Lim, Y., Sohn, I., Park, K., and Park, C. (2020). End-to-end deep learning architecture for continuous blood pressure estimation using attention mechanism. *Sensors*, 20(8):2338. (Cited on page 76.)
- [Eraldi-Gackiere and Graziani, 2007] Eraldi-Gackiere, D. and Graziani, P. (2007). *Exposition et désensibilisation: en thérapie comportementale et cognitive*. Dunod. (Cited on page 46.)
- [Espinoza and Paredes, 2020] Espinoza, W. J. M. and Paredes, E. A. A. (2020). Effect of a mobile application on the precision of the preliminary diagnosis of anxiety. *Cogent Engineering*, 7(1):1765689. (Cited on page 67.)

## Bibliography

---

- [Felman, 2018] Felman, A. (2018). What are anxiety disorders? Retrieved January 21, 2021, from web site: <https://www.medicalnewstoday.com/articles/323454.php>. (Cited on pages 2 and 40.)
- [Fisher et al., 2014] Fisher, R. S., Acevedo, C., Arzimanoglou, A., Bogacz, A., Cross, J. H., Elger, C. E., Engel Jr, J., Forsgren, L., French, J. A., Glynn, M., et al. (2014). Ilae official report: a practical clinical definition of epilepsy. *Epilepsia*, 55(4):475–482. (Cited on page 17.)
- [Fisher et al., 2017] Fisher, R. S., Cross, J. H., French, J. A., Higurashi, N., Hirsch, E., Jansen, F. E., Lagae, L., Moshé, S. L., Peltola, J., Roulet Perez, E., et al. (2017). Operational classification of seizure types by the international league against epilepsy: Position paper of the ilae commission for classification and terminology. *Epilepsia*, 58(4):522–530. (Cited on page 17.)
- [Fourati et al., 2017a] Fourati, R., Ammar, B., Aouiti, C., Medina, J. J. S., and Alimi, A. M. (2017a). Optimized echo state network with intrinsic plasticity for eeg-based emotion recognition. In Liu, D., Xie, S., Li, Y., Zhao, D., and El-Alfy, E. M., editors, *Neural Information Processing - 24th International Conference, ICONIP 2017, Guangzhou, China, November 14-18, 2017, Proceedings, Part II*, volume 10635 of *Lecture Notes in Computer Science*, pages 718–727. Springer. (Cited on page 21.)
- [Fourati et al., 2017b] Fourati, R., Ammar, B., Aouiti, C., Sanchez-Medina, J., and Alimi, A. M. (2017b). Optimized echo state network with intrinsic plasticity for eeg-based emotion recognition. In *International Conference on Neural Information Processing*, pages 718–727. Springer. (Cited on page 78.)
- [Fourati et al., 2020a] Fourati, R., Ammar, B., Jin, Y., and Alimi, A. M. (2020a). Eeg feature learning with intrinsic plasticity based deep echo state network. In *2020 International Joint Conference on Neural Networks (IJCNN)*, pages 1–8. IEEE. (Cited on page 78.)
- [Fourati et al., 2020b] Fourati, R., Ammar, B., Sanchez-Medina, J., and Alimi, A. M. (2020b). Unsupervised learning in reservoir computing for eeg-based emotion recognition. *IEEE Transactions on Affective Computing*. (Cited on pages 21, 24 and 78.)
- [García-Martínez et al., 2017] García-Martínez, B., Martínez-Rodrigo, A., Zangróniz, R., Pastor, J. M., and Alcaraz, R. (2017). Symbolic analysis of brain dynamics detects negative stress. *Entropy*, 19(5):196. (Cited on pages 20 and 24.)
- [Giannakakis et al., 2015] Giannakakis, G., Grigoriadis, D., and Tsiknakis, M. (2015). Detection of stress/anxiety state from eeg features during video watching. In *Engineering in Medicine and Biology Society (EMBC), 2015 37th Annual International Conference of the IEEE*, pages 6034–6037. IEEE. (Cited on pages 21, 24 and 48.)
- [Goldenberg, 2010] Goldenberg, M. M. (2010). Overview of drugs used for epilepsy and seizures: etiology, diagnosis, and treatment. *Pharmacy and Therapeutics*, 35(7):392. (Cited on page 73.)

## Bibliography

---

- [Gómez-Herrero et al., 2006] Gómez-Herrero, G., De Clercq, W., Anwar, H., Kara, O., Egiazarian, K., Van Huffel, S., and Van Paesschen, W. (2006). Automatic removal of ocular artifacts in the eeg without an eeg reference channel. In *Proceedings of the 7th Nordic Signal Processing Symposium-NORSIG 2006*, pages 130–133. IEEE. (Cited on page 52.)
- [Goodfellow et al., 2016] Goodfellow, I., Bengio, Y., and Courville, A. (2016). *Deep learning*. MIT press. (Cited on page 137.)
- [Goodfellow et al., 2014] Goodfellow, I. J., Pouget-Abadie, J., Mirza, M., Xu, B., Warde-Farley, D., Ozair, S., Courville, A. C., and Bengio, Y. (2014). Generative adversarial nets. In Ghahramani, Z., Welling, M., Cortes, C., Lawrence, N. D., and Weinberger, K. Q., editors, *Advances in Neural Information Processing Systems 27: Annual Conference on Neural Information Processing Systems 2014, December 8-13 2014, Montreal, Quebec, Canada*, pages 2672–2680. (Cited on page 136.)
- [Hamilton, 1959] Hamilton, M. (1959). The assessment of anxiety states by rating. *British journal of medical psychology*, 32(1):50–55. (Cited on pages vii, 45 and 47.)
- [Hinton et al., 2012] Hinton, G., Deng, L., Yu, D., Dahl, G. E., Mohamed, A.-r., Jaitly, N., Senior, A., Vanhoucke, V., Nguyen, P., Sainath, T. N., et al. (2012). Deep neural networks for acoustic modeling in speech recognition: The shared views of four research groups. *IEEE Signal processing magazine*, 29(6):82–97. (Cited on page 137.)
- [Hinton et al., 2006] Hinton, G. E., Osindero, S., and Teh, Y.-W. (2006). A fast learning algorithm for deep belief nets. *Neural computation*, 18(7):1527–1554. (Cited on page 137.)
- [Hjorth, 1970] Hjorth, B. (1970). Eeg analysis based on time domain properties. *Electroencephalography and clinical neurophysiology*, 29(3):306–310. (Cited on pages 53 and 54.)
- [Hochreiter and Schmidhuber, 1997] Hochreiter, S. and Schmidhuber, J. (1997). Long short-term memory. *Neural computation*, 9(8):1735–1780. (Cited on page 78.)
- [Horlings et al., 2008] Horlings, R., Datcu, D., and Rothkrantz, L. J. (2008). Emotion recognition using brain activity. In *Proceedings of the 9th international conference on computer systems and technologies and workshop for PhD students in computing*, page 6. ACM. (Cited on page 54.)
- [Howbert et al., 2014] Howbert, J. J., Patterson, E. E., Stead, S. M., Brinkmann, B., Vasoli, V., Crepeau, D., Vite, C. H., Sturges, B., Ruedebusch, V., Mavoori, J., et al. (2014). Forecasting seizures in dogs with naturally occurring epilepsy. *PloS one*, 9(1):e81920. (Cited on page 32.)
- [Hu et al., 2020] Hu, H., Li, Q., Zhao, Y., and Zhang, Y. (2020). Parallel deep learning algorithms with hybrid attention mechanism for image segmentation of lung tumors. *IEEE Transactions on Industrial Informatics*, 17(4):2880–2889. (Cited on page 76.)
- [Hu et al., 2019] Hu, W.-S., Li, H.-C., Pan, L., Li, W., Tao, R., and Du, Q. (2019). Feature extraction and classification based on spatial-spectral convlstm neural network for hyperspectral images. *arXiv preprint arXiv:1905.03577*. (Cited on page 112.)

## Bibliography

---

- [Hvass et al., 2017] Hvass, J., Larsen, O., Vendelbo, K., Nilsson, N., Nordahl, R., and Serafin, S. (2017). Visual realism and presence in a virtual reality game. In *2017 3DTV Conference: The True Vision-Capture, Transmission and Display of 3D Video (3DTV-CON)*, pages 1–4. IEEE. (Cited on page 48.)
- [Islam et al., 2016] Islam, M. K., Rastegarnia, A., and Yang, Z. (2016). A wavelet-based artifact reduction from scalp eeg for epileptic seizure detection. *IEEE journal of biomedical and health informatics*, 20(5):1321–1332. (Cited on page 26.)
- [Jatupaiboon et al., 2013] Jatupaiboon, N., Pan-ngum, S., and Israsena, P. (2013). Emotion classification using minimal eeg channels and frequency bands. In *2013 10th International Joint Conference on Computer Science and Software Engineering (JCSSE)*, pages 21–24. IEEE. (Cited on page 46.)
- [Jenke et al., 2014] Jenke, R., Peer, A., and Buss, M. (2014). Feature extraction and selection for emotion recognition from eeg. *IEEE Transactions on Affective Computing*, 5(3):327–339. (Cited on page 55.)
- [Jun and Smitha, 2016] Jun, G. and Smitha, K. G. (2016). Eeg based stress level identification. In *2016 IEEE International Conference on Systems, Man, and Cybernetics (SMC)*, pages 003270–003274. (Cited on page 22.)
- [Katsigiannis and Ramzan, 2018] Katsigiannis, S. and Ramzan, N. (2018). Dreamer: a database for emotion recognition through eeg and ecg signals from wireless low-cost off-the-shelf devices. *IEEE journal of biomedical and health informatics*, 22(1):98–107. (Cited on pages 24, 46 and 48.)
- [Kaushik et al., 2018] Kaushik, P., Gupta, A., Roy, P. P., and Dogra, D. P. (2018). Eeg-based age and gender prediction using deep blstm-lstm network model. *IEEE Sensors Journal*, 19(7):2634–2641. (Cited on page 79.)
- [Khosrowabadi et al., 2011] Khosrowabadi, R., Quek, C., Ang, K. K., Tung, S. W., and Heijnen, M. (2011). A brain-computer interface for classifying eeg correlates of chronic mental stress. In *IJCNN*, pages 757–762. (Cited on pages 22 and 24.)
- [Kiral-Kornek et al., 2018] Kiral-Kornek, I., Roy, S., Nurse, E., Mashford, B., Karoly, P., Carroll, T., Payne, D., Saha, S., Baldassano, S., O’Brien, T., et al. (2018). Epileptic seizure prediction using big data and deep learning: toward a mobile system. *EBioMedicine*, 27:103–111. (Cited on page 32.)
- [Kiranyaz et al., 2014] Kiranyaz, S., Ince, T., Zabihi, M., and Ince, D. (2014). Automated patient-specific classification of long-term electroencephalography. *Journal of biomedical informatics*, 49:16–31. (Cited on page 34.)
- [Koelstra et al., 2012] Koelstra, S., Muhl, C., Soleymani, M., Lee, J.-S., Yazdani, A., Ebrahimi, T., Pun, T., Nijholt, A., and Patras, I. (2012). Deap: A database for emotion analysis; using physiological signals. *IEEE Transactions on Affective Computing*, 3(1):18–31. (Cited on pages 21, 48 and 55.)

## Bibliography

---

- [Kropotov, 2010] Kropotov, J. D. (2010). *Quantitative EEG, event-related potentials and neurotherapy*. Academic Press. (Cited on page 11.)
- [Kuhlmann et al., 2018] Kuhlmann, L., Karoly, P., Freestone, D. R., Brinkmann, B. H., Temko, A., Barachant, A., Li, F., Titericz Jr, G., Lang, B. W., Lavery, D., et al. (2018). Epilepsyecosystem.org: crowd-sourcing reproducible seizure prediction with long-term human intracranial eeg. *Brain*, 141(9):2619–2630. (Cited on page 33.)
- [Larson, 2019] Larson, J. (2019). What are alpha brain waves and why are they important? *Web publication* <https://www.healthline.com/health/alpha-brain-wavesbenefits>. (Cited on page 50.)
- [LeCun et al., 2015] LeCun, Y., Bengio, Y., and Hinton, G. (2015). Deep learning. *Nature*, 521(7553):436–444. (Cited on page 32.)
- [Li et al., 2019] Li, Y., Zheng, W., Wang, L., Zong, Y., and Cui, Z. (2019). From regional to global brain: A novel hierarchical spatial-temporal neural network model for eeg emotion recognition. *IEEE Transactions on Affective Computing, to be published*. doi:10.1109/TAFFC.2019.2922912. (Cited on page 78.)
- [Lim and Chia, 2015] Lim, C.-K. A. and Chia, W. C. (2015). Analysis of single-electrode eeg rhythms using matlab to elicit correlation with cognitive stress. *International Journal of Computer Theory and Engineering*, 7(2):149. (Cited on pages 22 and 24.)
- [Litt and Lehnertz, 2002] Litt, B. and Lehnertz, K. (2002). Seizure prediction and the pre-seizure period. *Current opinion in neurology*, 15(2):173–177. (Cited on page 100.)
- [Liu et al., 2020] Liu, T., Truong, N. D., Nikpour, A., Zhou, L., and Kavehei, O. (2020). Epileptic seizure classification with symmetric and hybrid bilinear models. *IEEE journal of biomedical and health informatics*, 24(10):2844–2851. (Cited on pages 37 and 86.)
- [Luo et al., 2018] Luo, Y., Zhang, S.-Y., Zheng, W.-L., and Lu, B.-L. (2018). Wgan domain adaptation for eeg-based emotion recognition. In *International Conference on Neural Information Processing*, pages 275–286. Springer. (Cited on page 136.)
- [Luo et al., 2019] Luo, Y., Zhu, L.-Z., and Lu, B.-L. (2019). A gan-based data augmentation method for multimodal emotion recognition. In *International Symposium on Neural Networks*, pages 141–150. Springer. (Cited on page 136.)
- [Maier et al., 1988] Maier, W., Buller, R., Philipp, M., and Heuser, I. (1988). The hamilton anxiety scale: reliability, validity and sensitivity to change in anxiety and depressive disorders. *Journal of affective disorders*, 14(1):61–68. (Cited on pages vii, 45 and 47.)
- [McEvoy et al., 2015] McEvoy, K., Hasenstab, K., Senturk, D., Sanders, A., and Jeste, S. S. (2015). Physiologic artifacts in resting state oscillations in young children: methodological considerations for noisy data. *Brain imaging and behavior*, 9(1):104–114. (Cited on page 51.)
- [Meng et al., 2019] Meng, D., Peng, X., Wang, K., and Qiao, Y. (2019). Frame attention networks for facial expression recognition in videos. In *2019 IEEE International Conference on Image Processing (ICIP)*, pages 3866–3870. (Cited on page 112.)

## Bibliography

---

- [Miao et al., 2015] Miao, Y., Gowayed, M., and Metze, F. (2015). Eesen: End-to-end speech recognition using deep rnn models and wfst-based decoding. In *2015 IEEE Workshop on Automatic Speech Recognition and Understanding (ASRU)*, pages 167–174. IEEE. (Cited on page 76.)
- [Mohammad et al., 2017] Mohammad, N., Ara, S., Jannat, M. R., and Shifang, D. (2017). Towards automated epileptic seizure detection for lightweight devices through eeg signal processing. *Global Journal of Medical Research*. (Cited on page 34.)
- [Mormann et al., 2005] Mormann, F., Kreuz, T., Rieke, C., Andrzejak, R. G., Kraskov, A., David, P., Elger, C. E., and Lehnertz, K. (2005). On the predictability of epileptic seizures. *Clinical neurophysiology*, 116(3):569–587. (Cited on pages 102 and 104.)
- [Murdoch et al., 2019] Murdoch, M., Partin, M. R., Vang, D., and Kehle-Forbes, S. M. (2019). The psychological risk of minimal risk activities: A pre-and posttest study using the self-assessment manikin. *Journal of Empirical Research on Human Research Ethics*, 14(1):15–22. (Cited on page 48.)
- [Murugappan et al., 2010] Murugappan, M., Rizon, M., Nagarajan, R., and Yaacob, S. (2010). Inferring of human emotional states using multichannel eeg. *European Journal of Scientific Research*, 48(2):281–299. (Cited on page 56.)
- [Nahmias et al., 2020] Nahmias, D. O., Civillico, E. F., and Kontson, K. L. (2020). Deep learning and feature based medication classifications from eeg in a large clinical data set. *Scientific Reports*, 10(1):1–11. (Cited on page 37.)
- [Nair and Hinton, 2010] Nair, V. and Hinton, G. E. (2010). Rectified linear units improve restricted boltzmann machines. In *Icml*. (Cited on page 137.)
- [Nunez and Srinivasan, 2006] Nunez, P. L. and Srinivasan, R. (2006). *Electric fields of the brain: the neurophysics of EEG*. Oxford University Press, USA. (Cited on page 11.)
- [Obeid and Picone, 2016] Obeid, I. and Picone, J. (2016). The temple university hospital eeg data corpus. *Frontiers in neuroscience*, 10:196. (Cited on page 136.)
- [Oude, 2007] Oude, D. (2007). Eeg-based emotion recognition the influence of visual and auditory stimuli. *Emotion*, 57:1798–1806. (Cited on pages 22 and 51.)
- [Page et al., 2015] Page, A., Sagedy, C., Smith, E., Attaran, N., Oates, T., and Mohsenin, T. (2015). A flexible multichannel eeg feature extractor and classifier for seizure detection. *IEEE Transactions on Circuits and Systems II: Express Briefs*, 62(2):109–113. (Cited on page 31.)
- [Panayiotopoulos, 2005a] Panayiotopoulos, C. (2005a). Clinical aspects of the diagnosis of epileptic seizures and epileptic syndromes. In *The epilepsies: Seizures, syndromes and management*. Bladon Medical Publishing. (Cited on page 73.)
- [Panayiotopoulos, 2005b] Panayiotopoulos, C. (2005b). Optimal use of the eeg in the diagnosis and management of epilepsies. In *The epilepsies: seizures, syndromes and management*. Bladon Medical Publishing. (Cited on page 73.)

## Bibliography

---

- [Panoulas et al., 2008] Panoulas, K. I., Hadjileontiadis, L. J., and Panas, S. M. (2008). Hilbert-huang spectrum as a new field for the identification of eeg event related de-/synchronization for bci applications. In *Engineering in Medicine and Biology Society, 2008. EMBS 2008. 30th Annual International Conference of the IEEE*, pages 3832–3835. IEEE. (Cited on page 55.)
- [Park et al., 2011] Park, Y., Luo, L., Parhi, K. K., and Netoff, T. (2011). Seizure prediction with spectral power of eeg using cost-sensitive support vector machines. *Epilepsia*, 52(10):1761–1770. (Cited on page 102.)
- [Patidar and Panigrahi, 2017] Patidar, S. and Panigrahi, T. (2017). Detection of epileptic seizure using kraskov entropy applied on tunable-q wavelet transform of eeg signals. *Biomedical Signal Processing and Control*, 34:74–80. (Cited on pages 28 and 34.)
- [Patil et al., 2017] Patil, M. N. B., Mirajkar, R., Patil, S., and Patil, P. (2017). A method for detection and reduction of stress using eeg. *International Research Journal of Engineering and Technology (IRJET)*, 4(1):1528–1604. (Cited on page 24.)
- [Pellegrino, 2014] Pellegrino, G. (2014). Analysis for automatic detection of epileptic seizure from eeg signals. (Cited on page 17.)
- [Piho and Tjahjadi, 2018] Piho, L. and Tjahjadi, T. (2018). A mutual information based adaptive windowing of informative eeg for emotion recognition. *IEEE Transactions on Affective Computing, to be published*. doi:10.1109/TAFFC.2018.2840973. (Cited on page 64.)
- [Pitkänen et al., 2017] Pitkänen, A., Buckmaster, P., Galanopoulou, A. S., and Moshé, S. L. (2017). *Models of seizures and epilepsy*. Academic Press. (Cited on pages 100, 101 and 102.)
- [Prashant Lahane, 2016] Prashant Lahane, Amit Vaidya, C. U. S. S. A. R. (2016). Real time system to detect human stress using eeg signals. *International Journal of Innovative Research in Computer and Communication Engineering*, 4(4). (Cited on page 22.)
- [Qiu et al., 2018] Qiu, Y., Zhou, W., Yu, N., and Du, P. (2018). Denoising sparse autoencoder-based ictal eeg classification. *IEEE Transactions on Neural Systems and Rehabilitation Engineering*, 26(9):1717–1726. (Cited on pages 28 and 34.)
- [Quesney and Gloor, 1985] Quesney, L. and Gloor, P. (1985). Localization of epileptic foci. *Electroencephalography and clinical neurophysiology. Supplement*, 37:165–200. (Cited on page 3.)
- [Rasekhi et al., 2013] Rasekhi, J., Mollaei, M. R. K., Bandarabadi, M., Teixeira, C. A., and Dourado, A. (2013). Preprocessing effects of 22 linear univariate features on the performance of seizure prediction methods. *Journal of neuroscience methods*, 217(1-2):9–16. (Cited on page 102.)
- [Roy et al., 2019] Roy, S., Asif, U., Tang, J., and Harrer, S. (2019). Machine learning for seizure type classification: setting the benchmark. *arXiv preprint arXiv:1902.01012*. (Cited on pages 36 and 37.)

## Bibliography

---

- [Russell, 1980] Russell, J. A. (1980). A circumplex model of affect. *Journal of personality and social psychology*, 39(6):1161. (Cited on page 48.)
- [Sackellares, 2008] Sackellares, J. C. (2008). Seizure prediction. *Epilepsy Currents*, 8(3):55–59. (Cited on page 101.)
- [Saeed et al., 2017] Saeed, S. M. U., Anwar, S. M., and Majid, M. (2017). Quantification of human stress using commercially available single channel eeg headset. *IEICE Transactions on Information and Systems*, 100(9):2241–2244. (Cited on page 63.)
- [Saeed et al., 2015] Saeed, S. M. U., Anwar, S. M., Majid, M., and Bhatti, A. M. (2015). Psychological stress measurement using low cost single channel eeg headset. In *2015 IEEE International Symposium on Signal Processing and Information Technology (ISSPIT)*, pages 581–585. IEEE. (Cited on page 63.)
- [Saeed et al., 2018] Saeed, U., Muhammad, S., Anwar, S. M., Majid, M., Awais, M., and Alnowami, M. (2018). Selection of neural oscillatory features for human stress classification with single channel eeg headset. *BioMed research international*, 2018. (Cited on page 63.)
- [Samiee et al., 2015] Samiee, K., Kovacs, P., and Gabbouj, M. (2015). Epileptic seizure classification of eeg time-series using rational discrete short-time fourier transform. *IEEE transactions on Biomedical Engineering*, 62(2):541–552. (Cited on pages 28 and 34.)
- [Sanei and Chambers, 2013] Sanei, S. and Chambers, J. A. (2013). *EEG signal processing*. John Wiley & Sons. (Cited on page 13.)
- [Saputro et al., 2019] Saputro, I. R. D., Maryati, N. D., Solihati, S. R., Wijayanto, I., Hadiyoso, S., and Patmasari, R. (2019). Seizure type classification on eeg signal using support vector machine. In *Journal of Physics: Conference Series*, volume 1201, page 012065. IOP Publishing. (Cited on pages 36 and 37.)
- [Scheffer et al., 2017] Scheffer, I. E., Berkovic, S., Capovilla, G., Connolly, M. B., French, J., Guilhoto, L., Hirsch, E., Jain, S., Mathern, G. W., Moshé, S. L., et al. (2017). Ilae classification of the epilepsies: position paper of the ilae commission for classification and terminology. *Epilepsia*, 58(4):512–521. (Cited on pages 2, 18 and 19.)
- [Secerbegovic et al., 2017] Secerbegovic, A., Ibric, S., Nisic, J., Suljanovic, N., and Mujcic, A. (2017). Mental workload vs. stress differentiation using single-channel eeg. In *CMBEBIH 2017*, pages 511–515. Springer, Singapore. (Cited on page 63.)
- [Selim et al., 2019] Selim, S., Elhinamy, E., Othman, H., Abouelsaadat, W., and Salem, M. A.-M. (2019). A review of machine learning approaches for epileptic seizure prediction. In *2019 14th International Conference on Computer Engineering and Systems (ICCES)*, pages 239–244. IEEE. (Cited on page 106.)
- [Sharma and Pachori, 2017] Sharma, M. and Pachori, R. B. (2017). A novel approach to detect epileptic seizures using a combination of tunable-q wavelet transform and fractal dimension. *Journal of Mechanics in Medicine and Biology*, 17(07):1740003. (Cited on pages 27 and 34.)

## Bibliography

---

- [Shoeb, 2009] Shoeb, A. H. (2009). *Application of machine learning to epileptic seizure onset detection and treatment*. PhD thesis, Massachusetts Institute of Technology. (Cited on pages 25, 115 and 136.)
- [Shukla et al., 2019] Shukla, J., Barreda-Angeles, M., Oliver, J., Nandi, G., and Puig, D. (2019). Feature extraction and selection for emotion recognition from electrodermal activity. *IEEE Transactions on Affective Computing*. (Cited on page 48.)
- [Spielberger, 2013] Spielberger, C. D. (2013). *Anxiety: Current trends in theory and research*. Elsevier. (Cited on page 15.)
- [Sriraam et al., 2019] Sriraam, N., Temel, Y., Rao, S. V., Kubben, P. L., et al. (2019). A convolutional neural network based framework for classification of seizure types. In *2019 41st Annual International Conference of the IEEE Engineering in Medicine and Biology Society (EMBC)*, pages 2547–2550. IEEE. (Cited on pages 36 and 37.)
- [Subhani et al., 2017] Subhani, A. R., Mumtaz, W., Saad, M. N. B. M., Kamel, N., and Malik, A. S. (2017). Machine learning framework for the detection of mental stress at multiple levels. *IEEE Access*, 5:13545–13556. (Cited on page 63.)
- [Supratak et al., 2014] Supratak, A., Li, L., and Guo, Y. (2014). Feature extraction with stacked autoencoders for epileptic seizure detection. In *Engineering in Medicine and Biology Society (EMBC), 2014 36th Annual International Conference of the IEEE*, pages 4184–4187. IEEE. (Cited on page 34.)
- [Tatum, 2013] Tatum, W. O. (2013). Artifact-related epilepsy. *Neurology*, 80(1 Supplement 1):S12–S25. (Cited on page 20.)
- [Temko et al., 2011] Temko, A., Lightbody, G., Thomas, E. M., Boylan, G. B., and Marnane, W. (2011). Instantaneous measure of eeg channel importance for improved patient-adaptive neonatal seizure detection. *IEEE transactions on biomedical engineering*, 59(3):717–727. (Cited on page 76.)
- [Tichavský et al., 2006] Tichavský, P., Doron, E., Yeredor, A., and Nielsen, J. (2006). A computationally affordable implementation of an asymptotically optimal bss algorithm for ar sources. In *2006 14th European Signal Processing Conference*, pages 1–5. IEEE. (Cited on page 52.)
- [Toole and Boylan, 2017] Toole, J. M. and Boylan, G. B. (2017). Neural: quantitative features for newborn eeg using matlab. *arXiv preprint arXiv:1704.05694*. (Cited on page 57.)
- [Tsiouris et al., 2018] Tsiouris, K. M., Pezoulas, V. C., Zervakis, M., Konitsiotis, S., Koutsouris, D. D., and Fotiadis, D. I. (2018). A long short-term memory deep learning network for the prediction of epileptic seizures using eeg signals. *Computers in biology and medicine*, 99:24–37. (Cited on pages 76, 79, 107, 115, 116, 119 and 123.)
- [Vanitha and Krishnan, 2016] Vanitha, V. and Krishnan, P. (2016). Real time stress detection system based on eeg signals. *Biomedical Research*, pages 271–275. (Cited on pages 21 and 24.)

## Bibliography

---

- [Wang et al., 2018] Wang, G., Ren, D., Li, K., Wang, D., Wang, M., and Yan, X. (2018). Eeg-based detection of epileptic seizures through the use of a directed transfer function method. *IEEE Access*, 6:47189–47198. (Cited on pages 30 and 34.)
- [Xie et al., 2020] Xie, T., Cao, M., and Pan, Z. (2020). Applying self-assessment manikin (sam) to evaluate the affective arousal effects of vr games. In *Proceedings of the 2020 3rd International Conference on Image and Graphics Processing*, pages 134–138. (Cited on page 48.)
- [Xingjian et al., 2015] Xingjian, S., Chen, Z., Wang, H., Yeung, D.-Y., Wong, W.-K., and Woo, W.-c. (2015). Convolutional lstm network: A machine learning approach for precipitation nowcasting. In *Advances in neural information processing systems*, pages 802–810. (Cited on pages 74, 107 and 134.)
- [Yao et al., 2018] Yao, X., Li, X., Ye, Q., Huang, Y., Cheng, Q., and Zhang, G. (2018). A robust deep learning approach for automatic seizure detection. *arXiv preprint arXiv:1812.06562*. (Cited on pages 120, 121 and 123.)
- [Yao et al., 2021] Yao, X., Li, X., Ye, Q., Huang, Y., Cheng, Q., and Zhang, G.-Q. (2021). A robust deep learning approach for automatic classification of seizures against non-seizures. *Biomedical Signal Processing and Control*, 64:102215. (Cited on pages 78, 87 and 88.)
- [Yin et al., 2017] Yin, W., Kann, K., Yu, M., and Schütze, H. (2017). Comparative study of cnn and rnn for natural language processing. *arXiv preprint arXiv:1702.01923*. (Cited on page 76.)
- [Yuan and Jia, 2019] Yuan, Y. and Jia, K. (2019). Fusionatt: deep fusional attention networks for multi-channel biomedical signals. *Sensors*, 19(11):2429. (Cited on page 87.)
- [Yuan et al., 2018] Yuan, Y., Xun, G., Ma, F., Suo, Q., Xue, H., Jia, K., and Zhang, A. (2018). A novel channel-aware attention framework for multi-channel eeg seizure detection via multi-view deep learning. In *2018 IEEE EMBS International Conference on Biomedical & Health Informatics (BHI)*,, pages 206–209. (Cited on pages 29 and 34.)
- [Zabihi et al., 2016] Zabihi, M., Kiranyaz, S., Rad, A. B., Katsaggelos, A. K., Gabbouj, M., and Ince, T. (2016). Analysis of high-dimensional phase space via poincaré section for patient-specific seizure detection. *IEEE Transactions on Neural Systems and Rehabilitation Engineering*, 24(3):386–398. (Cited on page 34.)
- [Zanetti et al., 2019] Zanetti, M., Mizumoto, T., Faes, L., Fornaser, A., De Cecco, M., Maule, L., Valente, M., and Nollo, G. (2019). Multilevel assessment of mental stress via network physiology paradigm using consumer wearable devices. *Journal of Ambient Intelligence and Humanized Computing*, pages 1–10. (Cited on page 63.)
- [Zhang and Chen, 2017] Zhang, T. and Chen, W. (2017). Lmd based features for the automatic seizure detection of eeg signals using svm. *IEEE Transactions on Neural Systems and Rehabilitation Engineering*, 25(8):1100–1108. (Cited on pages 31 and 34.)

## Bibliography

---

- [Zhang et al., 2020a] Zhang, X., Pan, J., Shen, J., Din, Z. U., Li, J., Lu, D., Wu, M., and Hu, B. (2020a). Fusing of electroencephalogram and eye movement with group sparse canonical correlation analysis for anxiety detection. *IEEE Transactions on Affective Computing*, to be published. doi:10.1109/TAFFC.2020.2981440. (Cited on pages 20 and 23.)
- [Zhang et al., 2020b] Zhang, X., Yao, L., Dong, M., Liu, Z., Zhang, Y., and Li, Y. (2020b). Adversarial representation learning for robust patient-independent epileptic seizure detection. *IEEE Journal of Biomedical and Health Informatics*. (Cited on pages 76, 85 and 86.)
- [Zhao et al., 2018] Zhao, H., Guo, X., Wang, M., Li, T., Pang, C., and Georgakopoulos, D. (2018). Analyze eeg signals with extreme learning machine based on pmis feature selection. *International Journal of Machine Learning and Cybernetics*, 9(2):243–249. (Cited on page 61.)
- [Zheng et al., 2017] Zheng, W.-L., Zhu, J.-Y., and Lu, B.-L. (2017). Identifying stable patterns over time for emotion recognition from eeg. *IEEE Transactions on Affective Computing*. (Cited on pages 43 and 58.)
- [Zhuang et al., 2017] Zhuang, N., Zeng, Y., Tong, L., Zhang, C., Zhang, H., and Yan, B. (2017). Emotion recognition from eeg signals using multidimensional information in emd domain. *BioMed research international*, 2017. (Cited on page 55.)